INNOVATIVE CLEAN COAL TECHNOLOGY

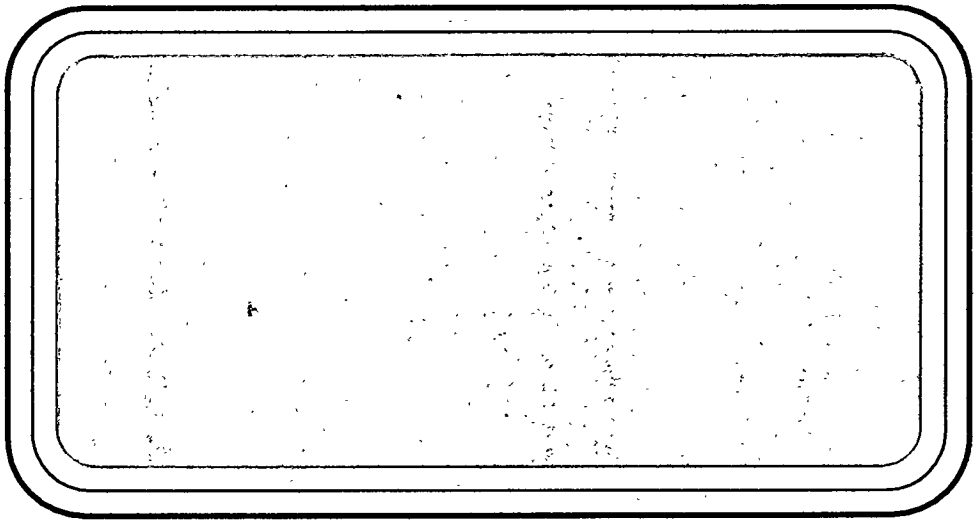

Prepared by:

Southern Company Services, Inc.
Birmingham, Alabama

INNOVATIVE CLEAN COAL TECHNOLOGY (ICCT)

DEMONSTRATION OF SELECTIVE CATALYTIC REDUCTION TECHNOLOGY FOR THE CONTROL OF NITROGEN OXIDE EMISSIONS FROM HIGH-SULFUR COAL-FIRED BOILERS

Technical Progress Report
First and Second Quarters 1995

FINAL

DOE Contract
DE-FC22-90PC89652

SCS Contract
C-91-000026

Prepared by:

W.S. Hinton & Associates
2708 Woodbreeze Drive
Cantonment, Florida 32533

Prepared for:

Southern Company Services, Inc.
600 North 18th Street
P.O. Box 2625
Birmingham, Alabama 35202-2625

Cleared by DOE Patent Counsel on March 13, 1996

DISCLAIMER

LEGAL NOTICE

This report was prepared for Southern Company Services, Inc. pursuant to a cooperative agreement partially funded by the U. S. Department of Energy and neither Southern Company Services, Inc. nor any of its subcontractors nor the U. S. Department of Energy, nor any person acting on behalf of either:

(a) Makes any warranty or representation, express or implied with respect to the accuracy, completeness, or usefulness of the information contained in this report, or that the use of any information, apparatus, method, or process disclosed in this report may not infringe privately-owned rights; or

(b) Assumes any liabilities with respect to the use of, or for damages resulting from the use of, any information, apparatus, method or process disclosed in this report.

Reference herein to any specific commercial product, process, or service by trade name, trademark, manufacturer, or otherwise, does not necessarily constitute or imply its endorsement, recommendation, or favoring by the U. S. Department of Energy. The views and opinion of authors expressed herein do not necessarily state or reflect those of the U. S. Department of Energy.

Section 1

SUMMARY

Background

The objective of this project is to demonstrate and evaluate commercially available Selective Catalytic Reduction (SCR) catalysts from U. S., Japanese and European catalyst suppliers on a high-sulfur U. S. coal-fired boiler. SCR is a post-combustion nitrogen oxide (NO_x) control technology that involves injecting ammonia (NH_3) into the flue gas generated from coal combustion in an electric utility boiler. The flue gas containing ammonia is then passed through a reactor containing a specialized catalyst. In the presence of the catalyst, the ammonia reacts with NO_x to convert it to nitrogen and water vapor.

Although SCR is widely practiced in Japan and Europe on gas-, oil-, and low-sulfur coal-fired boilers, there are several technical uncertainties associated with applying SCR to U. S. coals. These uncertainties include:

(1) potential catalyst deactivation due to poisoning by trace metal species present in U. S. coals that are not present in other fuels.

(2) performance of the technology and effects on the balance-of-plant equipment in the presence of high amounts of SO_2 and SO_3.

(3) performance of a wide variety of SCR catalyst compositions, geometries, and methods of manufacture under typical high-sulfur coal-fired utility operating conditions.

These uncertainties are being explored by operating a series of small-scale SCR reactors and simultaneously exposing different SCR catalysts to flue gas derived from the combustion of high sulfur U. S. coal.

The demonstration is being performed at Gulf Power Company's Plant Crist Unit No. 5 (75 MW nameplate capacity) near Pensacola, Florida. The project is funded by the U. S. Department of Energy (DOE), Southern Company Services, Inc. (SCS on behalf of the entire Southern electric system), the Electric Power Research Institute (EPRI), and Ontario Hydro. SCS is the participant responsible for managing all aspects of this project.

The project is being conducted in the following three phases:

Phase I -	Permitting, Environmental Monitoring Plan and Preliminary Engineering
Phase II -	Detailed Design Engineering and Construction
Phase III -	Operation, Testing, Disposition and Final Report

The project is in the operation and testing phase during this reporting period.

Operations

During the first and second quarters of 1995, all the reactors were operated in long-term base operating conditions, i.e. at an effective NH_3/NO_x ratio near 0.81 for 80% NO_x removal. Facility operation ceased on July 14, 1995. The short operational period in the third quarter, 1995 is included in this reporting period.

		Operating hours	
Catalyst supplier	Reactor designation	1st Qtr.	End of Project
W R. Grace	A (large)	9882	11012
Nippon Shokubai	B (large)	10699	11859
Siemens	C (large)	10755	11632
W. R. Grace	D (small)	9011	10151
Cormetech	E (small)	9011	10151
Haldor Topsoe	F (small)	9035	10175
Hitachi Zosen	G (small)	6153	7293
Cormetech	H (small)	--	982
Cormetech	J (small/low-dust)	4271	5363

Operation of the test facility progressed relatively smoothly during the reporting period. Total operating time during the period was reduced significantly due to the major host unit outage. The following chronological listing offers a brief history of test facility operation during the reporting period and points out operational highlights on a monthly basis.

Operational History Highlights

January, 1995

- Completion of fourth parametric test sequence
- Restart of test facility after maintenance and catalyst sampling outage
- Sampling of all catalysts except "A"
- Service water pump failure

February, 1995

- Shutdown of test facility in preparation for extended host unit outage (February 1, 1995)
- Special sampling of gas and solid phase ammonia for adsorption/desorption
- Inspection of air preheaters to investigate fouling

March, 1995

- Reassembling of air preheaters completed
- Completion of various maintenance items
- Start of preparation of specifications for dismantling bid

April, 1995

- Results of fourth parametric test sequence sent to project participants
- Modifications made to reactor "H" for high-velocity catalyst test
- Return of intermediate NO_x measurement system to manufacturer
- Preparation of paper for the EPRI/EPA Joint Symposium on NO_x control

May, 1995

- Completion of host unit outage
- Restart of test facility (May 22, 1995)
- Start of final abbreviated parametric test sequence
- Beginning of high velocity tests on reactor "H"
- Failure and repair of reactor "C" fan motor

June, 1995

- Released specifications for dismantling bids
- Final particulate and trace metal testing started
- Paper submitted to DOE for presentation at the Clean Coal Technology Conference

July, 1995

- Award of dismantling contract
- Completion of the final parametric test sequence
- Completion of operation phase of the project and final shutdown of the test facility (July 14, 1995)

Testing

The parametric and baseline tests performed during this reporting period are shown below. This sequence of tests represents the fifth and final parametric test sequence. The results of these tests were similar to those noted in previous parametric sequences.

Fifth (Final) Parametric Test Sequence

Flue gas flow rate Large / Small reactor	Flue gas temperature	NH_3/NO_x Ratio	Measurements
KSCFM	°F		
3.0 / 0.24	620	0.8	slip NH_3
5.0 / 0.40	620	0.8	intermediate & slip NH_3
7.5 / 0.60	620	1.0	slip NH_3
5.0 / 0.40	750	0.8	intermediate & slip NH_3
7.5 / 0.60	700	0.8	intermediate & slip NH_3
5.0 / 0.40 (Baseline)	750	0.8	intermediate & slip NH_3, SO_2/SO_3 HCl Concentration (Reactor A only), velocity profile, N_2O
3.0 / 0.24	700	0.8	intermediate NH_3
5.0 / 0.40	700	0.6	intermediate & slip NH_3
5.0 / 0.40	700	1.0	intermediate & slip NH_3
5.0 / 0.40	620	0.6	slip NH_3
5.0 / 0.40	620	1.0	slip NH_3
7.5 / 0.60	700	0.6	slip NH_3
7.5 / 0.60	700	1.0	slip NH_3
5.0 / 0.40	750	0.6	slip NH_3
5.0 / 0.40	750	1.0	slip NH_3

The testing showed that the reactors were continuing to operate within the specified design limits. Pressure drop trends were fairly smooth indicating little catalyst fouling or severe erosion. Responses of the catalysts in terms of ammonia slip to temperature again showed fairly significant improvements when temperature was increased from 620 to 700 °F, but comparably little improvement was noted with temperature increases past 700 °F. As expected, ammonia slip increased with increasing NO_x reduction efficiency and increased sharply past NO_x removal rates of 90%. Baseline SO_2 oxidation was comparable to that previously noted. Response of SO_2 oxidation to increases in flow rate was fairly flat with some linear response noted. Temperature response of SO_2 oxidation was somewhat sharper, however, but was still less sensitive than expected (this was also the finding in previous parametric sequences).

Section 2

INTRODUCTION

The Innovative Clean Coal Technology (ICCT) Program is designed to demonstrate clean coal technologies that are capable of retrofitting or repowering existing facilities to achieve significant reduction in sulfur dioxide (SO_2) and/or nitrogen oxides (NO_x) emissions. The technologies selected for demonstration are capable of being commercialized in the 1990s and are expected to be more cost effective than current technologies.

This ICCT project is jointly funded by the U. S. Department of Energy, the Electric Power Research Institute (EPRI), Ontario Hydro, and by Southern Company Services (SCS) on behalf of the entire Southern electric system. The project's objective is to demonstrate the selective catalytic reduction (SCR) process for the removal of nitrogen oxides (NO_x) from the flue gas of boilers that burn U.S. high-sulfur coal. The SCR technology involves the injection of NH_3 into the flue gas and the subsequent catalytic reduction of NO_x by NH_3 to produce molecular nitrogen (N_2) and water vapor.

A simplified SCR process flow diagram with major equipment is shown in Figure 1. Specifically, hot flue gas leaving the economizer section of the boiler is ducted to the SCR reactor. Prior to entering the reactor, NH_3 is injected into the flue gas at a sufficient distance upstream of the reactor to provide for complete mixing of the NH_3 and flue gas. The quantity of NH_3 can be adjusted to control the NO_x reduction efficiency. The flue gas leaving the catalytic reactor enters the air preheater where it transfers heat to the incoming combustion air. Provisions are often made for ash removal from the bottom of the reactor since some fallout of fly ash may occur. Duct work is also provided to bypass some flue gas around the economizer during periods when the boiler is operating at reduced load. This is done to maintain the temperature of the flue gas entering the catalytic reactor at the proper reaction temperature of about 700°F. The flue gas leaving the air preheater goes to the electrostatic precipitator (ESP) where fly ash is removed. The ESP is part of the existing plant and is generally unaffected by the SCR system except as higher SO_3 content affects the electrical resistivity of the fly ash or if ammonium bisulfate co-precipitates with the fly ash.

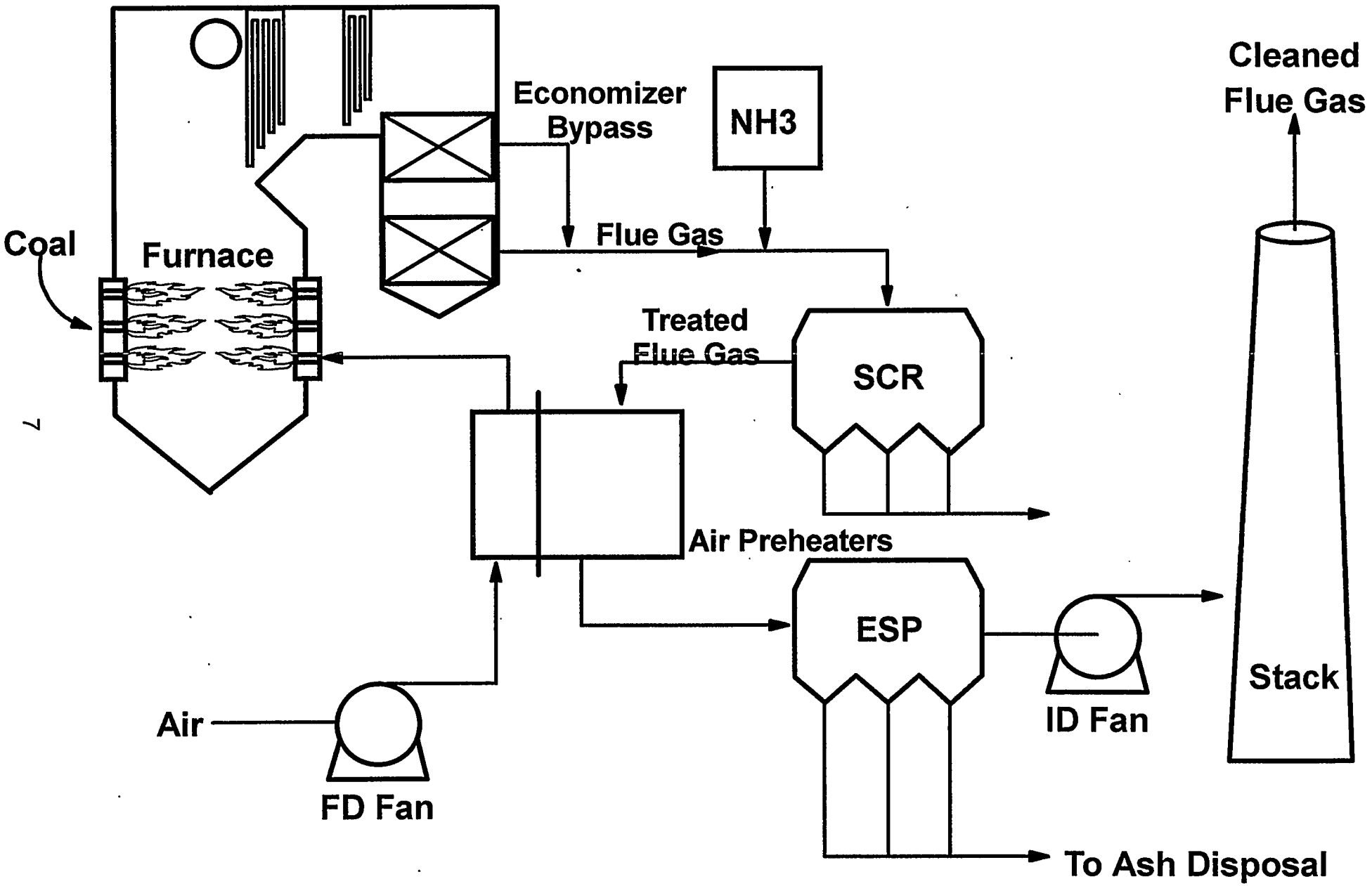

Figure 1. Flow Diagram of Typical SCR Installation.

s:\ptd\maj\maj\scrpint.pre

SCR technology is in commercial use in Japan and western Europe on gas-, oil-, and on low-sulfur, coal-fired power plants. The first utility applications of SCR technology started in Japan in 1977 for oil- and gas-fired boilers and subsequently in 1979 for coal-fired boilers. As of 1986, ninety utility boilers in Japan had been equipped with SCR technology including twenty-two coal-fired boilers. These coal-fired boilers represent a combined capacity in excess of 6500 MWe and are typically fired with a low-ash, low-sulfur coal.

In addition to Japanese experience, several countries in western Europe (most notably Germany and Austria) have passed stringent NO_x emission regulations that have all but mandated the installation of SCR. Prior to commercial SCR installations in Germany, utility companies demonstrated several types of SCR facilities in prototype demonstration programs similar to this ICCT project. Over 50 SCR pilot plants were built and operated in western Europe. These pilot plants ranged from 19 to 6200 SCFM and provided the data base that led to commercialization of the SCR technology in western Europe.

Previously completed U. S. work with the SCR process on utility boilers consists of three projects which were carried out in the late 1970s and early 1980s. One of these was carried out on a natural gas fired boiler by Southern California Edison. Another project consisted of a pilot test conducted for the EPA at Georgia Power's Plant Mitchell. This pilot plant treated a 1000 ACFM (0.5 MWe) slip stream of flue gas resulting from the combustion of low- to medium-sulfur coal. A third pilot-scale project, carried out at the Public Service Company of Colorado's Arapaho Station treated a 5000 ACFM (2.5 MWe) slip stream of flue gas resulting from the combustion of U. S. low-sulfur coal.

Although SCR is widely practiced in Japan and Europe, there are numerous technical uncertainties associated with applying SCR to U. S. coals. These uncertainties include:

(1) potential catalyst deactivation due to poisoning by trace metal species present in U. S. coals that are not present in other fuels.

(2) performance of the technology and effects on the balance-of-plant equipment in the presence of high amounts of SO_2 and SO_3.

(3) performance of a wide variety of SCR catalyst compositions, geometries and methods of manufacture under typical high-sulfur coal-fired utility operating conditions.

These uncertainties are being explored by operating a series of small-scale SCR reactors and simultaneously exposing different SCR catalysts to flue gas derived from the combustion of high sulfur U. S. coal.

The first uncertainty above is being handled by evaluating SCR catalyst performance for two years under realistic operating conditions found in U. S. pulverized coal-fired utility boilers. The deactivation rates for the catalysts exposed to flue gas from high sulfur U. S. coal will be documented to determine accurate catalyst life, and thus, accurate process economics.

The second uncertainty above is being explored by performing parametric testing and through the installation/operation of air preheaters downstream of the larger reactors. During parametric testing, operating conditions are adjusted above and below design values to observe deNO_x performance and ammonia slip as functions of the change in operating conditions. Air preheater performance is observed to evaluate effects from SCR operation upon heat transfer, and therefore, upon boiler efficiency.

The third uncertainty is being handled by using honeycomb- and plate-type SCR catalysts from U. S., Japan and Europe of various commercial composition. Results from the tests with these catalysts expands our knowledge of performance on a variety of SCR catalysts under U. S. utility operating conditions with high-sulfur coal.

The intent of this project is to demonstrate commercial catalyst performance, proper operating conditions, and catalyst life for the SCR process. This project is also demonstrating the technical and economic viability of SCR while reducing NO_x emissions by at least 80%.

The project is being conducted at Gulf Power Company's Plant Crist Unit 5, a commercially operating 75 MW unit, located in Pensacola, Florida, on U. S. coals with a sulfur content near 3.0%. Unit 5 is a tangentially-fired, dry bottom boiler, with hot and cold side ESPs for particulate control. The SCR process used in this demonstration is designed to treat a slip-stream of flue gas and features multiple reactors installed in parallel. With all reactors in operation, the maximum amount of combustion flue gas that can be treated is 17,400 standard cubic feet per minute (SCFM) which is roughly equivalent to 8.7 MWe.

The SCS facility is a slip-stream SCR test facility consisting of three 2.5 MWe (5000 SCFM) SCR reactors and six 0.20 MWe (400 SCFM) reactors that operate in parallel for side-by-side

comparisons of commercially available SCR catalyst technologies obtained from suppliers throughout the world. Figure 2 presents a simplified process flow diagram for the SCR test facility. The large (2.5 MWe) SCR reactors contain commercially available SCR catalysts as offered by SCR catalyst suppliers. These reactors are coupled with small-scale air preheaters to evaluate the long-term effects of SCR reaction chemistry on air preheater deposit formation and the deposits' effects on an air preheater. The small reactors are used to test additional commercially available catalysts. This demonstration facility size is adequate to develop performance data to evaluate SCR capabilities and costs that are applicable to boilers using high-sulfur U. S. coals.

The demonstration project is organized into three phases: (1) Phase I - Permitting, Environmental Monitoring Plan and Preliminary Engineering; (2) Phase II - Detail Design Engineering and Construction; and (3) Phase III - Operation, Testing, Disposition, and Final Report. The cooperative agreement was signed June 14, 1990, and the project completion date is now projected to be at the end of 1995. The original total estimated project costs were $15.6 million but project growth increased the expected total cost to $23 million. The co-funders are SCS ($10 million), DOE ($9.4 million), EPRI ($2.9 million) and Ontario Hydro ($0.75 million).

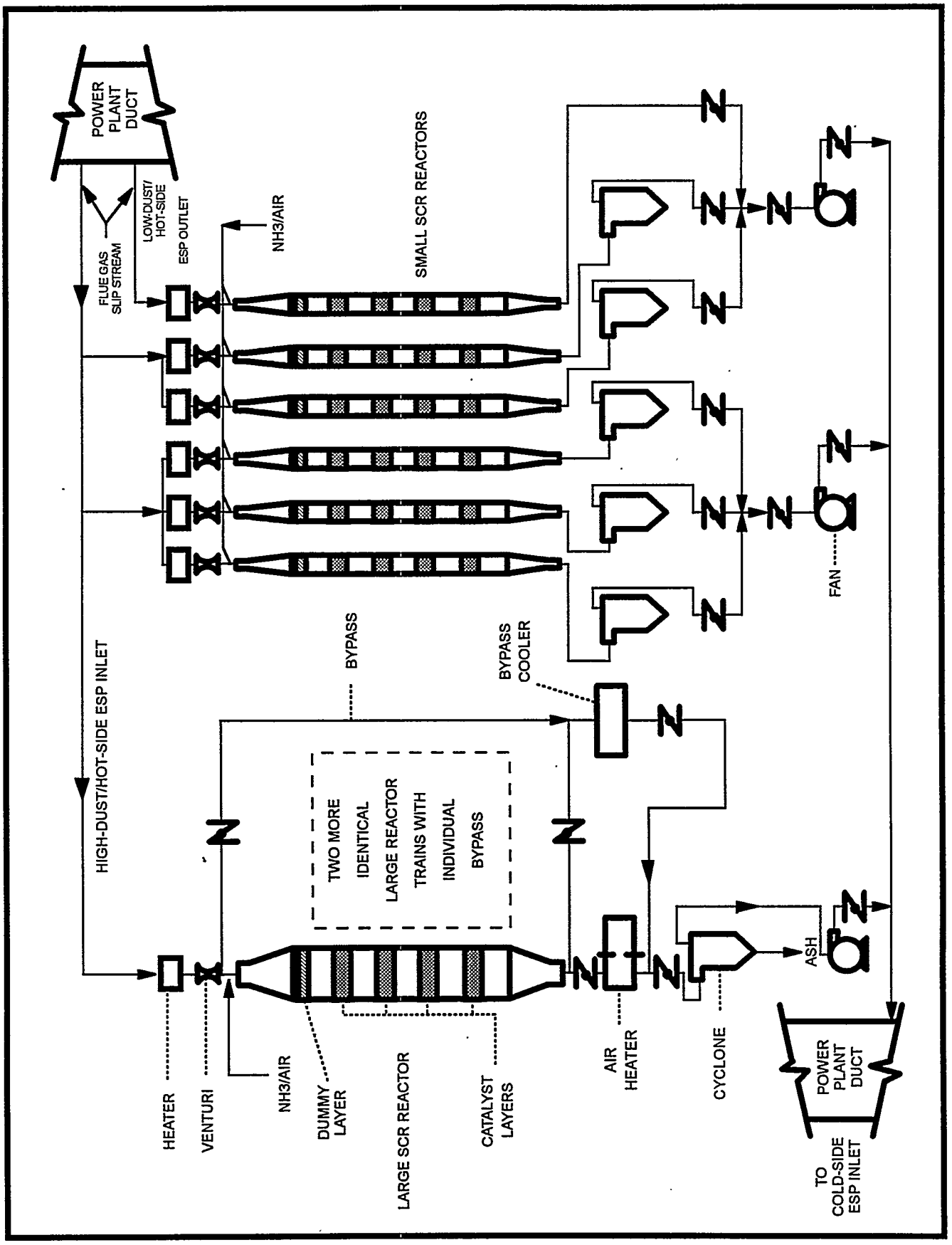

Figure 2. Prototype SCR Demonstration Facility-Process Flow Diagram

Section 3

PROJECT DESCRIPTION

Within the three phases of the project, the following tasks are to be conducted to effectively demonstrate the SCR process:

Phase I - Permitting, Environmental Monitoring Plan and Preliminary Engineering

Task 1.1.1 - Prototype Plant Permitting Activities
Task 1.1.2 - Develop Environmental Monitoring Program
Task 1.1.3 - Preliminary Engineering
Task 1.1.4 - Engineering and Construction Contracts Scope Development
Task 1.1.5 - Project Management and Reporting

Phase II - Detailed Design Engineering and Construction

Task 1.2.1 - Detailed Design Engineering
Task 1.2.2 - Construction
Task 1.2.3 - Operation Staff Training
Task 1.2.4 - Planning for Detailed Testing
Task 1.2.5 - Start-Up/Shakedown
Task 1.2.6 - Project Management and Reporting

Phase III - Operations, Testing, Disposition and Final Report

Task 1.3.1 - SCR Demonstration Facility Operations and Maintenance
Task 1.3.2 - Process Evaluation
Task 1.3.3 - Environmental Data Management and Reporting
Task 1.3.4 - Economic Evaluation
Task 1.3.5 - Dismantling/Disposition
Task 1.3.6 - Project Management and Reporting

Section 4

PROJECT STATUS

Progress during January - July, 1995, is summarized below for each of the on-going tasks in the Scope of Work.

PHASE III - OPERATIONS, TESTING, DISPOSITION, AND FINAL REPORT

Task 1.3.1 - SCR Demonstration Facility Operations and Maintenance

The catalyst suppliers, assigned reactors, and the total number of operating hours with exposure to flue gas for each reactor at the end of the first and second quarters in 1995 are as follows:

		Operating hours	
Catalyst supplier	Reactor designation	1st Qtr.	End of Project
W. R. Grace	A (large)	9882	11012
Nippon Shokubai	B (large)	10699	11853
Siemens	C (large)	10755	11632
W. R. Grace	D (small)	9011	10151
Cormetech	E (small)	9011	10151
Haldor Topsoe	F (small)	9035	10175
Hitachi Zosen	G (small)	6753	7293
Cormetech	H (small)	--	982
Cormetech	J (small/low-dust)	4271	5363

During the first and second quarters of 1995, all the reactors were operated in long-term base operating conditions, i.e. at an effective NH_3/NO_x ratio near 0.81 for 80% NO_x removal. In addition to the long-term base operating conditions, the fifth sequence of parametric tests was completed for Reactors A - J by July 14, 1995.

Operation of the test facility progressed relatively smoothly during the reporting period. Total operating time during the period was reduced significantly due to the major host unit outage (February 2 through May 15). The following chronological listing offers a brief history of test

facility operation during the reporting period and points out operational highlights on a monthly basis.

The test facility was returned to service during the first week of January after a brief maintenance and catalyst sampling outage. Maintenance performed during the outage included replacement of the service water pump packing, replacement of the "B" air preheater clutch and cleaning of the cyclone hoppers. Air preheater washes were also performed at this time. Significant improvements in air preheater pressure drop were realized from this washing, resulting in a fan speed reduction of 20% at baseline operation. All catalysts were sampled just before start-up with the exception of reactor "A" which was sampled in March. The facility operation progressed smoothly throughout the month of January with the exception of the failure of the service water pump and some ash fouling problems with the "C" cyclone hopper. The service water pump was damaged due to debris fouling the pump intake. Estimates for repair exceeded $20,000 and the decision was made to operate the test facility on a temporary cooling water connection to Plant Crist for the remainder of test facility operations. The fourth parametric test was completed during the month (reported previously in the July through December, 1994 progress report).

The test facility was shut down on February 1, 1995 as a result of a major maintenance outage scheduled for the host unit. The test facility outage continued until May 22, 1995, when test facility operation was resumed. Tests to evaluate ammonia partitioning between the gas and solid phase were conducted just before the outage. Also, ash samples were collected to perform laboratory tests on fly ash concerning ammonia absorption/desorption characteristics. During the month of February, air preheater fouling was investigated by disassembling both of the rotary air preheaters and by inspecting the hot-gas portion of the heat pipe. The air heaters were washed at this time and wash water samples sent to ABB Air Preheater.

The reassembly of the test facility air preheaters was completed in March. Other maintenance items included repair and cleaning of the gas sampling and analysis system, including maintenance of sample lines, pumps, valves, and other system components. Preparation of specifications for dismantling bids was begun.

Results of the fourth parametric test sequence (completed in January) were sent to project participants in April. No significant differences were noted in the data compared to previous parametric sequences. General maintenance on the test facility continued and preparations were begun to modify reactor "H" for proposed high-velocity tests using a Cormetech catalyst. Other

notable items during the month included the return of the intermediate NO_x measurement system to Monitor Labs for refund (this system proved unacceptable for the application). Also, a paper was prepared for presentation at the EPRI/EPA 1995 Joint Symposium on Stationary Combustion NO_x Control in Kansas City, Missouri.

Boiler operation resumed over the weekend of May 20, 1995, and the SCR facility resumed operation on May 22, 1995. The first several days of operation were spent calibrating instrumentation, etc. and with general facility check-out. Prior to the facility start-up, modifications to the "H" reactor were completed and installation of the high-velocity test catalysts was made. Testing on the fifth test sequence was begun after facility check-out. A short host unit outage to adjust turbine blade balance forced the test facility off line on May 28, 1995. Operations resumed on May 31, 1995. Failure of the reactor "C" fan motor on May 23, 1995 prevented operation of this reactor for approximately two weeks while repairs to the motor were made. High velocity tests on reactor "H" were begun late in the month, marking the end of nearly two years of shut-down for this reactor.

The testing on reactor "H" was performed to determine the effects of high flue gas velocities on the catalyst. The reactor was operated at a linear velocity from roughly 2.5 to 3 times that of the other reactors. No unusual degradation was noted in the catalyst after nearly 1000 hours of operation. However, it is unclear what the long-term effect on catalyst life would be due to the difficulty in extrapolating this short-term information to long-term operation (i.e. several years).

Parametric testing continued throughout the month of June. Particulate and trace-metal testing was also begun by an SRI off-site test crew. This crew was used to supplement the normal test staff to aid in the completion of the fifth parametric testing requirements by mid-July. A paper was also submitted for presentation at the Annual DOE Clean Coal Technology Conference in September, 1995.

The final parametric test sequence was completed on Thursday, July 13, 1995. Shutdown of the test facility began by mid-day and was completed by the end of the day, July 14, 1995. Thus, the operating and testing phase of the project was completed.

Chronological History

January, 1995

- Completion of fourth parametric test sequence
- Restart of test facility after maintenance and catalyst sampling outage (February 1, 1995)
- Sampling of all catalysts except "A"
- Service water pump failure

February, 1995

- Shutdown of test facility in preparation for extended host unit outage
- Special sampling of gas and solid phase ammonia for adsorption/desorption
- Inspection of air preheaters to investigate fouling

March, 1995

- Reassembling of air preheaters completed
- Completion of various maintenance items
- Start of preparation of specifications for dismantling bid

April, 1995

- Results of fourth parametric test sequence sent to project participants
- Modifications made to reactor "H" for high-velocity catalyst test
- Return of intermediate NO_x measurement system to manufacturer
- Preparation of paper for the EPRI/EPA Joint Symposium on NO_x control

May, 1995

- Completion of host unit outage
- Restart of test facility (May 22, 1995)
- Start of final abbreviated parametric test sequence
- Beginning of high velocity tests on reactor "H"
- Failure and repair of reactor "C" fan motor

June, 1995

- Released specifications for dismantling bids
- Final particulate and trace metal testing started
- Paper submitted to DOE for presentation at the Clean Coal Technology Conference

July, 1995

- Selection and award of dismantling contract
- Completion of the final parametric test sequence
- Completion of operation phase of the project and final shutdown of the test facility (July 14, 1996)

- Measurement Accuracy/Repeatability

The majority of manual measurements are made using triplicate samples. This insures the quality of the data and helps to remove operating variability from the results. Since triplicate measurements usually require several hours to complete, they also help to evaluate and insure that steady-state operation has been achieved for the particular test conditions. Each of the triplicate samples are analyzed in duplicate in the laboratory. Thus, six values are acquired for each average reported measured value. Detection limits for ammonia slip measurements are normally approximately 1 ppm with analytical repeatability to within 0.1 ppm. Intermediate ammonia detection limits are somewhat higher, namely 1 to 2 ppm with analytical repeatability to within 1 ppm. SO_2 measurements normally have detection limits of 5 ppm with analytical repeatability to within 1% of the measured value. SO_3 detection limits are normally 0.4 ppm with an analytical repeatability to within 0.4% of the measured value.

Task 1.3.2 - Process Evaluation

- Coal Chemistry

Coal samples were analyzed monthly for major components and certain trace elements. The monthly results, quarterly averages for January through March and April through June, yearly averages, and project-to-date averages are shown in Table 1.

- Flue Gas Composition

Several flue gas constituents are measured continuously by the gas analyzer system (described previously) at the SCR test facility inlet. Table 2 shows the constituent concentrations in terms of average values, normal high values, and normal low values over the reporting period. These quarterly values were determined using daily averages, daily highs, and daily lows during periods that the host boiler was on-line (operating at greater than 40 MWe).

Table 1. Coal Analysis Data

SCS ID No.			1st Qtr. 95	2nd Qtr. 95	1994	1995	Project Life
Test	Method	Units	Average	Average*	Average	Average	Average
Moisture, Total	ASTM D 3302	% by Wt.	12.42	10.58	11.16	11.04	10.87
Ash	ASTM D 3180	% by Wt.	9.46	8.63	9.18	8.84	9.30
Gross Calorific Value	ASTM D 3180	Btu/lb	13080	13459	13267	13364	13268
Sulfur, Total	ASTM D 3180	% by Wt.	2.24	1.74	2.64	1.87	2.58
Sulfur, lb/MMBtu	ASTM D 3180	lb/MMBtu	1.71	1.30	1.99	1.40	1.95
Carbon	ASTM D 3180	% by Wt.	74.26	75.74	74.76	75.37	74.82
Hydrogen	ASTM D 3180	% by Wt.	4.99	5.00	4.97	5.00	5.00
Nitrogen	ASTM D 3180	% by Wt.	1.60	1.58	1.59	1.59	1.58
Oxygen	ASTM D 3180	% by Wt.	7.45	7.31	6.86	7.35	6.73
Carbon, Fixed	ASTM D 3180	% by Wt.	53.42	54.48	53.38	54.22	52.83
Volatile Matter	ASTM D 3180	% by Wt.	37.12	36.89	37.44	36.95	37.88
Aluminum	ASTM D 3682	% by Wt.	1.10	1.02	1.12	1.04	1.09
Antimony	ASTM D 3683	mg/kg	<0.2	0.6	<1.0	0.5	<1.0
Arsenic	Spec. Chem. Acta. 44B	mg/kg	3.6	4.2	2.8	4.0	3.2
Barium	ASTM D 3683	mg/kg	22	36	33	33	40
Beryllium	ASTM D 3683	mg/kg	2	2	3	2	3
Cadmium	ASTM D 3683	mg/kg	0.22	0.13	<1.00	0.15	<1.00
Calcium	ASTM D 3682	% by Wt.	0.25	0.23	0.22	0.23	0.24
Chlorine	ASTM D 4208	mg/kg	3073	1400	2144	1818	1767
Chromium	ASTM D 3683	mg/kg	20	14	21	16	19
Cobalt	ASTM D 3683	mg/kg	8	6	7	7	7
Copper	ASTM D 3683	mg/kg	10	10	9	10	9
Fluorine	ASTM D 3761	mg/kg	72	48	61	54	56
Iron	ASTM D 3682	% by Wt.	1.10	0.85	1.12	0.92	1.08
Lead	Spec. Chem. Acta. 44B	mg/kg	11.1	10.7	11.5	10.8	11.7
Lithium	ASTM D 3683	mg/kg	18	11	10	13	9
Magnesium	ASTM D 3682	% by Wt.	0.06	0.08	0.06	0.08	0.06
Manganese	ASTM D 3683	mg/kg	23	24	25	24	24
Mercury	ASTM D 3684	mg/kg	<0.02	0.05	0.06	0.05	0.07
Molybdenum	ASTM D 3683	mg/kg	—	—	7.1	—	7.8
Nickel	ASTM D 3683	mg/kg	18	12	15	14	15
Phosphorus	ASTM D 3682	% by Wt.	0.01	0.01	0.01	0.01	0.02
Potassium	ASTM D 3682	% by Wt.	0.18	0.13	0.19	0.14	0.20
Selenium	Spec. Chem. Acta. 44B	mg/kg	1.4	2.6	<2.0	2.3	<2.0
Silica	ASTM D 3682	% by Wt.	2.05	2.20	2.25	2.16	2.27
Sodium	ASTM D 3682	% by Wt.	0.09	0.07	0.06	0.08	0.06
Titanium	ASTM D 3682	% by Wt.	0.06	0.06	0.06	0.06	0.06
Vanadium	ASTM D 3683	mg/kg	28	28	40	28	41
Zinc	ASTM D 3683	mg/kg	52	23	48	30	39

*2nd quarter average includes data for April through the end of the project on July 14.

TABLE 2. TEST FACILITY GAS CONCENTRATIONS

January - March 1995

Constituent	Average	High	Low
Unit #5 Load (MW)	57	71	39
Inlet NO_x (ppm)	398	477	335
Inlet O_2 (%)	5.1	7.4	3.2
Inlet CO_2 (%)	15.2	17.4	11.6
Inlet CO (ppm)	7	28	2
Inlet SO_2 (ppm)	*	*	*

* Problems with SO_2 analyzers prevent SO_2 reporting for this period.

April - July 1995

Constituent	Average	High	Low
Unit #5 Load (MW)	74	87	48
Inlet NO_x (ppm)	334	365	286
Inlet O_2 (%)	4.4	6.9	3.0
Inlet CO_2 (%)	15.4	17.1	12.7
Inlet CO (ppm)	4.2	4.3	2.7
Inlet SO_2 (ppm)	948	1096	731

- Mass Concentration and Particle Size Distribution

The mass concentration and particle size distribution measurements to confirm all reactors were receiving fly ash similar in concentration and particle size to that of the fly ash in the main plant ductwork were reported in the previous quarterly progress report for April - September 1993. Mass concentration was measured for each reactor during previous parametric testing. These were made for profile characterizations rather than reactor to reactor comparisons. Detailed mass concentration profile measurements were not made during this reporting period, but are described in previous reports.

- Fly Ash Chemistry and Resistivity

Ash mineral analyses and fly ash resistivity data were reported previously in the April - September, 1993 progress report.

- NH_3/NO_x Ratio

During long-term baseline operation, the SCR reactors were operated to achieve near 80% NO_x reduction when calculated on a constant oxygen basis. Modifications to the control system were made to include oxygen inleakage corrections when calculating the appropriate ammonia flow rate. This greatly enhanced the ability to operate the SCR reactors very near an actual NH_3/NO_x ratio of 0.80 giving roughly 80% NO_x reduction when calculated on a constant oxygen basis. This is assuming that little or no NO_2 is present resulting in an effective 1:1 NH_3:NO_x stoichiometry. In practice, small amounts (1-2%) of NO_2 present result in a slightly reduced NO_x reduction efficiency. Initial estimates based on literature values indicated that NO_2 concentrations may be as high on 5% of the total NO_x present. However, closer analysis of the monitoring equipment indicated the actual NO_2 present at the SCR facility is actually closer to 1% of the total NO_x present. In addition to long-term baseline operation, various parametric tests were performed requiring variation in the NH_3/NO_x ratio. During these tests, the effective NH_3/NO_x ratio was varied from a high of approximately 1.0 to a low of approximately 0.6 on each reactor. These parametric tests were conducted over relatively short periods of time and represent only a small fraction of the total reactor operating time.

- Ammonia Distribution

Ammonia distribution within the individual SCR reactors is extremely important in controlling ammonia slip and maintaining reactor efficiency. Assuming a perfectly smooth NO_x distribution, it is desirable to maintain an ammonia distribution that is as smooth as possible. The general criteria set for the test facility is to maintain ammonia distribution to within 10% of the average. Ammonia distributions were measured during the Fourth quarter, 1993, downstream of the dummy bed on each reactor at nine equally spaced points on the large reactors and four on the small reactors. Ammonia distribution measurements indicated that all distributions were within the 10% limit with averages comparing favorably with the predicted value.

- Flue Gas Temperature

The SCR facility is equipped with an economizer by-pass duct. This allows for high temperature flue gas extracted upstream of the host unit economizer to be mixed with flue gas extracted downstream of the host unit economizer. By adjusting the relative flows of these two components of the test facility feed gas, the temperature to the test facility can be adjusted. Under normal operation, the flue gas temperature to the test facility is maintained at 650° F. This is possible when the host unit is running at relatively high loads, however, at low unit load, the test facility inlet gas temperature often drops below 650°F even with full use of the economizer by-pass duct. Also, under some circumstances, while the host unit is operating at very high load, the feed gas to the test facility may exceed 650°F even with no economizer by-pass gas being used. The average flue gas temperature to the test facility as well as the daily high and low temperature are shown below for this reporting period. As with the previously shown gas concentration data, this data is constructed using daily averages, daily highs, and daily lows, during periods of on-line host boiler operation.

Test Facility Inlet Gas Temperature (° F)

1995

Date	Average	High	Low
Jan. - Mar.	666	687	627
Apr. - July	664	686	636

Each reactor is equipped with a flue gas heater which maintains strict control over the temperature of the flue gas entering the reactors. Under normal operating conditions the flue gas is maintained at 700°F at the entrance to the reactors. This requires that the gas be heated from approximately 650°F to 700°F under normal operating conditions. Of course, heat loss in the system requires some additional flue gas heating over the 50°F temperature difference noted. Under parametric conditions, the flue gas temperature to the reactors is varied from a low of approximately 620°F to a high of 750°F. Under these conditions, the economizer bypass duct flow rate may be adjusted to assist the heaters in obtaining the appropriate temperature. Under high temperature parametric conditions, heat loss through the system is more apparent, and flue

gas temperatures of 780°F just downstream of the heater may be required to give 750°F at the reactor inlet. Lower temperature parametric conditions do not show as extreme a temperature loss between the heaters and the inlet to the reactors. As a result, the heater exit temperature is normally much closer to the reactor inlet gas temperature during low temperature parametric tests and normal operating conditions.

- Air Preheater Performance Data

The three large reactors of the SCR facility are each equipped with an air preheater. Reactor A is equipped with a two layer Ljungstrom® type rotary air preheater supplied by ABB Air Preheater, Inc. of Wellsville, New York. Reactor B is equipped with a three layer Ljungstrom® type rotary air preheater nearly identical to the A preheater, also supplied by ABB. Reactor C is equipped with an ABB Q-pipe which is a heat pipe design utilizing toluene and naphthalene as the working fluids. The original design of the SCR facility included air preheater bypass ducting which allowed the air preheaters to be bypassed during any condition other than normal operating conditions. This was done to insure that the air preheater's long-term fouling characteristics were not skewed by extreme conditions during some of the short term parametric tests. The large reactor fan design requires relatively cool gas (less than 350°F). To accommodate this restriction, the air preheater bypass ducting was equipped with heat exchangers which were designed to cool the flue gas in place of the air preheaters. Unfortunately, the design of the by-pass heat exchangers caused immediate fouling upon use, making them unsatisfactory for the application. Consequently, the SCR facility is forced to use the three large reactor air preheaters at all times when on-line to maintain proper flue gas conditions for the large reactor fans. As a result, the air preheaters are exposed to the harsh conditions created by some of the parametric tests. However, these test periods are very short compared to the overall operating time at standard conditions, and it is assumed that overall fouling characteristics of the air preheaters are not greatly affected by the current operational requirements. Tables 3 and 4 show the average operating parameters for the three air preheaters over the reporting period shown. These values include any parametric test conditions that were performed during the specific time period.

Manual air preheater tests were not performed during this reporting period due to the limited operational period available. Priority was placed on completion of the fifth parametric test sequence on the test facility catalysts.

TABLE 3.

AVERAGE AIR PREHEATER OPERATIONAL PARAMETERS, JAN.-MAR. 1995

PARAMETER	APH A	APH B	APH C
GAS FLOW RATE (SCFM)	4972	4954	4967
AIR FLOW RATE (SCFM)	3914	3716	6396
INLET GAS TEMP. (°F)	662	669	670
EXIT GAS TEMP. (°F)	299	299	320
INLET AIR TEMP. (°F)	69	69	69
EXIT AIR TEMP. (°F)	572	583	423
GAS SIDE PRESS. DROP ("H_2O)	5.68	8.48	9.02
AIR SIDE PRESS. DROP ("H_2O)	2.29	3.30	NA
AIR/GAS DIFF. PRESS. ("H_2O)	0.51	0.52	NA
INLET GAS O_2 (% WET)	4.95	5.86	5.55
EXIT GAS O_2 (% WET)	8.30	9.26	NA

TABLE 4.

AVERAGE AIR PREHEATER OPERATIONAL PARAMETERS, APR. - JULY 1995

PARAMETER	APH A	APH B	APH C
GAS FLOW RATE (SCFM)	5540	5128	5233
AIR FLOW RATE (SCFM)	4109	4565	10166
INLET GAS TEMP. (°F)	667	671	665
EXIT GAS TEMP. (°F)	300	300	300
INLET AIR TEMP. (°F)	97	97	97
EXIT AIR TEMP. (°F)	584	520	345
GAS SIDE PRESS. DROP ("H_2O)	5.96	4.34	6.60
AIR SIDE PRESS. DROP ("H_2O)	2.70	2.04	NA
AIR/GAS DIFF. PRESS. ("H_2O)	0.52	0.53	NA
INLET GAS O_2 (% WET)	5.01	5.62	6.57
EXIT GAS O_2 (% WET)	9.23	10.19	NA

- Special Ammonia Impacts Study

A special study was conducted to evaluate the characteristics of ammonia volatilization, ammonia extraction, and metals extraction to determine any adverse effects on fly ash that may be present related to the application of SCR technology. Appendix A contains the final report from Southern Research Institute concerning this study. A summary of the results is shown below.

Ammonia Extractability and Volatilization from SCR Fly Ash

Almost no ammonia volatilized from the SCR ash until a significant amount of water vapor was absorbed by the ash. A plausible mechanism for the apparent volatilization that occurred is than enough water was gained by the ash to form a moist layer with a pH high enough to evolve gas-phase ammonia from the ammonium compounds on the ash. Nearly all of the ammonia on the ash evolved to the gas phase in the closed-container experiments. Ammonia concentrations in enclosed spaces depend on the ammonia concentration of the ash, the volume of air above the ash available for dilution, and the presence of a humid atmosphere.

The extraction of ammonia from fly ash seems to depend upon pH. Evidently, all or nearly all of the ammonia present was extracted in a buffered solution at pH 4.7 and pH 6.2, but not all was recovered in alkaline unbuffered extracts. In the pH 6.2 buffer, however, the completeness of extraction seemed to fall off somewhat as the ratio of ash to buffer increased. At 3 g of ash per 50 ml of pH 6.32 buffer, the amount of ammonia extracted was about 200 μg/g whereas at 1 g per 50 ml, the amount was near 250 μg/g.

Ammonia concentration in the ash was much higher for the smaller particle sizes, but most of the total ammonia was found to reside with the larger particles simply because these comprise the vast majority of the ash mass. The implication is that very little slip ammonia will exit the process in the gas phase when high efficiency particulate emission controls are in place since all detectable ammonia is in the solid phase at the air heater exit and most of the ammonia is associated with the larger particle sizes which are most readily collected.

Metals Extractability from SCR Fly Ash

The SCR fly ash samples were subjected to extraction with water, and the extracts were analyzed for each of 28 metals. This was done to ascertain whether exposure of the fly ash to ammonia vapor caused an enhancement of the metals extractabilities under conditions resembling those that might exist in an ash pond.

Of the 28 metal included in the study, only 17 could be detected in the fly-ash extracts. Of these 17 detectable metals, only barium underwent an increase in extractability following exposure to ammonia. The magnitude of the increase was found to depend directly on the magnitude of the NH_3/NO_x ratios tested. Of the 16 additional metals that could be detected in the fly-ash extracts, none displayed what was considered to be a genuine enhancement in extractability, and several exhibited deceases in extractability as a result of exposure of the fly ash to ammonia. Finally, a deliberate downward adjustment in the pH of one sample solution caused enhancements in the extractabilities of several metals, most notably Mg, but also Mn, Ca, As and Fe to a lesser degree.

- Catalyst-Specific Performance Parameters

The long term NO_x reduction and parametric test results characterizing the performance for Reactors A - J for this reporting period are discussed in the following sections. The parametric tests were composed of fifteen reactor operating conditions defined by variations in the flue gas flow rate, temperature, and NH_3/NO_x ratio. The test conditions for the fifth parametric sequence are shown in Table 5. The particular measurements that were performed (intermediate ammonia, slip ammonia, SO_2, SO_3, HCl, N_2O, and velocity and mass concentration profiles) are also shown in this table at the various test conditions. Although similar test conditions may be indicated, measurements were not taken simultaneously (e.g., ammonia and SO_2 data for the same conditions were not collected during the exact same test run, but rather under similar process conditions at different times).

TABLE 5. PARAMETRIC TEST CONDITIONS (5th Sequence)

Flue gas flow rate Large / Small reactor	Flue gas temperature	NH_3/NO_x Ratio	Measurements
KSCFM	°F		
3.0 / 0.24	620	0.8	slip NH_3
5.0 / 0.40	620	0.8	intermediate & slip NH_3
7.5 / 0.60	620	1.0	slip NH_3
5.0 / 0.40	750	0.8	intermediate & slip NH_3
7.5 / 0.60	700	0.8	intermediate & slip NH_3
5.0 / 0.40 (design conditions)	750	0.8	intermediate & slip NH_3, SO_2/SO_3 HCl Concentration (Reactor A only), velocity profile, N_2O
3.0 / 0.24	700	0.8	intermediate NH_3
5.0 / 0.40	700	0.6	intermediate & slip NH_3
5.0 / 0.40	700	1.0	intermediate & slip NH_3
5.0 / 0.40	620	0.6	slip NH_3
5.0 / 0.40	620	1.0	slip NH_3
7.5 / 0.60	700	0.6	slip NH_3
7.5 / 0.60	700	1.0	slip NH_3
5.0 / 0.40	750	0.6	slip NH_3
5.0 / 0.40	750	1.0	slip NH_3

- Reactor Pressure Drops

Overall reactor pressure drops (inlet to outlet, including dummy layer and all catalysts) are shown in Figure 3 for Reactors A - J during January through March and in Figure 4 for Reactors A - J for April through July, 1995. The plots only show data for which the test facility was operating. Thus, roughly only one month of facility operation is depicted on each plot. Figure 3, presenting data acquired prior to the host unit outage, shows a constant pressure drop over the period for nearly all reactors. Reactor J (Cormetech, low-dust) is somewhat more erratic due to the propensity for large particulate matter to collect on the catalyst screens. This phenomenon was described in previous reports. Figure 4 presents data collected after the host unit outage and is

similar to that shown in Figure 3. A steady increase in pressure drop is noted across reactor J, likely due to the build-up of large particulate matter on the catalyst screens. Reactor H (Cormetech, high-velocity) shows initially a very high pressure drop. This was due to particulate matter fouling the catalyst screens early in the operation of this reactor (reactor restarted mid-May, 1995). This particulate matter was likely the result of the extended shut-down period for this reactor. Cleaning of the reactor after the initial fouling episode reduced the overall pressure drop to levels in keeping with the other test facility reactors.

FIGURE 3

PRESSURE DROP VS. TIME

1st QUARTER 1995

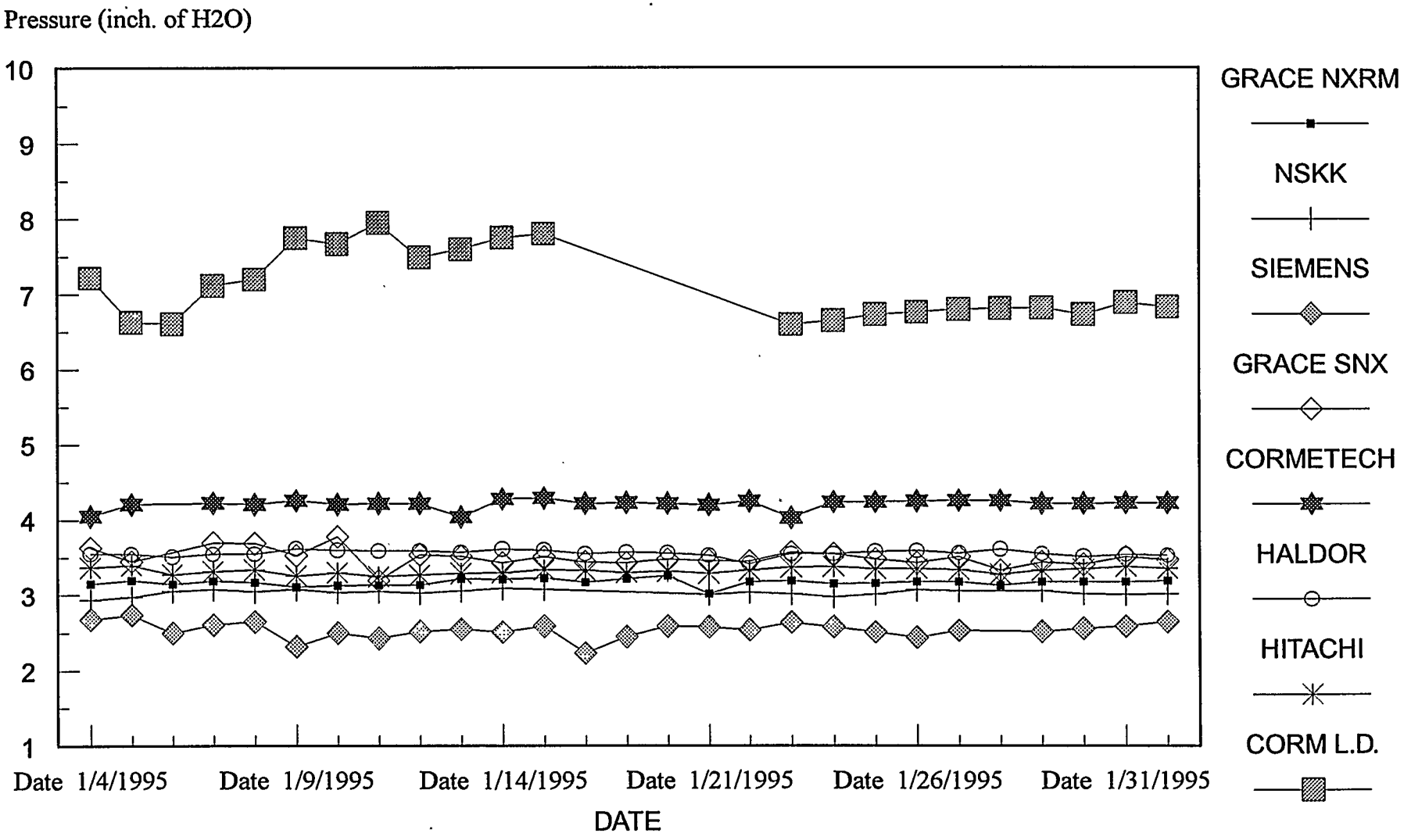

FIGURE 4

PRESSURE DROP VS. TIME

2nd QUARTER 1995

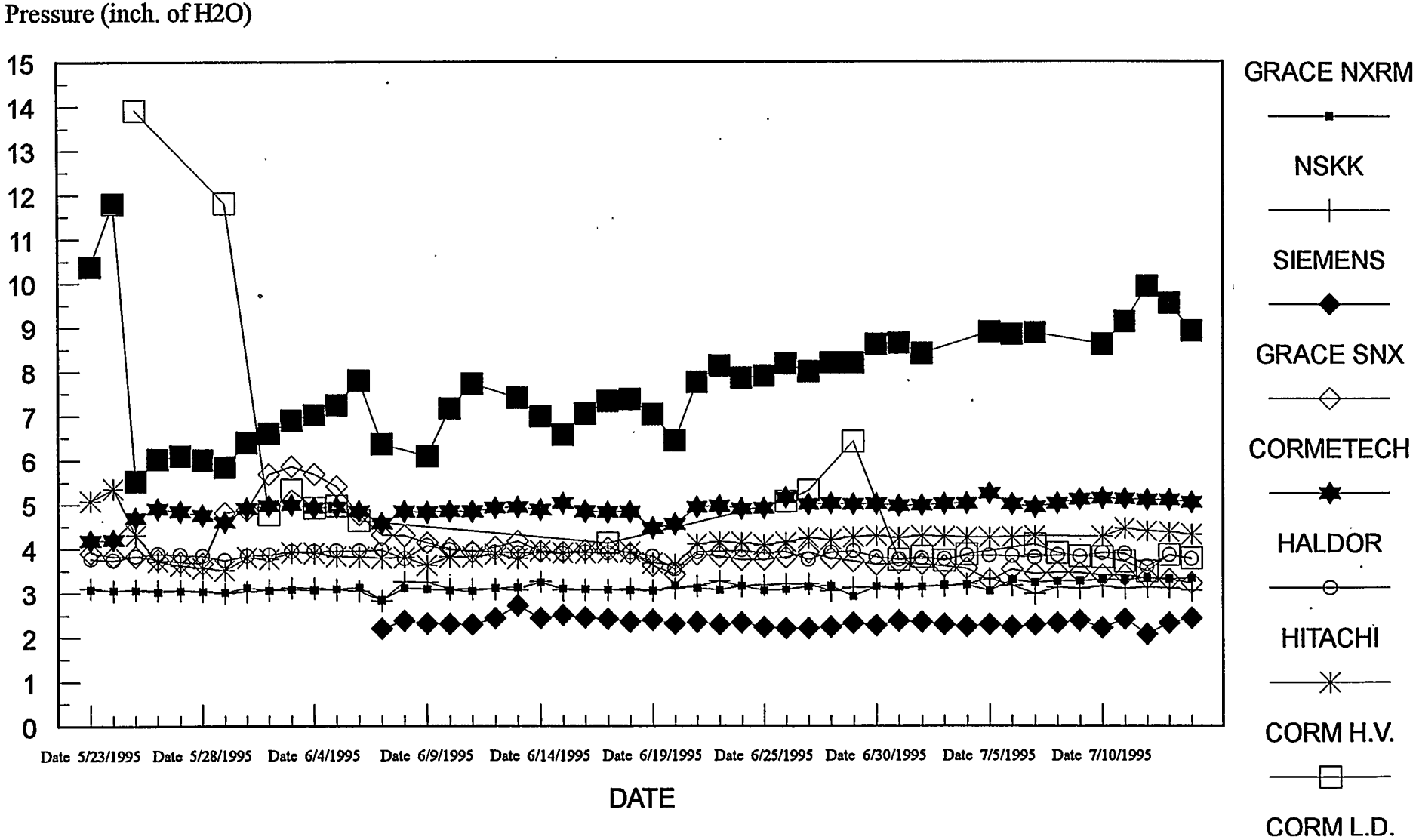

- Reactor A

Table 6 shows the test data for the fifth parametric sequence for intermediate ammonia, slip ammonia, and sulfur dioxide oxidation collected during this reporting period for the Grace Noxeram catalyst. All the ammonia data are corrected to reactor inlet oxygen concentration. The long term NO_x reduction is also given in this table as an average over the operating periods shown, i.e., for January through March and April through July of 1995. The long term NO_x reduction data indicates the average performance of the catalyst at or near the design operating conditions of 0.8 NH_3/NO_x ratio, 5000 SCFM flow rate, and 700 °F reactor temperature. As can be noted in the both quarter data averages, analytical errors and drift in calibrations led to values falsely indicating NO_x reduction being higher than the NH_3/NO_x ratio.

The intermediate ammonia measurements were made after the first catalyst bed and at conditions thought to give the best kinetic information. The NO_x removals reported with the intermediate ammonia measurements are computed from the measured ammonia concentration using standard material balance techniques.

The ammonia slip data given in Table 6 are presented below in three plots: ammonia slip versus each of flow rate, NH_3/NO_x ratio, and temperature. Figure 5 shows ammonia slip versus flow rate for roughly 90% NO_x reduction and 630 °F. As expected, the trend shows increasing ammonia slip with increasing reactor flow rate. The ammonia slip is, however, relatively minor indicating the ability of the catalyst design to withstand significant increases in flow while maintaining ammonia slip limits. Since a portion of the overall reaction rate is due to mass transfer limitations, improvements in bulk mass transfer coefficients are likely mitigating the effect of increased flow on slip ammonia increases. This plot demonstrates the ability of an SCR system to follow load variations dictated by the host boiler while maintaining design specifications.

Figure 6 shows ammonia slip versus NH_3/NO_x ratio at low temperature and design flow rate. The plot shows sharp increases in ammonia slip as the NH_3/NO_x ratio approaches 1.0. This finding is in keeping with published data of this type. At NH_3/NO_x ratios near 1.0, non-idealities in the reactor system force the catalyst to slip higher concentrations of ammonia since areas are present in the reactor where NO_x is the limiting reagent.

Ammonia slip versus temperature for design flow and roughly 60% NO_x reduction is plotted in Figure 7. The trend of the plot is unclear since all values were below the ammonia slip detection limit.

SO_2 oxidation at design temperature and flow rate was 0.55%. The SO_2 oxidation data is corrected to reactor outlet oxygen concentrations. The value for sulfur trioxide produced in the reactor is based on measured inlet and outlet sulfur trioxide concentration values (table showing SO_2 oxidation rate quotes reactor flow rate as calculated for the reactor exit, since outlet SO_3 is measured at this point).

Flue gas velocity (nine-point) profiles were conducted near design operating conditions (700 °F, 5000 SCFM) at the reactor inlet and reactor outlet. The flue gas velocity profiles are presented in Figure 8 (reactor inlet) and Figure 9 (reactor outlet). The average inlet and outlet velocities were 14.1 ± 1.6 ft/sec and 11.7 ± 2.1 ft/sec, respectively.

HCl concentration (at 3% O_2, dry) was measured at the design operating conditions before the point of ammonia injection (184 ± 6 ppmv), at the reactor inlet (132 ± 8 ppmv), and at the reactor outlet (86 ± 16 ppmv). The N_2O concentrations were also measured at the reactor inlet (2.0 ppmv) and at the reactor outlet (1.6 ppmv, both measurements are dry at 3% O_2).[1]

TABLE 6. REACTOR A DATA (5th Sequence)

INTERMEDIATE AMMONIA PARAMETRIC TEST DATA

FLOW RATE (SCFM)	TEMP. (°F)	INLET O_2 (%)	INLET NO_x (ppmv)	NH_3/NO_x RATIO	INT. NH_3 (ppmv)	INT. NO_x REDUCTION (%)
5671	637	4.673	286	0.744	19.6	67.6
3394	704	4.353	293	0.748	3.6	73.6
5705	706	4.537	290	0.557	8.5	52.8
5462	706	5.668	275	0.761	13.0	71.3
5654	706	5.651	338	0.934	37.0	82.5
6875	706	5.651	323	0.741	27.5	65.6
5580	757	4.986	297	0.753	14.6	70.4

SLIP AMMONIA PARAMETRIC TEST DATA

FLOW RATE (SCFM)	TEMP. (°F)	INLET O_2 (%)	INLET NO_x (ppmv)	NH_3/NO_x RATIO	SLIP NH_3 (ppmv)
3172	623	4.932	325	0.774	BDL
5282	624	5.646	328	0.581	BDL
5279	626	5.395	322	0.773	BDL
5823	637	4.800	311	0.919	1.3
6989	629	5.601	304	0.916	2.1
5250	705	6.108	302	0.585	BDL
5216	702	6.118	338	0.780	3.3
5803	706	4.931	317	0.923	BDL
6117	709	4.987	289	0.583	BDL
6015	703	5.939	230	0.580	BDL
6193	705	5.924	310	0.911	1.2
5392	757	8.803	294	0.575	BDL
5409	757	9.239	293	0.771	BDL
5829	756	4.873	301	0.920	1.3

TABLE 6. REACTOR A DATA (5TH SEQUENCE) - Continued

SULFUR DIOXIDE OXIDATION PARAMETRIC TEST DATA

FLOW RATE (SCFM)	TEMP. (°F)	OUTLET O_2 (%)	INLET SO_2 (ppmv)	NH_3/NO_x RATIO	MEAS. SO_3 IN (ppmv)	SO_3 OUT (ppmv)	SO_3 formed (ppmv)	OXID. RATE (%)
4781	705	4.037	1065	0.785	0.8	6.7	5.9	0.55

LONG TERM NO_x REDUCTION

TIME PERIOD	FLOW RATE (SCFM)	INLET NO_x (ppmv)	NH_3/NO_x RATIO	OUTLET NO_x (ppmv)	NO_x RED (%)
JAN. - MAR.	4974	404	0.79	48	88
APRIL - JULY	5540	340	0.76	61	80

FIGURE 5

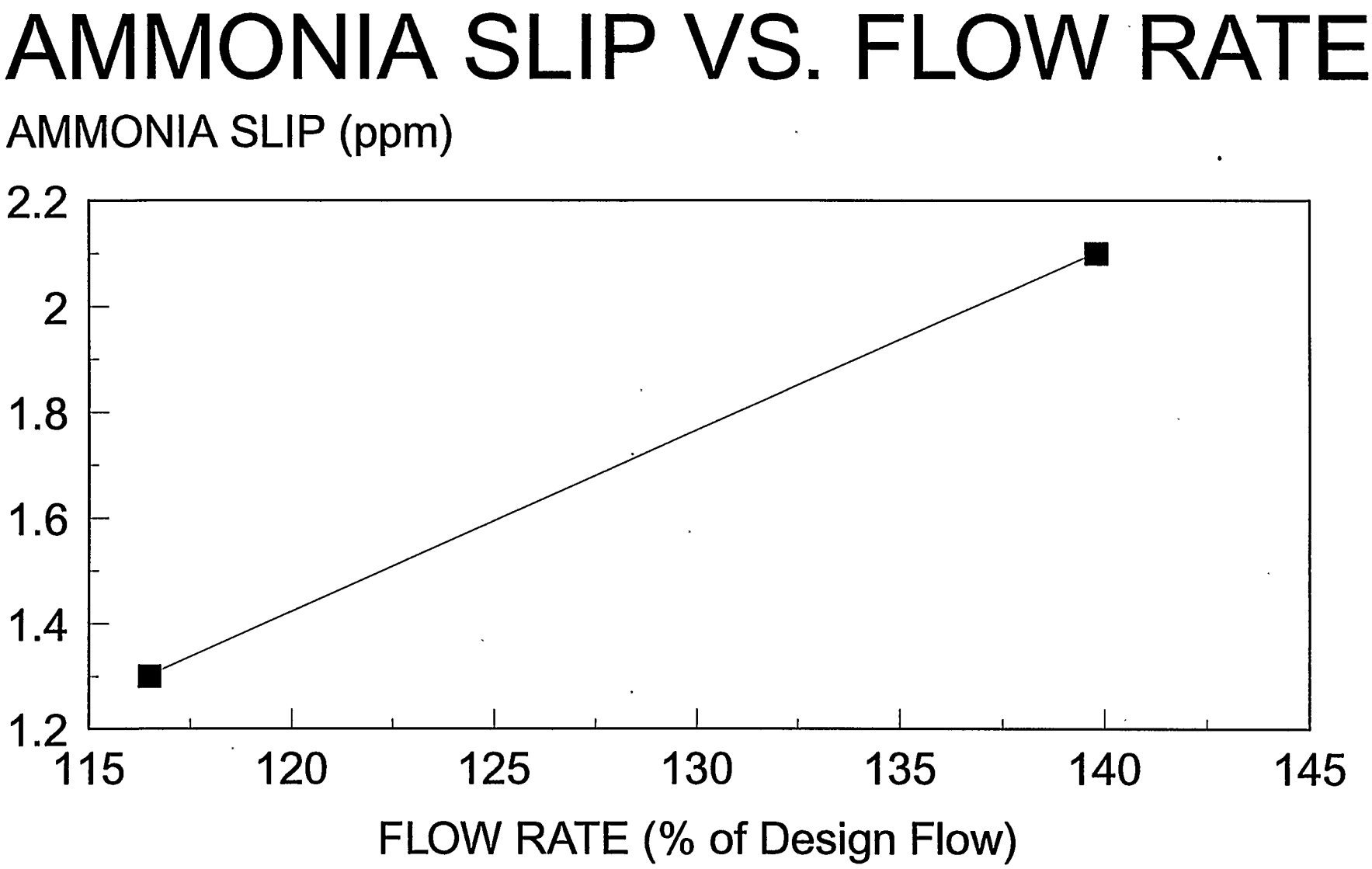
AMMONIA SLIP VS. FLOW RATE
AMMONIA SLIP (ppm)
2.2
2
1.8
1.6
1.4
1.2
115
120
125
130
135
140
145
FLOW RATE (% of Design Flow)
GRACE NXRM: NH3/NOx=0.90, 630 F

FIGURE 6

AMMONIA SLIP VS. NH3/NOx RATIO

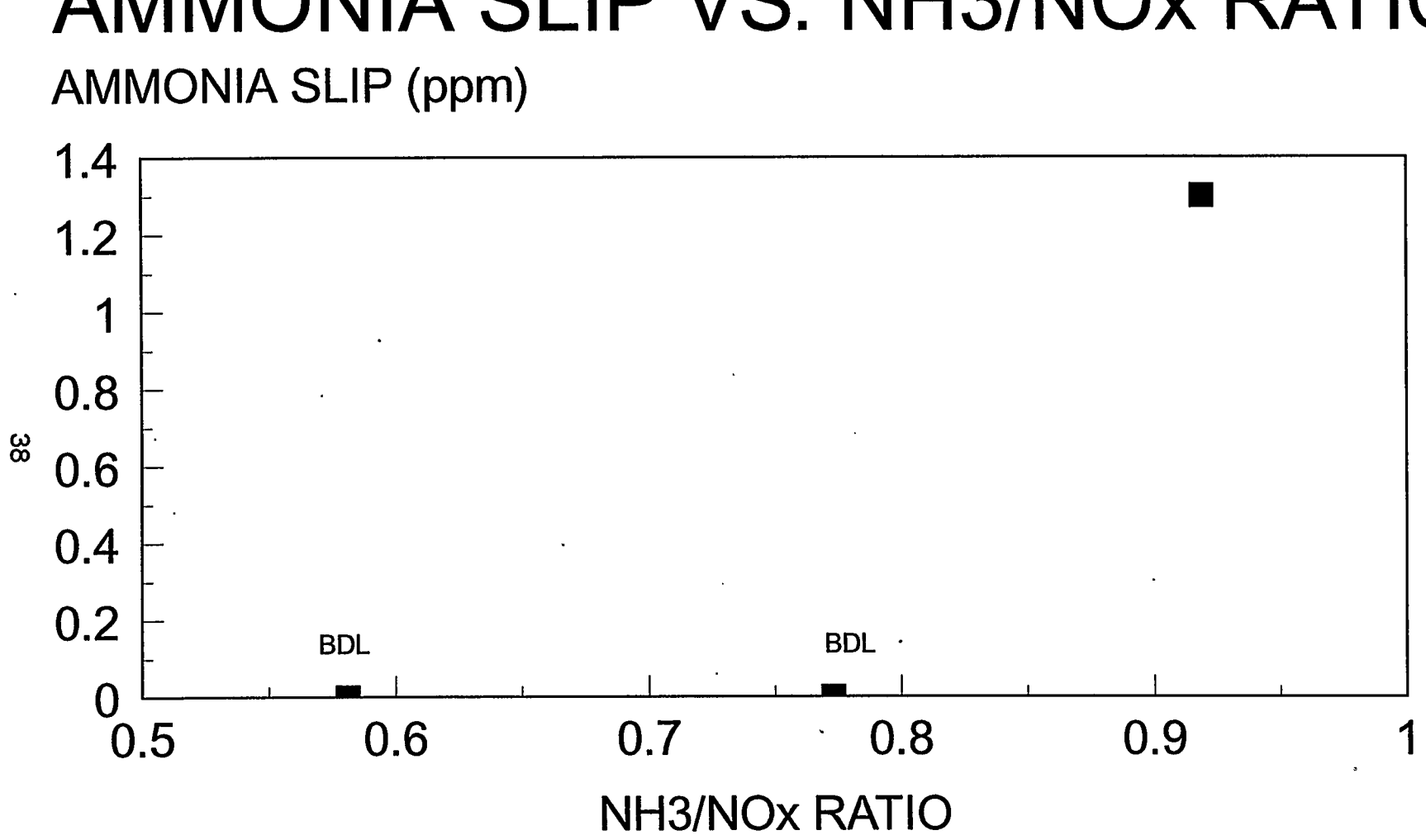

GRACE NXRM: Design Flow, 620 F

(BDL) Below lower detection limit of 0.7-0.9ppm

FIGURE 7

AMMONIA SLIP VS. TEMPERATURE

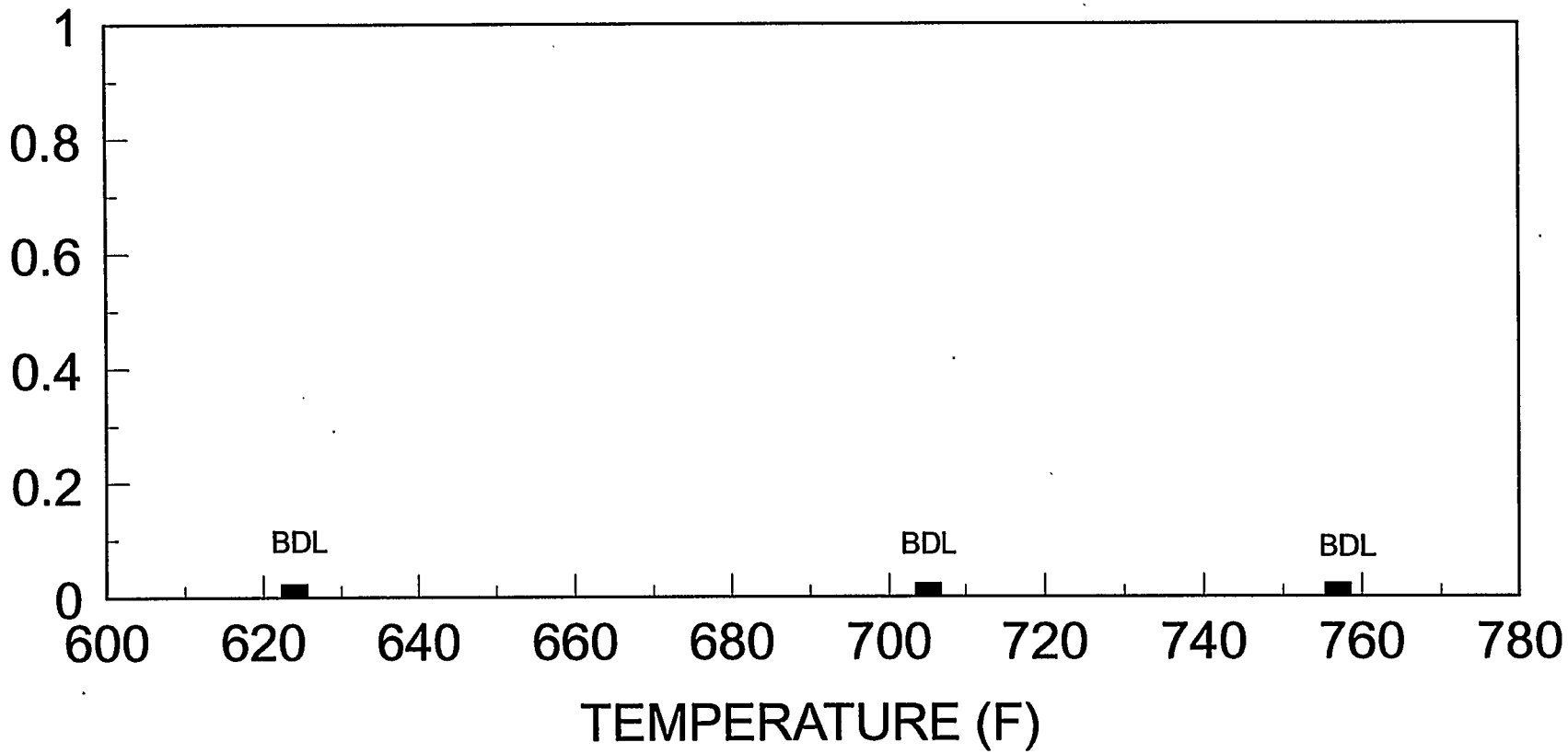

GRACE NXRM: Design Flow, NH3/NOx=0.60

(BDL) Below lower detection limit

FIGURE 8

REACTOR A

CATALYST LAYER 1 INLET

Velocity Profile
ft/s

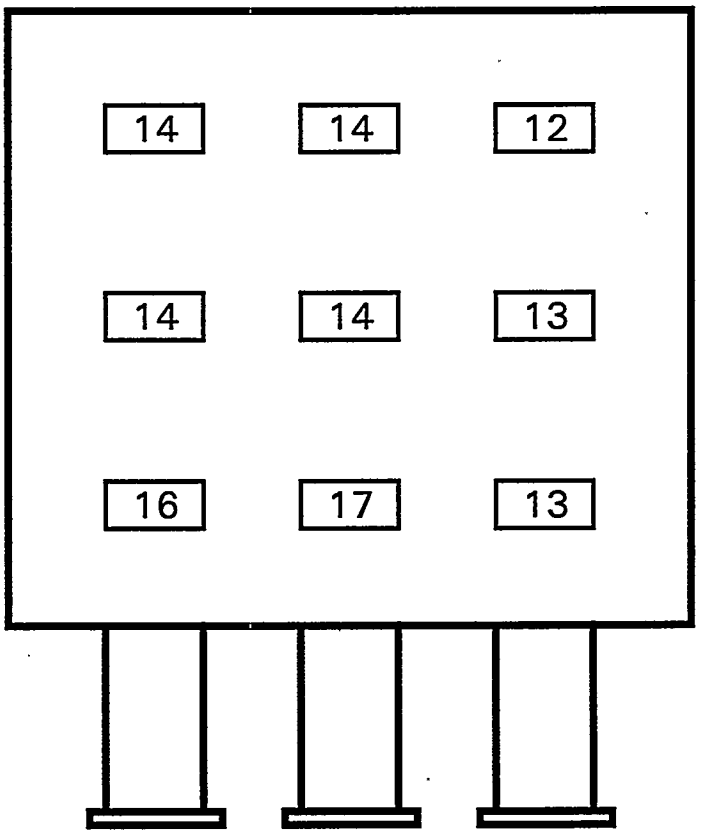

Average = 14 ft/s
σ = 2 ft/s

FIGURE 9

REACTOR A
REACTOR EXIT

Velocity Profile
ft/s

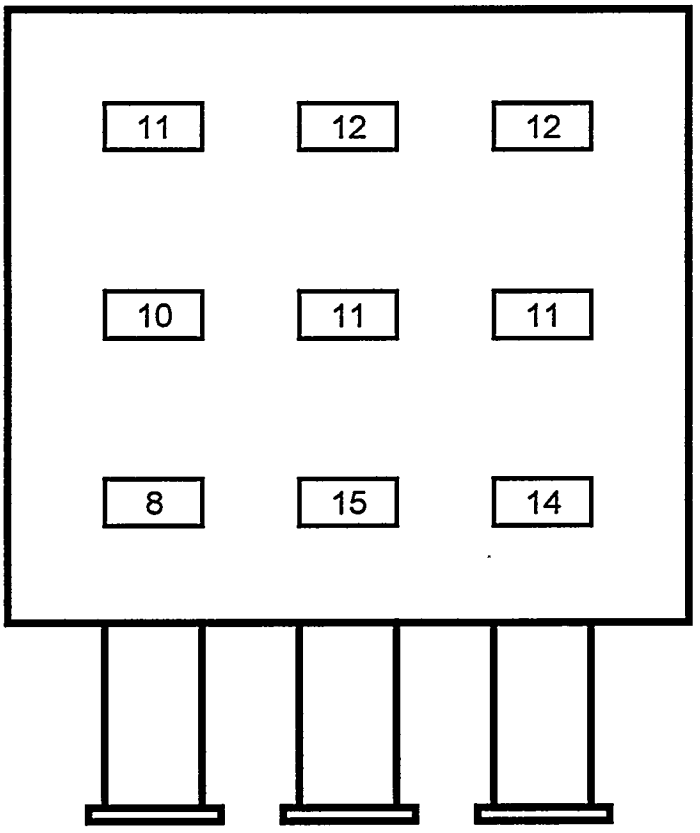

Average = 12 ft/s
σ = 2 ft/s

- Reactor B

Table 7 shows the parametric test data on intermediate ammonia, slip ammonia, and sulfur dioxide oxidation collected during this reporting period for the NSKK catalyst. All the ammonia data are corrected to reactor inlet oxygen concentration. The long term NO_x reduction is also given in this table as an average over the operating periods shown, i.e., for January - March and April - July of 1995. The long term NO_x reduction data indicates the average performance of the catalyst at or near the design operating conditions of 0.8 NH_3/NO_x ratio, 5000 SCFM flow rate, and 700 °F reactor temperature. As can be noted in the both quarter data averages, analytical errors and drift in calibrations led to values falsely indicating NO_x reduction being higher than the NH_3/NO_x ratio.

The intermediate ammonia measurements were made after the first catalyst bed and at conditions thought to give the best kinetic information. The NO_x removals reported with the intermediate ammonia measurements are computed from the measured ammonia concentration using standard material balance techniques.

The ammonia slip data given in Table 7 are presented below in three plots: ammonia slip versus each of flow rate, NH_3/NO_x ratio, and temperature. Figure 10 shows ammonia slip versus flow rate for roughly 100% NO_x reduction and 700 °F. As expected, the trend shows increasing ammonia slip with increasing reactor flow rate. The ammonia slip is, however, relatively minor indicating the ability of the catalyst design to withstand significant increases in flow while maintaining ammonia slip limits. Since a portion of the overall reaction rate is due to mass transfer limitations, improvements in bulk mass transfer coefficients are likely mitigating the effect of increased flow on slip ammonia increases. This plot demonstrates the ability of an SCR system to follow load variations dictated by the host boiler while maintaining design specifications.

Figure 11 shows ammonia slip versus NH_3/NO_x ratio at design temperature and flow rate. The plot shows sharp increases in ammonia slip as the NH_3/NO_x ratio approaches 1.0. This finding is in keeping with published data of this type. At NH_3/NO_x ratios near 1.0, non-idealities in the reactor system force the catalyst to slip higher concentrations of ammonia since areas are present in the reactor where NO_x is the limiting reagent.

Ammonia slip versus temperature for design flow and roughly 100% NO_x reduction is plotted in Figure 12. Some improvement (decrease) in ammonia slip is noted between 620 and 700 °F, likely due to improvements in the kinetic reaction rate with increasing temperature. The slight

increase in ammonia slip between 700 and 750 °F is likely due to measurement variability and is not considered significant. In this case the data should not be construed as demonstrating increases in ammonia slip with increasing temperature above 700 °F. It is expected that the 700 and 750 °F values are roughly equivalent which may be due in part to mass transfer limitations that have become controlling at these higher temperatures. In general, the plot demonstrates that in terms of ammonia slip, significant improvements are not realized with temperature above 700 °F. Losses in boiler efficiency would probably outweigh any improvement that may be obtained in ammonia slip by designing an SCR reactor to operate at a temperature near 700 °F.

SO_2 oxidation at design temperature and flow rate was 0.01%. The SO_2 oxidation data is corrected to reactor outlet oxygen concentrations. The value for sulfur trioxide produced in the reactor is based on measured inlet and outlet sulfur trioxide concentration values (table showing SO_2 oxidation rate quotes reactor flow rate as calculated for the reactor exit, since outlet SO_3 is measured at this point).

Flue gas velocity (nine-point) profiles were conducted near design operating conditions (700 °F, 5000 SCFM) at the reactor inlet and reactor outlet. The flue gas velocity profiles are presented in Figure 13 (reactor inlet) and Figure 14 (reactor outlet). The average inlet and outlet velocities were 13.2 ± 1.8 ft/sec and 13.0 ± 1.6 ft/sec, respectively. The N_2O concentrations were also measured at the reactor inlet (2.0 ppmv) and at the reactor outlet (1.6 ppmv, both measurements are dry at 3% O_2).[1]

TABLE 7. REACTOR B DATA (5th Sequence)

INTERMEDIATE AMMONIA PARAMETRIC TEST DATA

FLOW RATE (SCFM)	TEMP. (°F)	INLET O_2 (%)	INLET NO_x (ppmv)	NH_3/NO_x RATIO	INT. NH_3 (ppmv)	INT. NO_x REDUCTION (%)
5191	627	4.687	349	0.797	46.9	66.3
3121	707	4.851	347	0.794	10.9	76.3
5200	706	3.761	308	0.596	19.1	53.5
5155	703	4.040	305	0.797	32.3	69.1
5205	707	3.678	302	0.992	45.3	84.2
6750	707	3.718	304	0.795	40.3	66.3
5164	753	6.275	296	0.879	26.2	79.1

SLIP AMMONIA PARAMETRIC TEST DATA

FLOW RATE (SCFM)	TEMP. (°F)	INLET O_2 (%)	INLET NO_x (ppmv)	NH_3/NO_x RATIO	SLIP NH_3 (ppmv)
3046	621	4.880	310	0.797	BDL
5067	626	3.918	354	0.598	BDL
5085	625	3.896	347	0.795	BDL
5241	626	4.239	331	0.993	2.0
6501	629	4.035	336	0.992	5.1
5068	705	6.158	238	0.593	BDL
5074	704	6.097	337	0.789	BDL
5230	706	4.129	329	0.994	1.1
6148	709	3.795	328	0.598	BDL
6133	709	5.297	320	0.798	BDL
6298	707	4.448	343	0.991	2.2
5096	756	4.091	343	0.597	BDL
5121	757	5.723	364	0.793	BDL
5228	756	3.325	318	0.997	1.4

TABLE 7. REACTOR B DATA (5TH SEQUENCE) - Continued

SULFUR DIOXIDE OXIDATION PARAMETRIC TEST DATA

FLOW RATE (SCFM)	TEMP. (°F)	OUTLET O_2 (%)	INLET SO_2 (ppmv)	NH_3/NO_x RATIO	MEAS. SO_3 IN (ppmv)	SO_3 OUT (ppmv)	SO_3 formed (ppmv)	OXID. RATE (%)
5190	706	5.390	1046	0.798	0.3	0.5	0.2	0.01

LONG TERM NO_x REDUCTION

TIME PERIOD	FLOW RATE (SCFM)	INLET NO_x (ppmv)	NH_3/NO_x RATIO	OUTLET NO_x (ppmv)	NO_x RED (%)
JAN. - MAR.	4954	399	0.79	32	89
APRIL - JULY	5128	338	0.80	51	83

FIGURE 10

AMMONIA SLIP VS. FLOW RATE

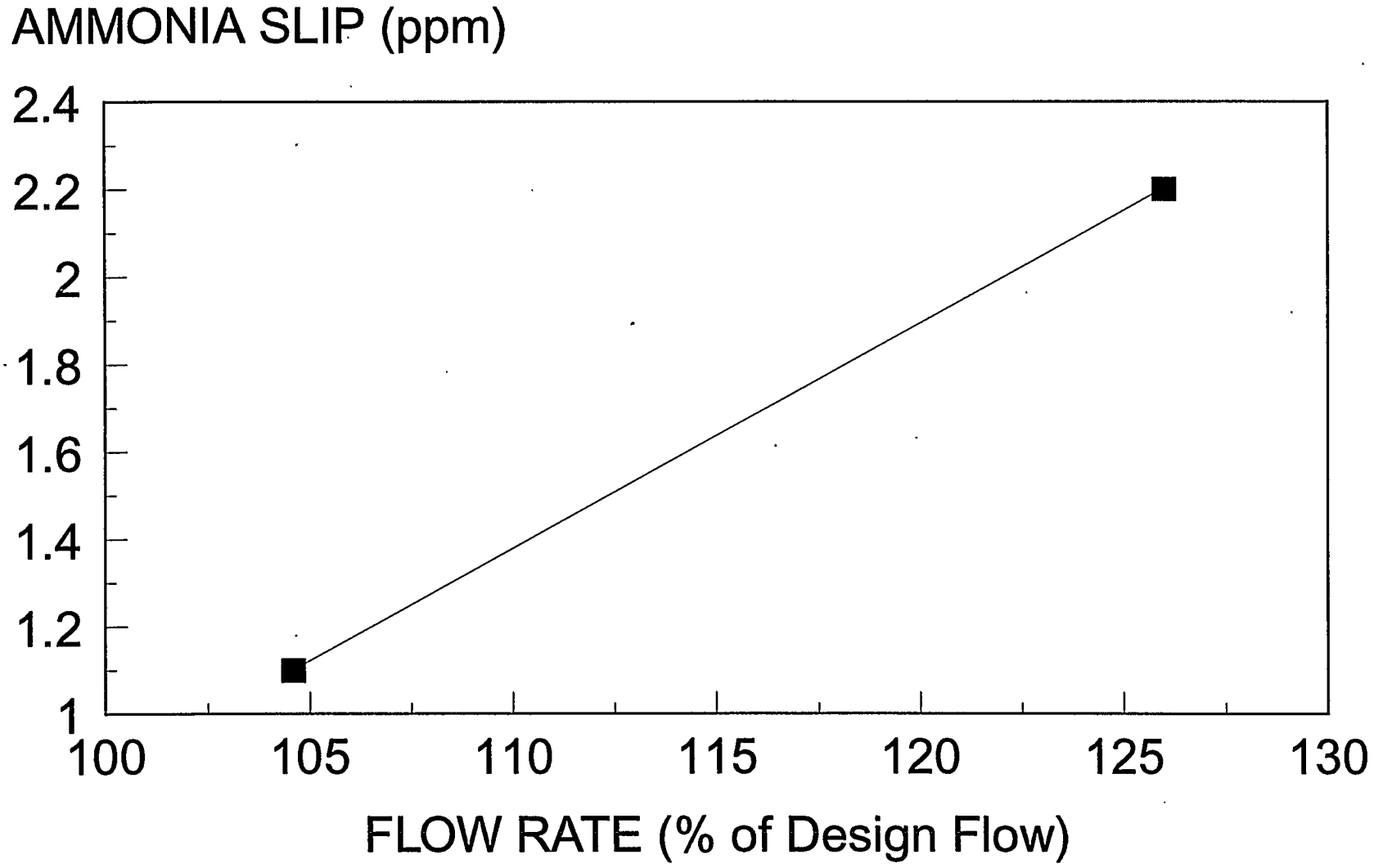

NSKK: NH3/NOx=1.00, 700 F

Figure 11

AMMONIA SLIP VS. NH3/NOx RATIO

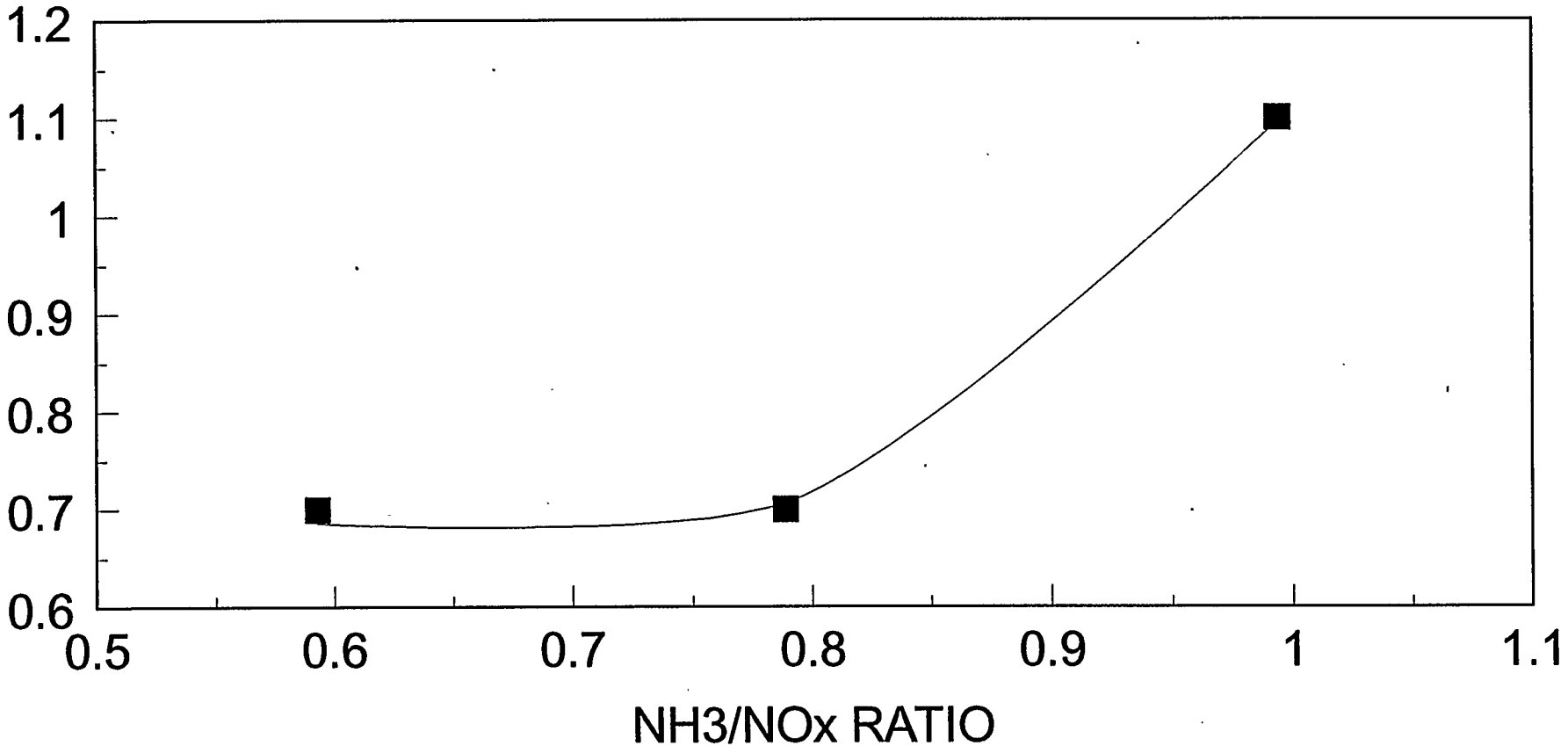

NSKK: Design Flow, 700 F

FIGURE 12

AMMONIA SLIP VS. TEMPERATURE

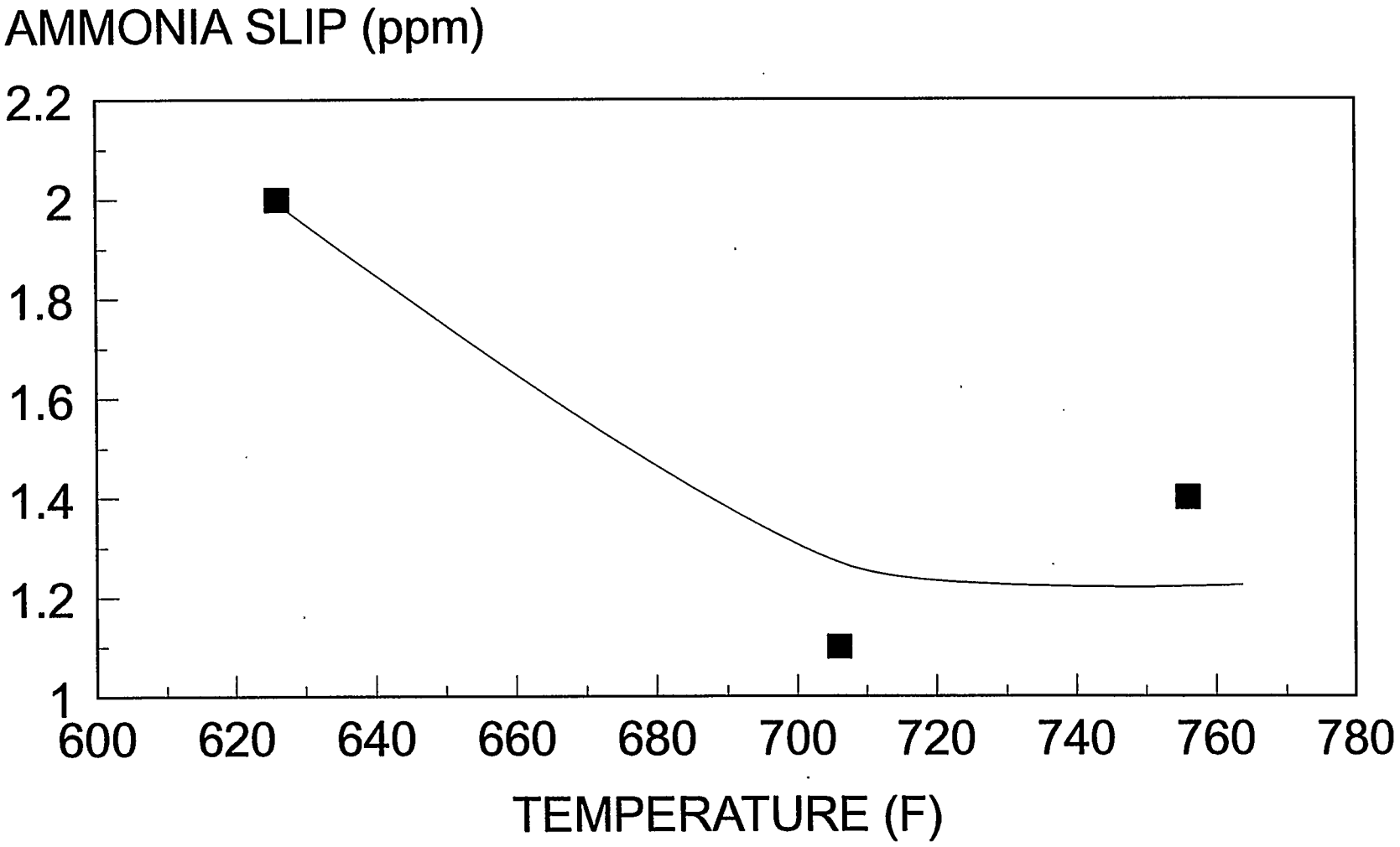

NSKK: Design Flow, NH3/NOx=1.00

FIGURE 13

REACTOR B

CATALYST LAYER 1 INLET

Velocity Profile
ft/s

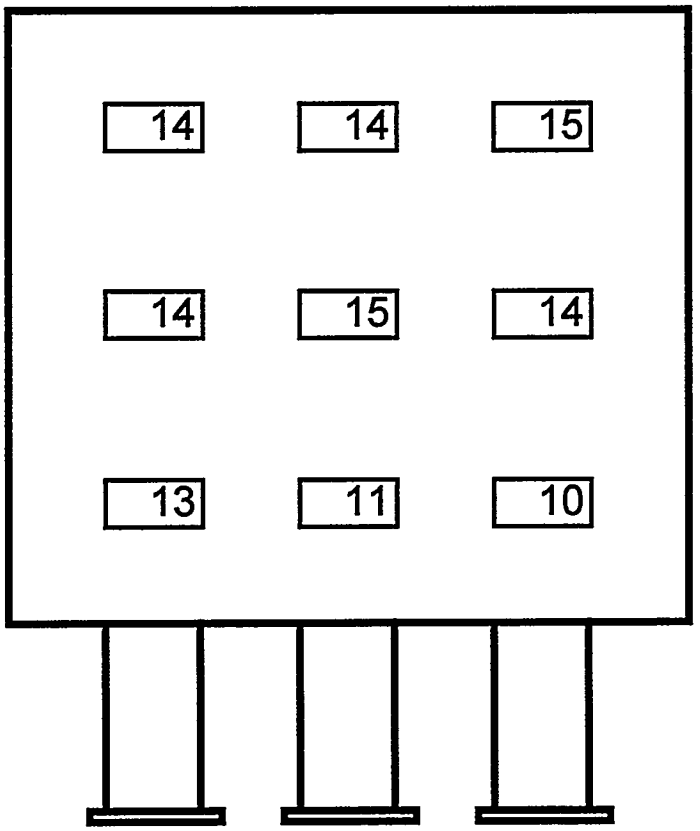

Average = 13 ft/s
σ = 2 ft/s

FIGURE 14

REACTOR B
REACTOR EXIT

Velocity Profile
ft/s

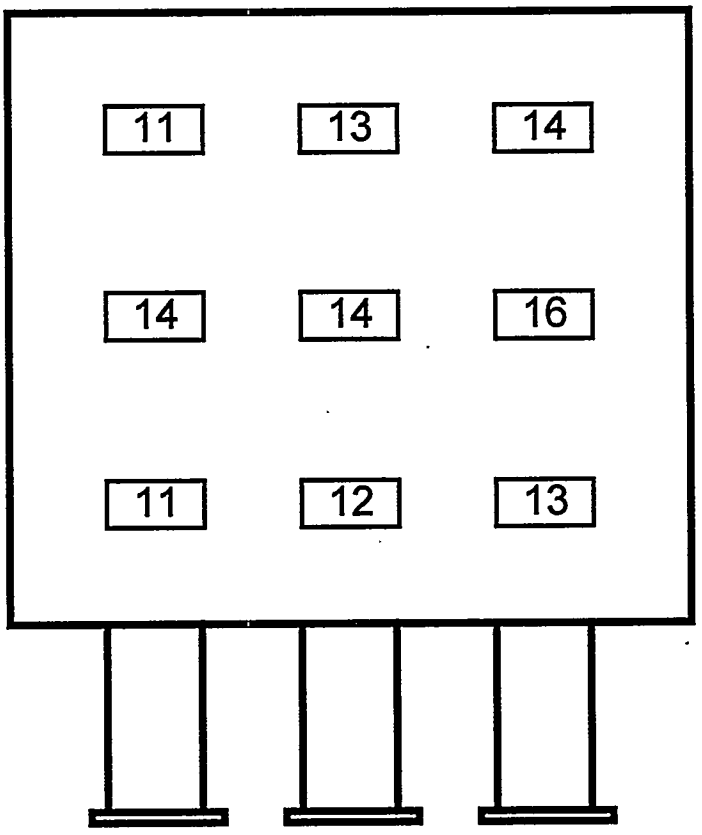

Average = 13 ft/s
σ = 2 ft/s

- Reactor C

Table 8 shows the parametric test data on intermediate ammonia, slip ammonia, and sulfur dioxide oxidation collected during this reporting period for the Siemens catalyst. All the ammonia data are corrected to reactor inlet oxygen concentration. The long term NO_x reduction is also given in this table as an average over the operating periods shown, i.e., for January - March and April - July of 1995. The long term NO_x reduction data indicates the average performance of the catalyst at or near the design operating conditions of 0.8 NH_3/NO_x ratio, 5000 SCFM flow rate, and 700°F reactor temperature. As can be noted in both quarter data averages, analytical errors and drift in calibrations led to values falsely indicating NO_x reduction being higher than the NH_3/NO_x ratio.

The intermediate ammonia measurements were made after the first catalyst bed and at conditions thought to give the best kinetic information. The NO_x removals reported with the intermediate ammonia measurements are computed from the measured ammonia concentration using standard material balance techniques.

The ammonia slip data given in Table 8 are presented below in three plots: ammonia slip versus each of flow rate, NH_3/NO_x ratio, and temperature. Figure 15 shows ammonia slip versus flow rate for roughly 60% NO_x reduction and 700 °F. As expected, the trend shows increasing ammonia slip with increasing reactor flow rate. The ammonia slip is, however, relatively minor indicating the ability of the catalyst design to withstand significant increases in flow while maintaining ammonia slip limits. Since a portion of the overall reaction rate is due to mass transfer limitations, improvements in bulk mass transfer coefficients are likely mitigating the effect of increased flow on slip ammonia increases. This plot demonstrates the ability of an SCR system to follow load variations dictated by the host boiler while maintaining design specifications.

Figure 16 shows ammonia slip versus NH_3/NO_x ratio at design temperature and flow rate. The plot shows a slight increase in ammonia slip as the NH_3/NO_x ratio increased from 0.6 to 0.8. This finding is in keeping with published data of this type.

Ammonia slip versus temperature for design flow and roughly 80% NO_x reduction is plotted in Figure 17. Some improvement (decrease) in ammonia slip is noted between 620 and 700 °F, likely due to improvements in the kinetic reaction rate with increasing temperature. The slight increase in ammonia slip between 700 and 750 °F points is likely due to measurement variability and is not considered significant. In this case the plot should not be construed as demonstrating

increases in ammonia slip with increasing temperature above 700 °F. It is expected that the 700 and 750 °F values are roughly equivalent which may be due in part to mass transfer limitations that have become controlling at these higher temperatures. In general, the plot demonstrates that in terms of ammonia slip, significant improvements are not realized with temperatures above 700°F. Losses in boiler efficiency would probably outweigh any improvements that may be obtained in ammonia slip by designing an SCR reactor to operate at a temperature near 750 °F.

SO_2 oxidation at design temperature and flow rate was 0.59%. The SO_2 oxidation data is corrected to reactor outlet oxygen concentrations. The value for sulfur trioxide produced in the reactor is based on measured inlet and outlet sulfur trioxide concentration values (table showing SO_2 oxidation rate quotes reactor flow rate as calculated for the reactor exit, since outlet SO_3 is measured at this point).

Flue gas velocity (nine-point) profiles were conducted near design operating conditions (700 °F, 5000 SCFM) at the reactor inlet and reactor outlet. The flue gas velocity profiles are presented in Figure 18 (reactor inlet) and Figure 19 (reactor outlet). The average inlet and outlet velocities were 15 ± 1 ft/sec and 13 ± 1 ft/sec, respectively. The N_2O concentrations were also measured at the reactor inlet (2.0 ppmv) and at the reactor outlet (1.6 ppmv, both measurements are dry at 3% O_2).[1]

TABLE 8. REACTOR C DATA (5TH SEQUENCE)

INTERMEDIATE AMMONIA PARAMETRIC TEST DATA

FLOW RATE (SCFM)	TEMP. (°F)	INLET O_2 (%)	INLET NO_x (ppmv)	NH_3/NO_x RATIO	INT. NH_3 (ppmv)	INT. NO_x REDUCTION (%)
5392	632	4.582	362	0.690	41.8	57.5
3240	703	4.578	346	0.692	16.7	64.3
5421	708	3.518	305	0.515	17.3	45.8
5181	708	3.727	307	0.749	31.4	64.7
5434	707	3.573	306	0.857	56.4	67.3
7072	706	3.522	325	0.683	52.6	52.1
5321	756	4.081	306	0.712	34.5	59.9

SLIP AMMONIA PARAMETRIC TEST DATA

FLOW RATE (SCFM)	TEMP. (°F)	INLET O_2 (%)	INLET NO_x (ppmv)	NH_3/NO_x RATIO	SLIP NH_3 (ppmv)
3073	624	6.150	357	0.763	BDL
5083	627	3.681	382	0.582	3.0
5075	626	3.617	380	0.776	12.0
5677	631	4.224	321	0.799	39.7
5668	623	4.240	339	0.798	40.1
5042	707	3.556	335	0.580	2.1
5048	707	3.294	334	0.787	5.0
5698	707	3.594	330	0.795	24.1
6902	707	4.223	342	0.591	5.6
6933	705	4.706	381	0.771	11.6
5604	708	4.074	342	0.648	29.9
5103	756	4.675	384	0.577	2.7
5103	756	4.463	385	0.770	5.4
5662	756	4.272	312	0.799	9.3

TABLE 8. REACTOR C DATA (5TH SEQUENCE) - Continued

SULFUR DIOXIDE OXIDATION PARAMETRIC TEST DATA

FLOW RATE (SCFM)	TEMP. (°F)	OUTLET O_2 (%)	INLET SO_2 (ppmv)	NH_3/NO_x RATIO	MEAS. SO_3 IN (ppmv)	SO_3 OUT (ppmv)	SO_3 formed (ppmv)	OXID. RATE (%)
5996	705	5.240	1027	0.676	1.1	7.1	6.0	0.59

LONG TERM NO_x REDUCTION

TIME PERIOD	FLOW RATE (SCFM)	INLET NO_x (ppmv)	NH_3/NO_x RATIO	OUTLET NO_x (ppmv)	NO_x RED. (%)
JAN. - MAR.	4967	410	0.79	32	89
APRIL - JULY	5233	345	0.71	42	85

FIGURE 15

AMMONIA SLIP VS. FLOW RATE

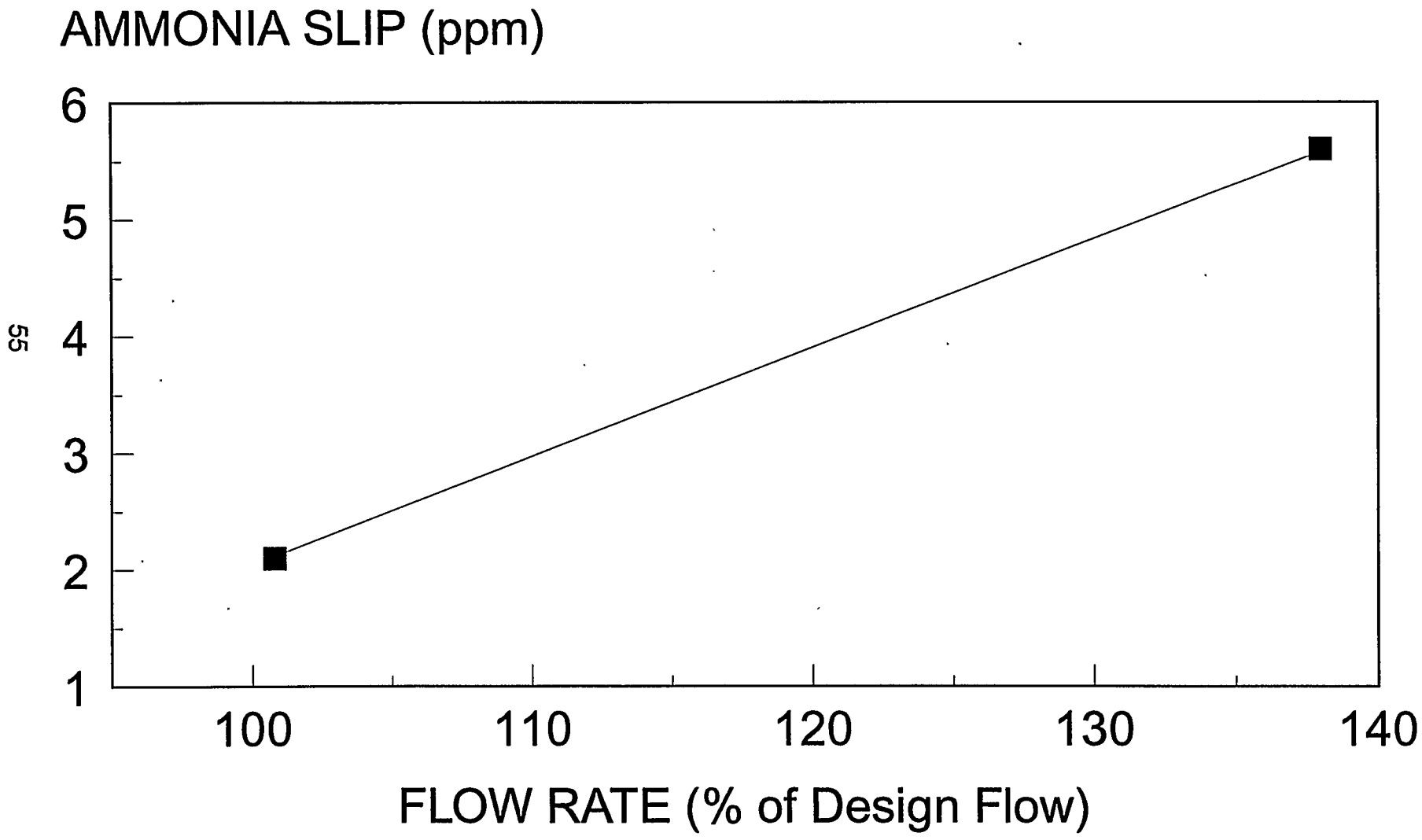

FIGURE 16

AMMONIA SLIP VS. NH3/NOx RATIO

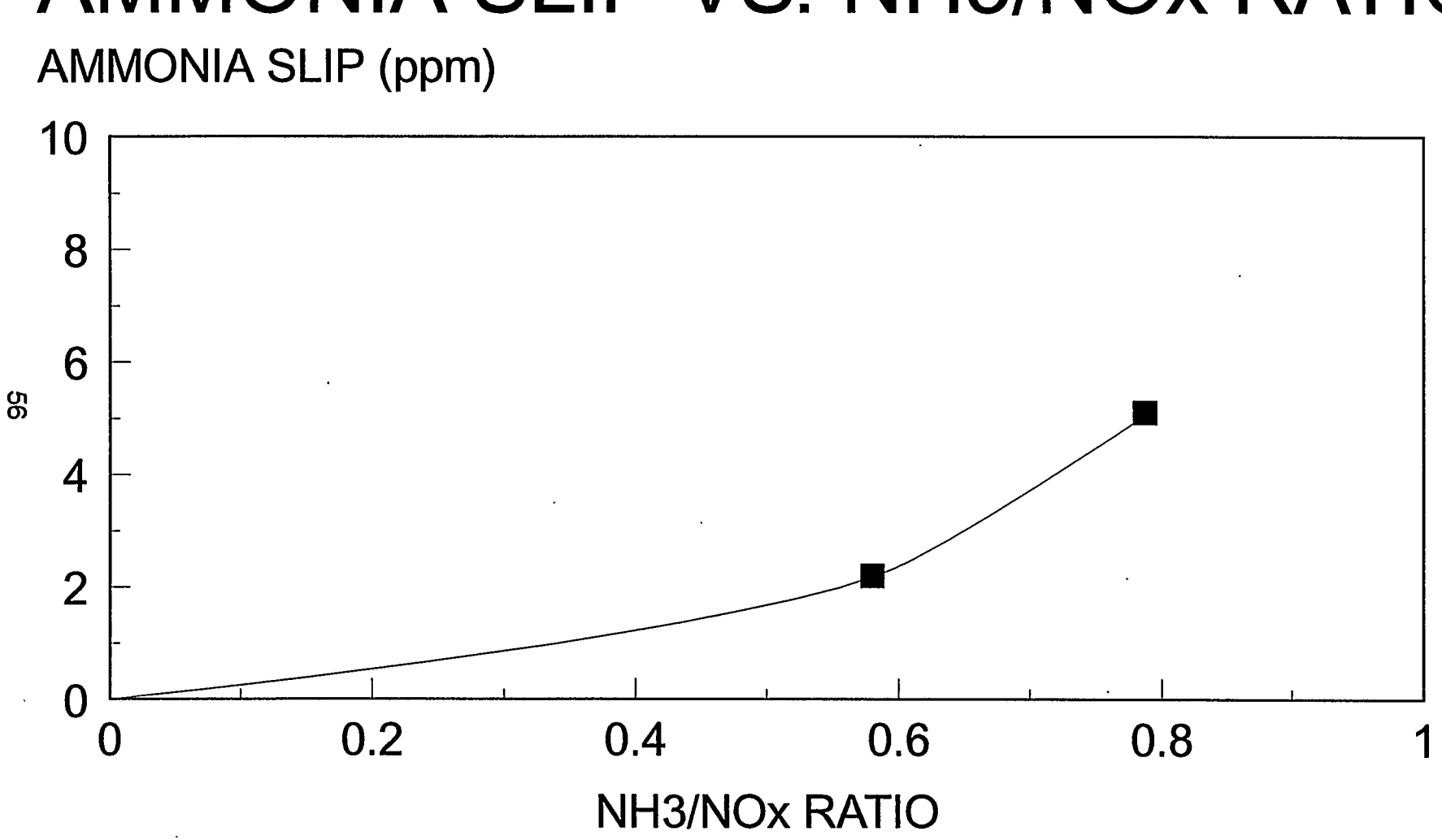

SIEMENS: Design Flow, 700 F

FIGURE 17

AMMONIA SLIP VS. TEMPERATURE

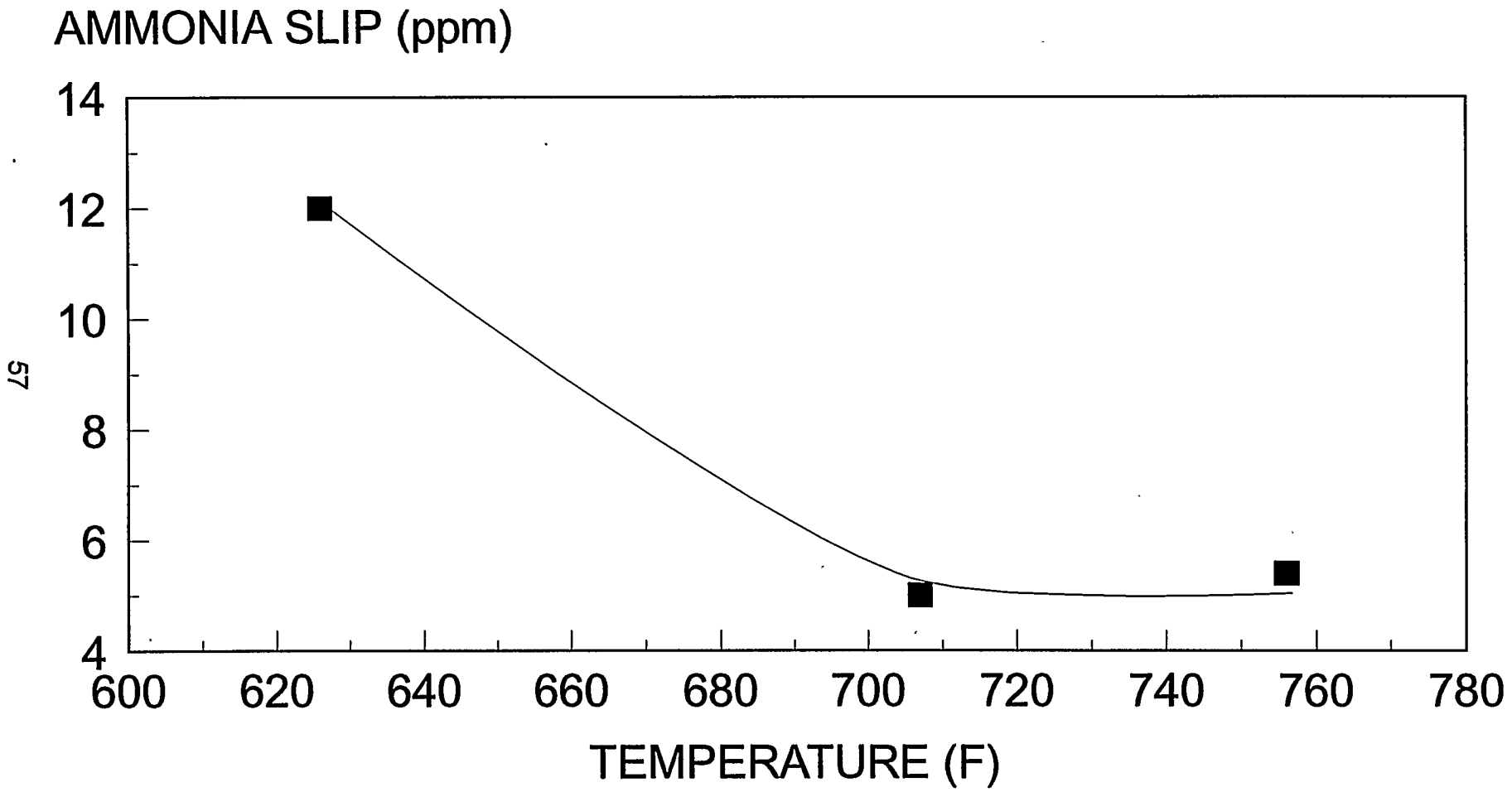

SIEMENS: Design Flow, NH3/NOx=0.80

FIGURE 18

REACTOR C

CATALYST LAYER 1 INLET

Velocity Profile
ft/s

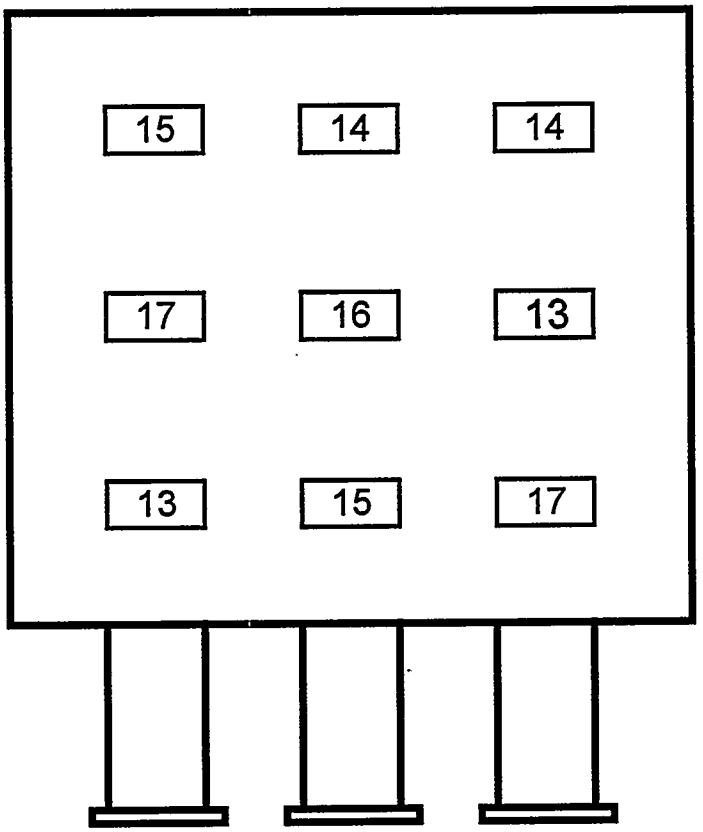

Average = 15 ft/s
σ = 1 ft/s

FIGURE 19

REACTOR C

REACTOR EXIT

Velocity Profile
ft/s

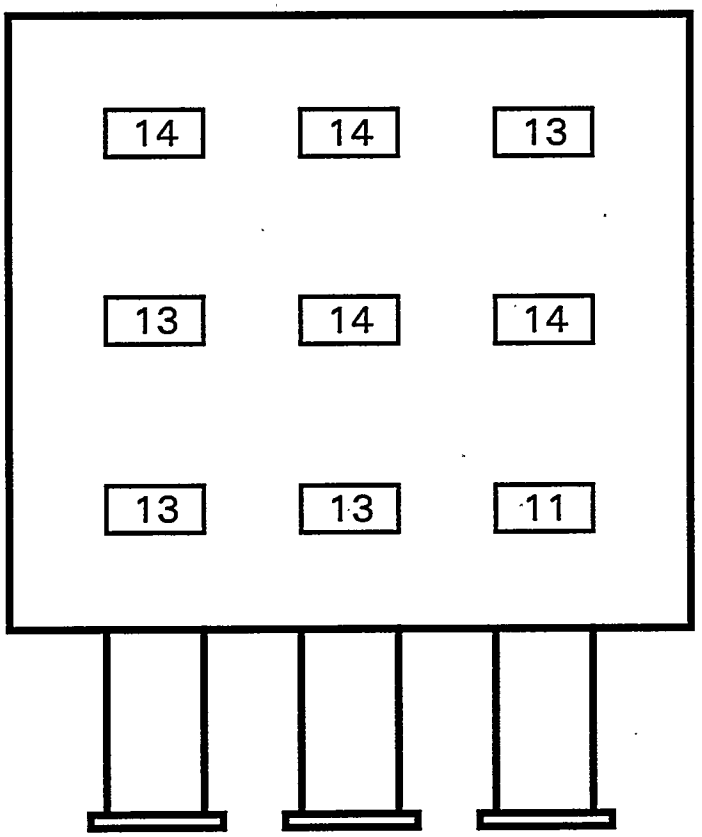

Average = 13 ft/s
σ = 1 ft/s

- Reactor D

Table 9 shows the parametric test data on intermediate ammonia, slip ammonia, and sulfur dioxide oxidation collected during this reporting period for the Grace Synox catalyst. All the ammonia data are corrected to reactor inlet oxygen concentration. The long term NO_x reduction is also given in this table as an average over the operating periods shown, i.e., for January - March and April - July of 1995. The long term NO_x reduction data indicates the average performance of the catalyst at or near the design operating conditions of 0.8 NH_3/NO_x ratio, 400 SCFM flow rate, and 700 °F reactor temperature. As can be noted in the first quarter data averages, analytical errors and drift in calibrations led to values falsely indicating NO_x reduction being higher than the NH_3/NO_x ratio.

The intermediate ammonia measurements were made after the first catalyst bed and at conditions thought to give the best kinetic information. The NO_x removals reported with the intermediate ammonia measurements are computed from the measured ammonia concentration using standard material balance techniques.

The ammonia slip data given in Table 9 are presented below in three plots: ammonia slip versus each of flow rate, NH_3/NO_x ratio, and temperature. Figure 20 shows ammonia slip versus flow rate for roughly 100% NO_x reduction and 620 °F. As expected, the trend shows increasing ammonia slip with increasing reactor flow rate. A fairly significant increase in ammonia slip is noted with flow rate. However, this ammonia slip is not likely to be nearly as significant at lower NO_x removal rates. A portion of the overall reaction rate is due to mass transfer limitations, improvements in bulk mass transfer coefficients are likely mitigating the effect of increased flow on slip ammonia increases.

Figure 21 shows ammonia slip versus NH_3/NO_x ratio at low temperature and design flow rate. The plot shows sharp increases in ammonia slip as the NH_3/NO_x ratio approaches 1.0. This finding is in keeping with published data of this type. At NH_3/NO_x ratios near 1.0, non-idealities in the reactor system force the catalyst to slip higher concentrations of ammonia since areas are present in the reactor where NO_x is the limiting reagent.

Ammonia slip versus temperature for design flow and roughly 80% NO_x reduction is plotted in Figure 22. Some improvement (decrease) in ammonia slip is noted between 620 and 700 °F,

likely due to improvements in the kinetic reaction rate with increasing temperature. Only slight improvements are noted with increasing temperature above 700 °F. This may possibly be due to mass transfer limitations that have become controlling at these higher temperatures. In general, the plot demonstrates that in terms of ammonia slip, significant improvements are not realized with temperatures above 700 °F. Losses in boiler efficiency would probably outweigh any improvements that may be obtained in ammonia slip by designing an SCR reactor to operate at temperatures near 750 °F.

SO_2 oxidation at design temperature and flow rate was -0.25%. In this case, there was an apparent loss in sulfur trioxide across the reactor. It is believed that the apparent loss is caused by acid condensation on cold spots at the reactor surface. The SO_2 oxidation data is corrected to reactor outlet oxygen concentrations. The value for sulfur trioxide produced in the reactor is based on measured inlet and outlet sulfur trioxide concentration values (table showing SO_2 oxidation rate quotes reactor flow rate as calculated for the reactor exit, since outlet SO_3 is measured at this point).

Flue gas velocity (three-point) profiles were conducted near design operating conditions (700 °F, 400 SCFM) at the reactor inlet and reactor outlet. The flue gas velocity profiles are presented in Figure 23 (reactor inlet) and Figure 24 (reactor outlet). The average inlet and outlet velocities were 14.3 ± 1.3 ft/sec and 13.8 ± 1.6 ft/sec, respectively. The N_2O concentrations were also measured at the reactor inlet (2.0 ppmv) and at the reactor outlet (2.1 ppmv, both measurements are dry at 3% O_2).[1]

TABLE 9. REACTOR D DATA (5TH SEQUENCE)

INTERMEDIATE AMMONIA PARAMETRIC TEST DATA

FLOW RATE (SCFM)	TEMP. (°F)	INLET O_2 (%)	INLET NO_x (ppmv)	NH_3/NO_x RATIO	INT. NH_3 (ppmv)	INT. NO_x REDUCTION (%)
352	625	4.714	319	0.788	93.2	49.6
217	700	5.379	281	0.787	48.4	61.5
352	704	6.903	327	0.593	45.3	45.4
363	704	4.287	321	0.789	63.3	59.2
354	698	4.885	324	0.990	87.3	72.1
469	706	5.701	319	0.790	79.4	54.1
343	756	4.623	340	0.790	74.1	57.2

SLIP AMMONIA PARAMETRIC TEST DATA

FLOW RATE (SCFM)	TEMP. (°F)	INLET O_2 (%)	INLET NO_x (ppmv)	NH_3/NO_x RATIO	SLIP NH_3 (ppmv)
225	624	4.529	301	0.801	0.8
378	625	4.751	345	0.597	1.7
374	626	3.881	327	0.809	4.8
330	624	4.274	322	0.979	11.3
490	625	4.699	238	0.989	29.7
382	706	5.141	231	0.608	1.4
385	706	6.020	339	0.793	2.6
328	703	5.060	319	0.989	3.9
506	708	4.185	338	0.597	3.9
563	705	4.490	335	0.795	8.2
481	705	4.673	338	0.988	16.1
367	755	5.548	364	0.597	1.3
365	755	5.303	365	0.801	2.2
329	757	4.565	307	0.979	3.9

TABLE 9. REACTOR D DATA (5TH SEQUENCE) - Continued

SULFUR DIOXIDE OXIDATION PARAMETRIC TEST DATA

FLOW RATE (SCFM)	TEMP. (°F)	OUTLET O_2 (%)	INLET SO_2 (ppmv)	NH_3/NO_x RATIO	MEAS. SO_3 IN (ppmv)	SO_3 OUT (ppmv)	SO_3 formed (ppmv)	OXID. RATE (%)
402	707	7.330	840.	0.751	3.0	0.9	-2.1	-0.25

LONG TERM NO_x REDUCTION

TIME PERIOD	FLOW RATE (SCFM)	INLET NO_x (ppmv)	NH_3/NO_x RATIO	OUTLET NO_x (ppmv)	NO_x RED. (%)
JAN. - MAR.	404	423	0.80	38	89
APRIL - JULY	359	336	0.79	64	78

FIGURE 20

AMMONIA SLIP VS. FLOW RATE

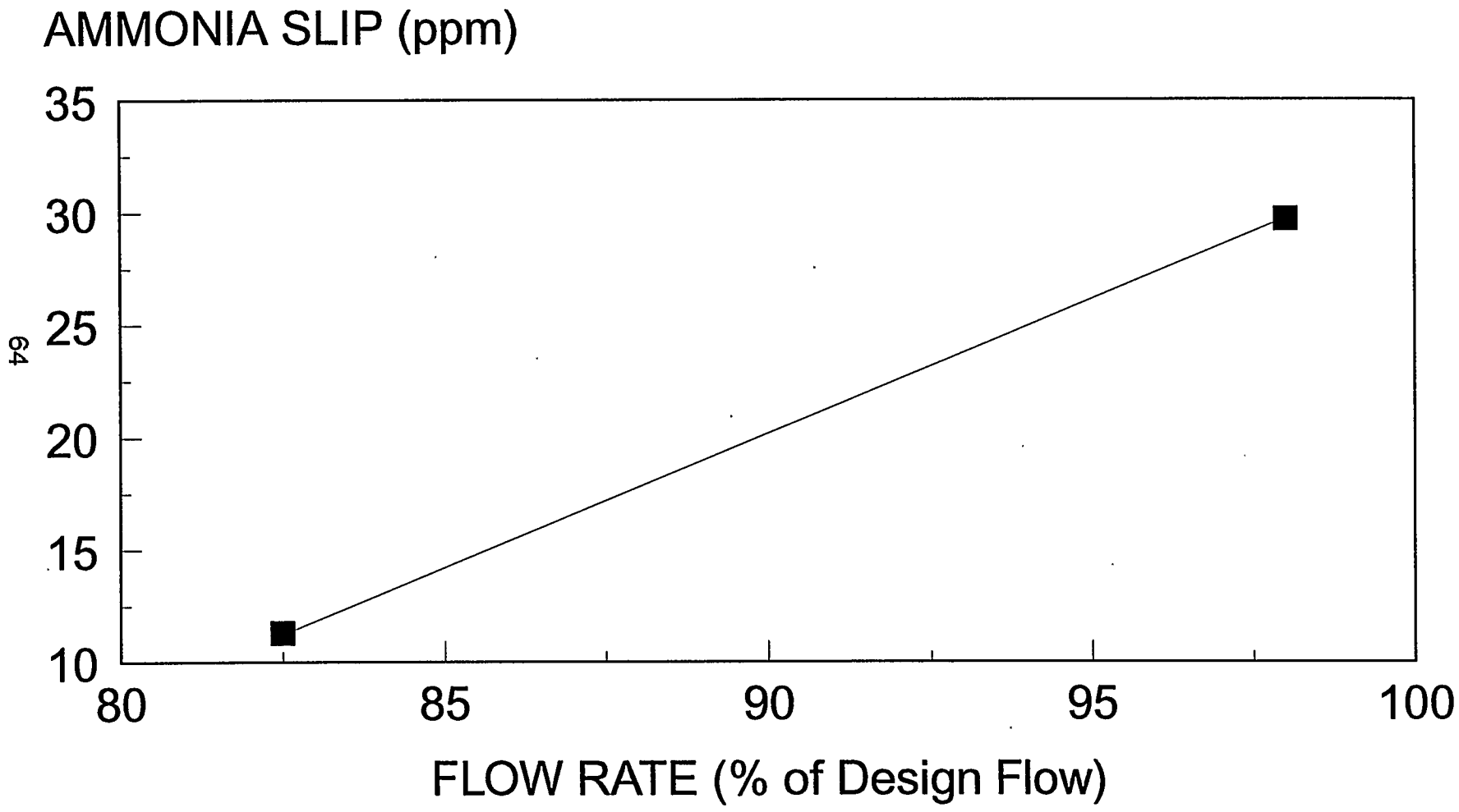

GRACE SNX: NH3/NOx=1.00, 620 F

FIGURE 21

AMMONIA SLIP VS. NH3/NOx RATIO

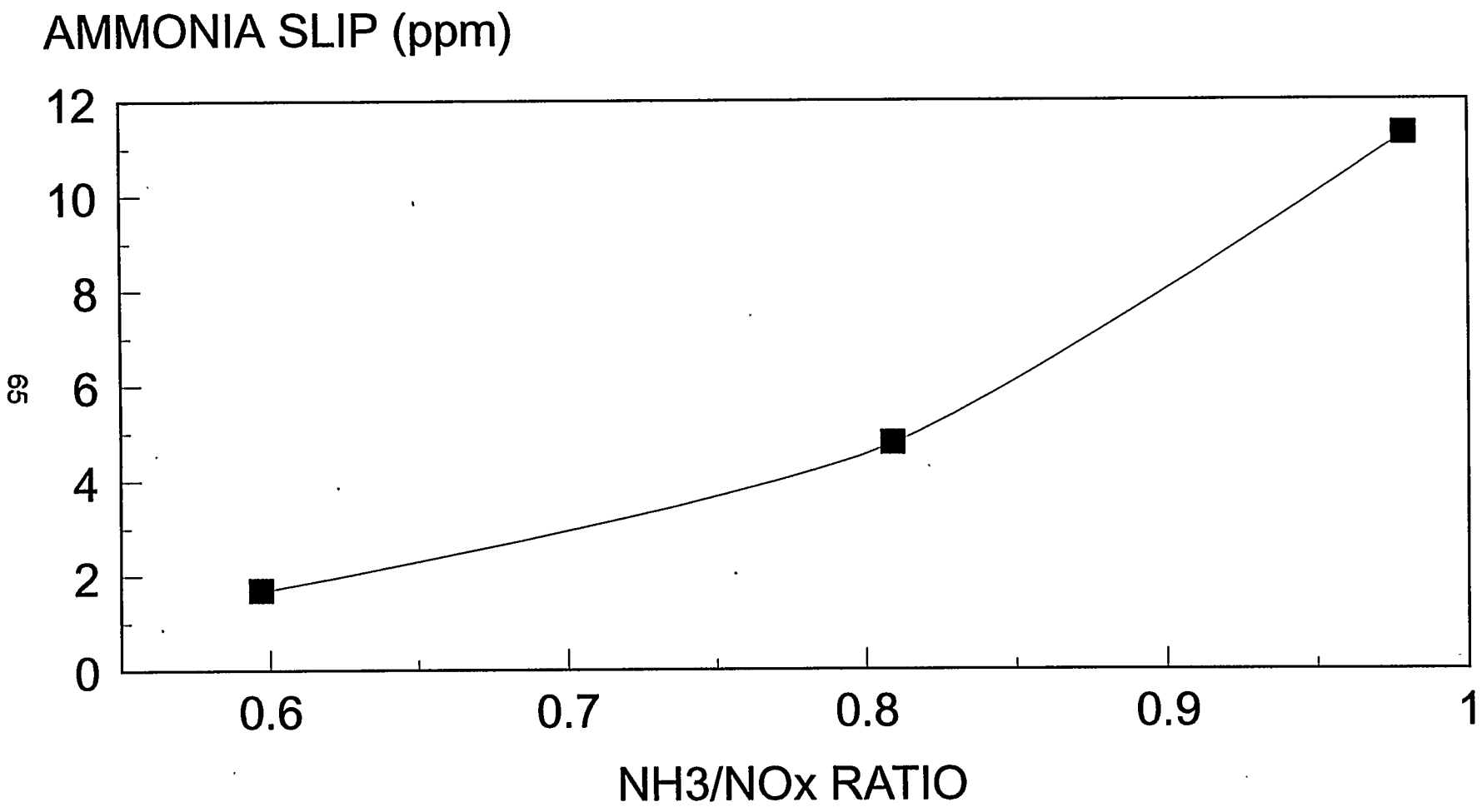

GRACE SNX: Design Flow, 620 F

FIGURE 22

AMMONIA SLIP VS. TEMPERATURE

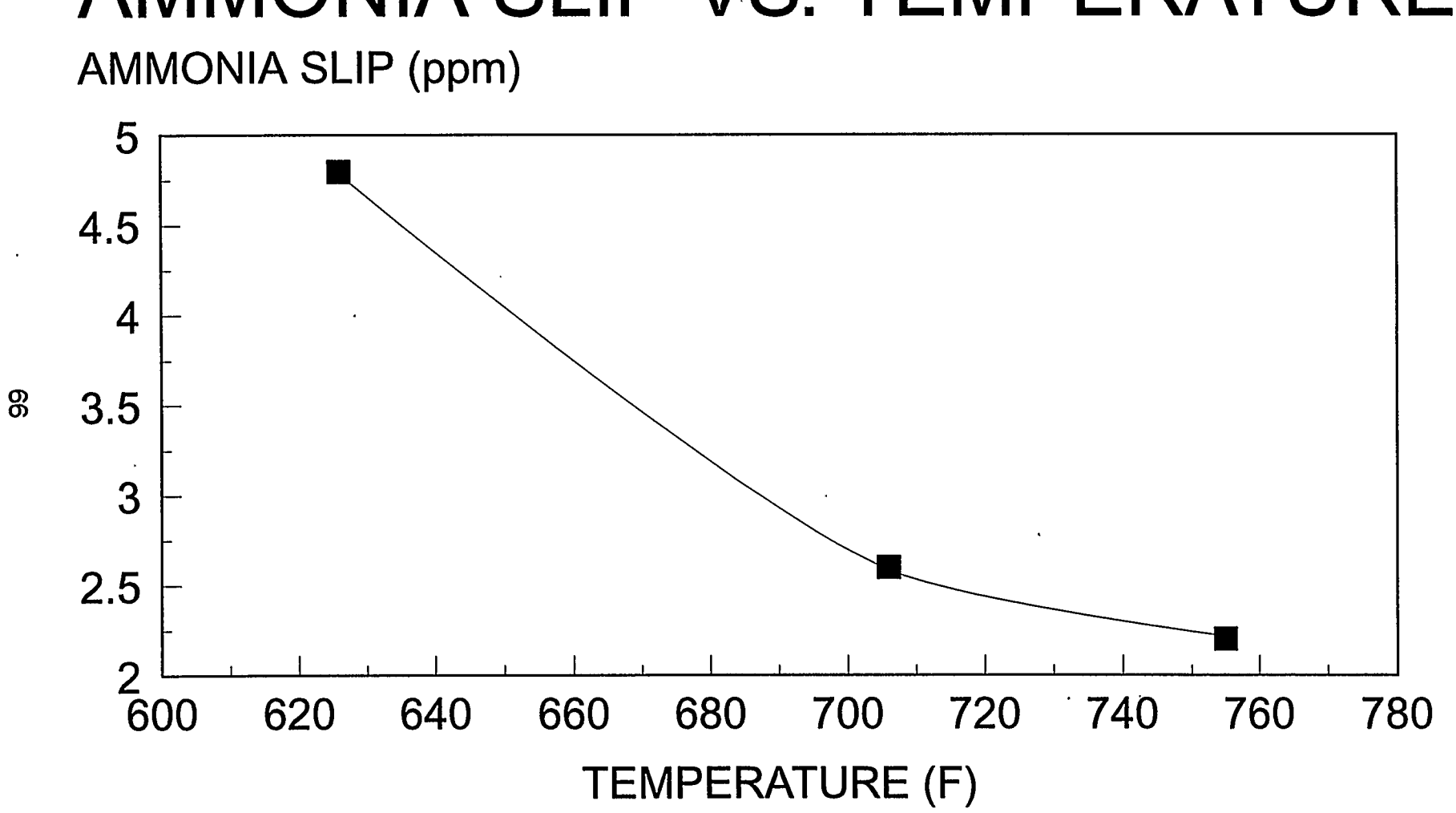

GRACE SNX: Design Flow, NH3/NOx=0.80

FIGURE 23

REACTOR D

CATALYST LAYER 1 INLET

Velocity Profile
ft/s

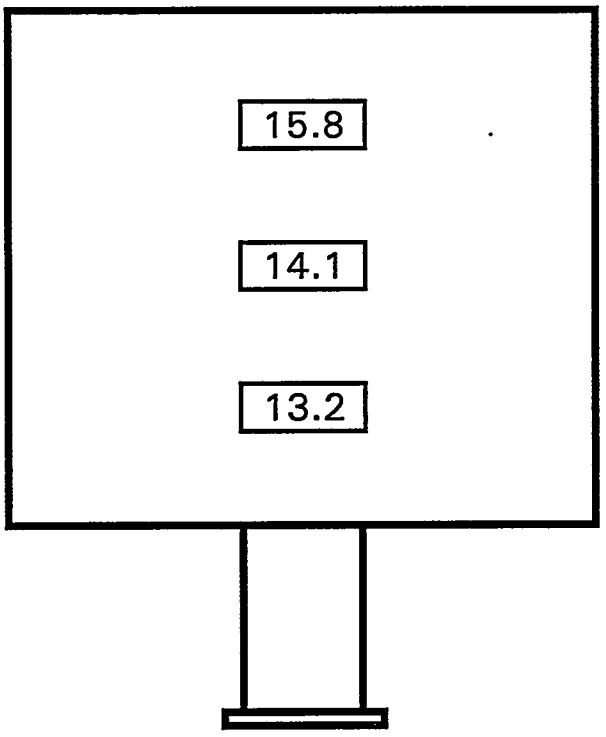

Average = 14 ft/s
σ = 1 ft/s

FIGURE 24

REACTOR D

REACTOR EXIT

Velocity Profile
ft/s

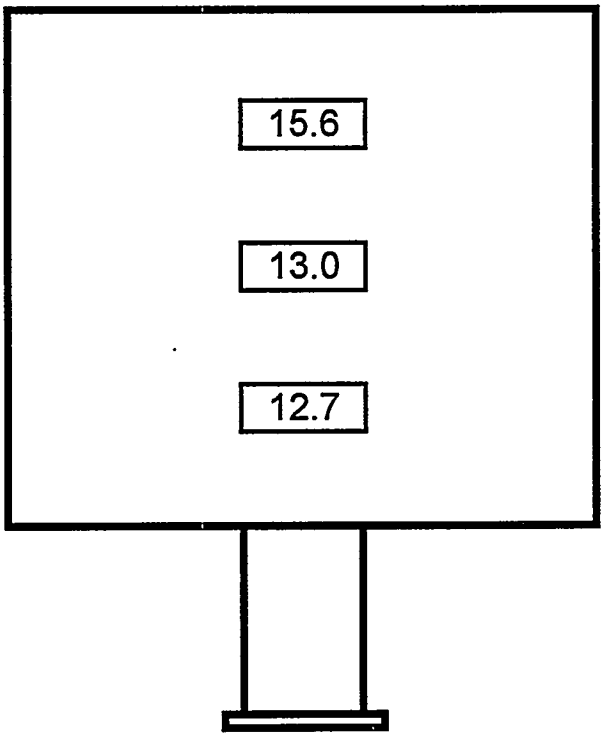

Average = 14 ft/s
σ = 2 ft/s

- Reactor E

Table 10 shows the parametric test data on intermediate ammonia, slip ammonia, and sulfur dioxide oxidation collected during this reporting period for the Cormetech high-dust catalyst. All the ammonia data are corrected to reactor inlet oxygen concentration. The long term NO_x reduction is also given in this table as an average over the operating periods shown, i.e., for January - March and April - July of 1995. The long term NO_x reduction data indicates the average performance of the catalyst at or near the design operating conditions of 0.8 NH_3/NO_x ratio, 400 SCFM flow rate, and 700 °F reactor temperature. As can be noted in the first quarter data averages, analytical errors and drift in calibrations led to values falsely indicating NO_x reduction being higher than the NH_3/NO_x ratio.

The intermediate ammonia measurements were made after the first catalyst bed and at conditions thought to give the best kinetic information. The NO_x removals reported with the intermediate ammonia measurements are computed from the measured ammonia concentration using standard material balance techniques.

The ammonia slip data given in Table 10 are presented below in three plots: ammonia slip versus each of flow rate, NH_3/NO_x ratio, and temperature. Figure 25 shows ammonia slip versus flow rate for roughly 65% NO_x reduction and 625 °F. As expected, the trend shows increasing ammonia slip with increasing reactor flow rate. The ammonia slip is, however, relatively minor indicating the ability of the catalyst design to withstand significant increases in flow while maintaining ammonia slip limits. Since a portion of the overall reaction rate is due to mass transfer limitations, improvements in bulk mass transfer coefficients are likely mitigating the effect of increased flow on slip ammonia increases. This plot demonstrates the ability of an SCR system to follow load variations dictated by the host boiler while maintaining design specifications.

Figure 26 shows ammonia slip versus NH_3/NO_x ratio at low temperature and design flow rate. The plot shows a slight increase in ammonia slip as the NH_3/NO_x ratio increases from 0.55 to 0.75. This finding is in keeping with published data of this type.

Ammonia slip versus temperature for design flow and roughly 70% NO_x reduction is plotted in Figure 27. The trend of the plot is unclear since all values are at or below the ammonia slip detection limit.

SO_2 oxidation at design temperature and flow rate was -0.04%. In this case, there was an apparent loss in sulfur trioxide across the reactor. It is believed that the apparent loss is caused by acid condensation on cold spots at the reactor surface. The SO_2 oxidation data is corrected to reactor outlet oxygen concentrations. The value for sulfur trioxide produced in the reactor is based on measured inlet and outlet sulfur trioxide concentration values (table showing SO_2 oxidation rate quotes reactor flow rate as calculated for the reactor exit, since outlet SO_3 is measured at this point).

Flue gas velocity (three-point) profiles were conducted near design operating conditions (700 °F, 400 SCFM) at the reactor inlet and reactor outlet. The flue gas velocity profiles are presented in Figure 28 (reactor inlet) and Figure 29 (reactor outlet). The average inlet and outlet velocities were 16.1 ± 1.2 ft/sec and 13.0 ± 3.7 ft/sec, respectively. The N_2O concentrations were also measured at the reactor inlet (2.0 ppmv) and at the reactor outlet (1.8 ppmv, both measurements are dry at 3% O_2).[1]

TABLE 10. REACTOR E DATA (5TH SEQUENCE)

INTERMEDIATE AMMONIA PARAMETRIC TEST DATA

FLOW RATE (SCFM)	TEMP. (°F)	INLET O_2 (%)	INLET NO_x (ppmv)	NH_3/NO_x RATIO	INT. NH_3 (ppmv)	INT. NO_x REDUCTION(%)
429	621	4.357	309	0.665	13.7	62.0
259	706	4.673	311	0.664	4.60	64.9
433	706	4.570	329	0.490	10.2	45.9
416	705	3.982	339	0.693	12.1	65.7
439	705	4.818	349	0.804	20.7	74.4
609	704	4.404	351	0.643	30.7	55.6
433	756	5.514	325	0.638	11.3	60.4

SLIP AMMONIA PARAMETRIC TEST DATA

FLOW RATE (SCFM)	TEMP. (°F)	INLET O_2 (%)	INLET NO_x (ppmv)	NH_3/NO_x RATIO	SLIP NH_3 (ppmv)
253	624	4.619	331	0.714	BDL
416	625	4.200	345	0.555	BDL
415	625	4.110	348	0.725	BDL
452	627	4.357	387	0.615	0.8
672	627	4.116	335	0.728	3.1
413	704	5.386	249	0.553	BDL
405	702	5.651	343	0.748	0.8
448	706	4.286	326	0.735	BDL
569	705	3.461	339	0.549	0.7
563	704	4.727	334	0.740	0.8
612	706	4.385	344	0.725	2.2
426	756	4.493	367	0.457	BDL
425	756	4.384	376	0.608	BDL
449	756	3.402	315	0.740	BDL

TABLE 10. REACTOR E DATA (5TH SEQUENCE) - Continued

SULFUR DIOXIDE OXIDATION PARAMETRIC TEST DATA

FLOW RATE (SCFM)	TEMP. (°F)	OUTLET O_2 (%)	INLET SO_2 (ppmv)	NH_3/NO_x RATIO	MEAS. SO_3 IN (ppmv)	SO_3 OUT (ppmv)	SO_3 formed (ppmv)	OXID. RATE (%)
502	706	9.422	849	0.760	3.5	3.2	-0.3	-0.04

LONG TERM NO_x REDUCTION

TIME PERIOD	FLOW RATE (SCFM)	INLET NO_x (ppmv)	NH_3/NO_x RATIO	OUTLET NO_x (ppmv)	NO_x RED. (%)
JAN. - MAR.	400	413	0.79	77	80
APRIL - JULY	431	338	0.66	109	62

FIGURE 25

AMMONIA SLIP VS. FLOW RATE

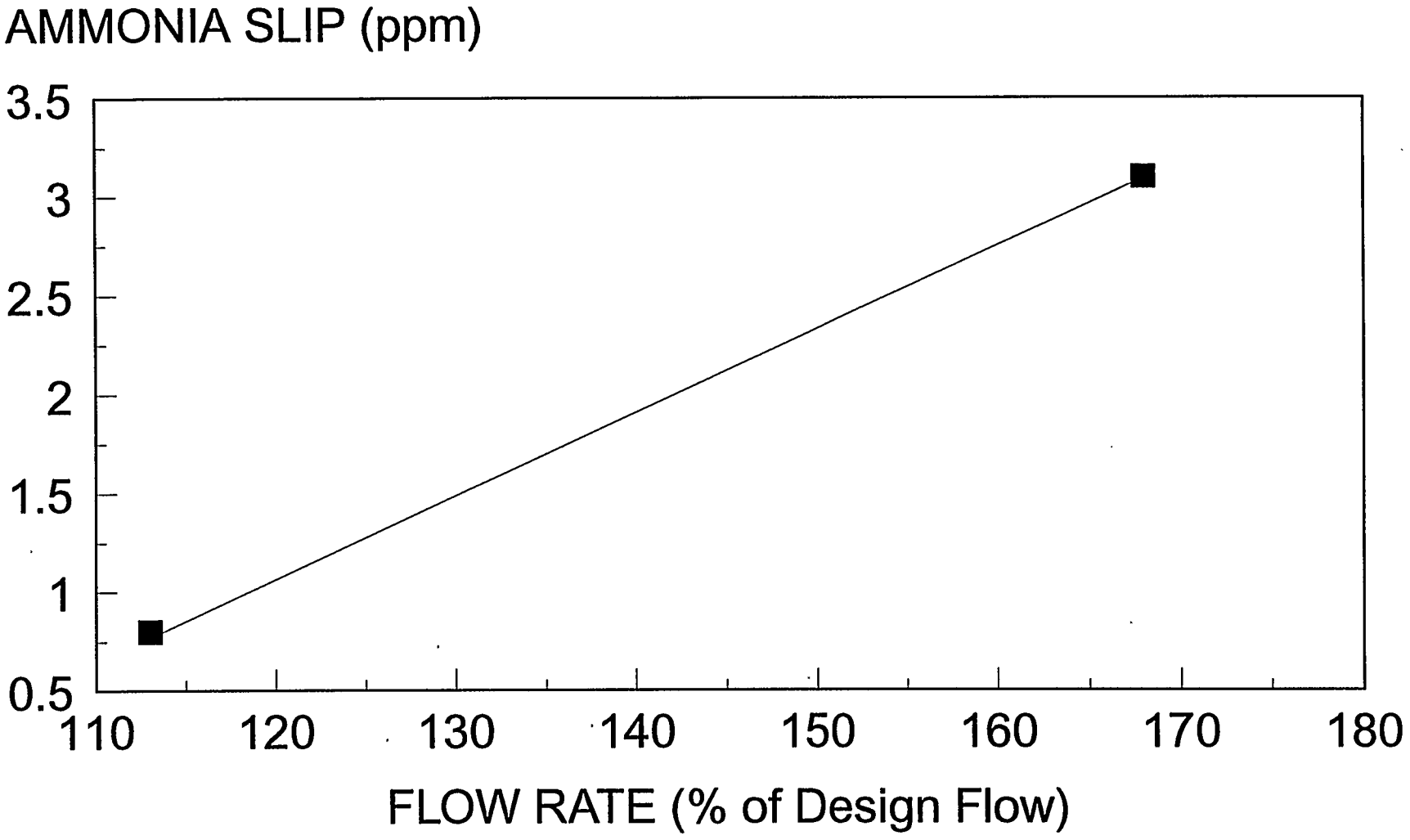

CORM HD: NH3/NOx=0.65, 625 F

FIGURE 26

AMMONIA SLIP VS. NH3/NOx RATIO

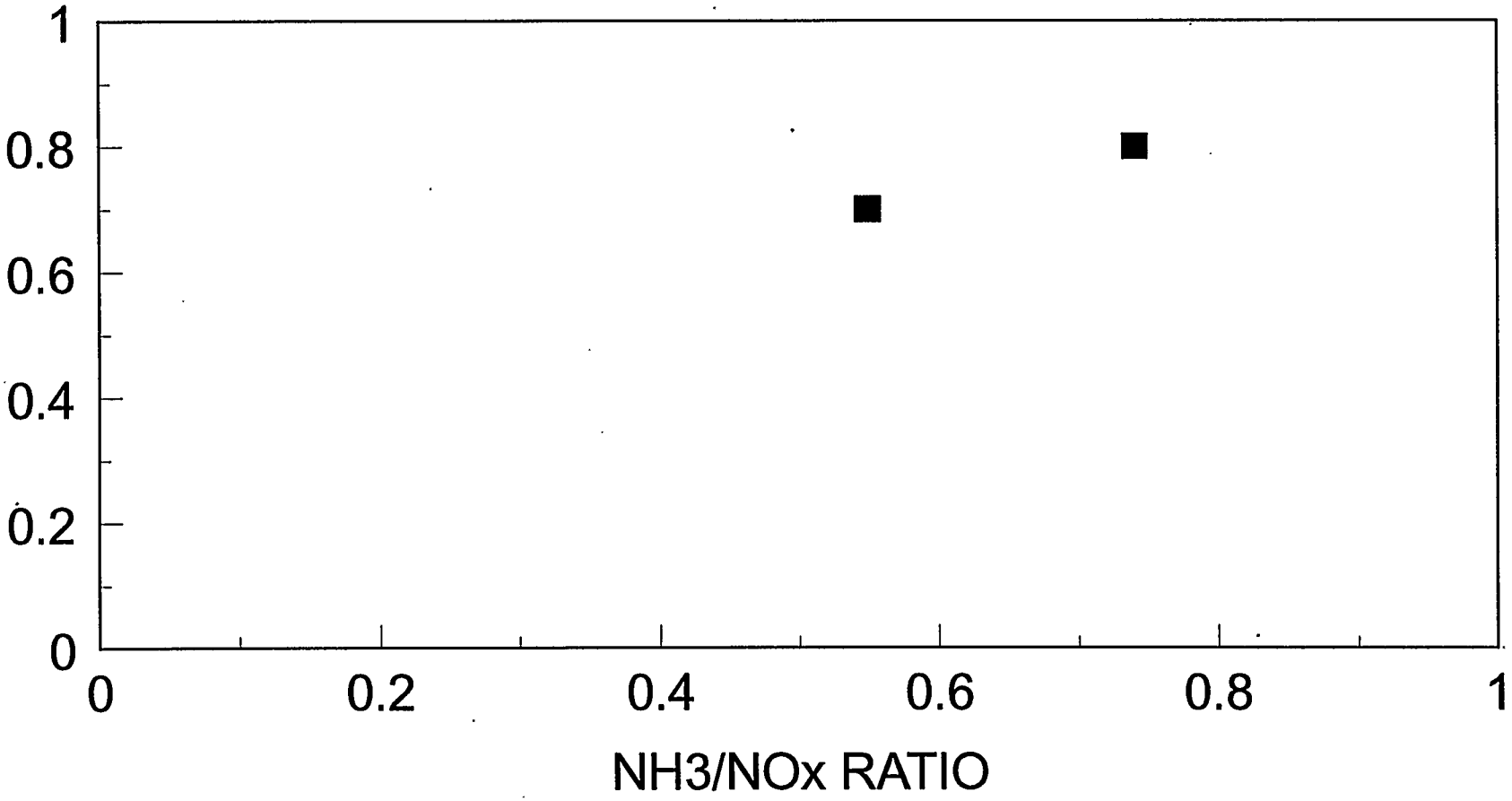

CORM HD: High Flow, 700 F

FIGURE 27

AMMONIA SLIP VS. TEMPERATURE

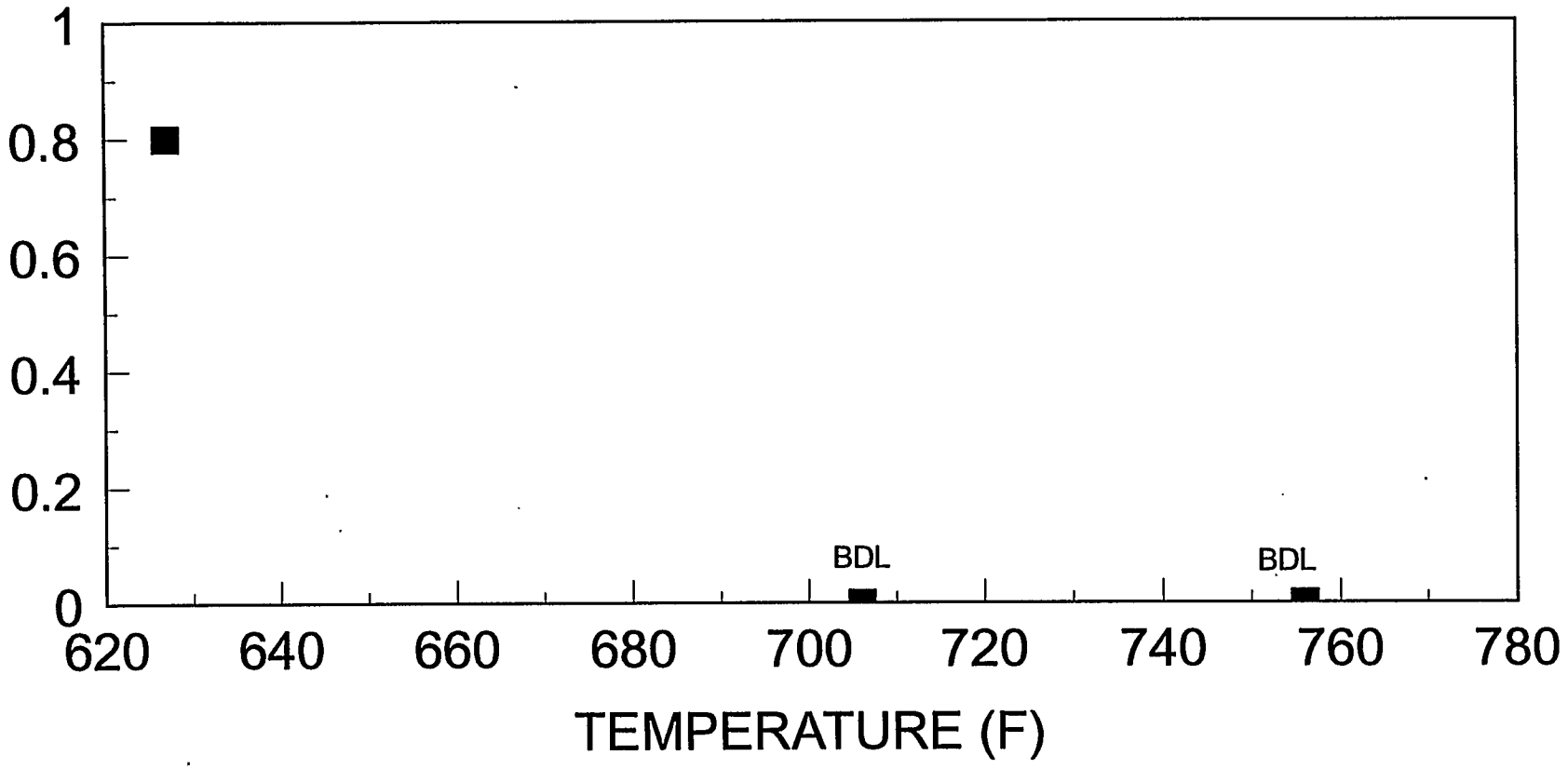

CORM HD: Design Flow, NH3/NOx=0.70

(BDL) Below lower detection limit

FIGURE 28

REACTOR E

CATALYST LAYER 1 INLET

Velocity Profile
ft/s

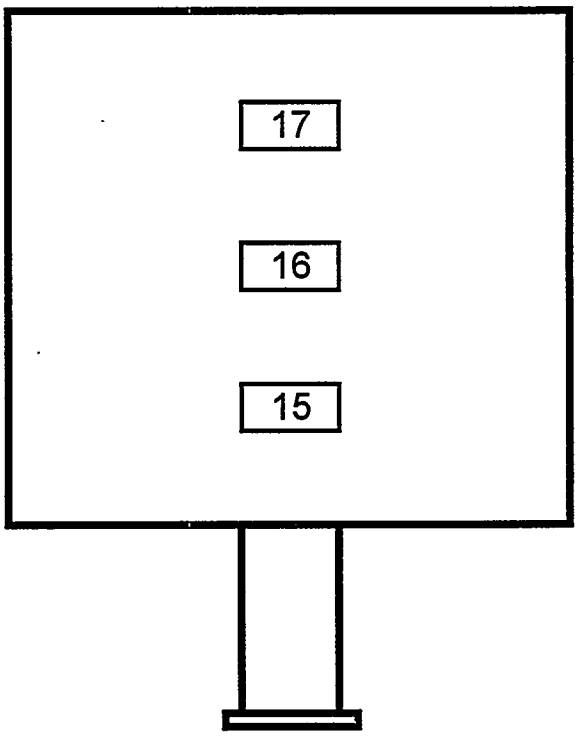

Average = 16 ft/s
σ = 1 ft/s

FIGURE 29

REACTOR E

REACTOR EXIT

Velocity Profile
ft/s

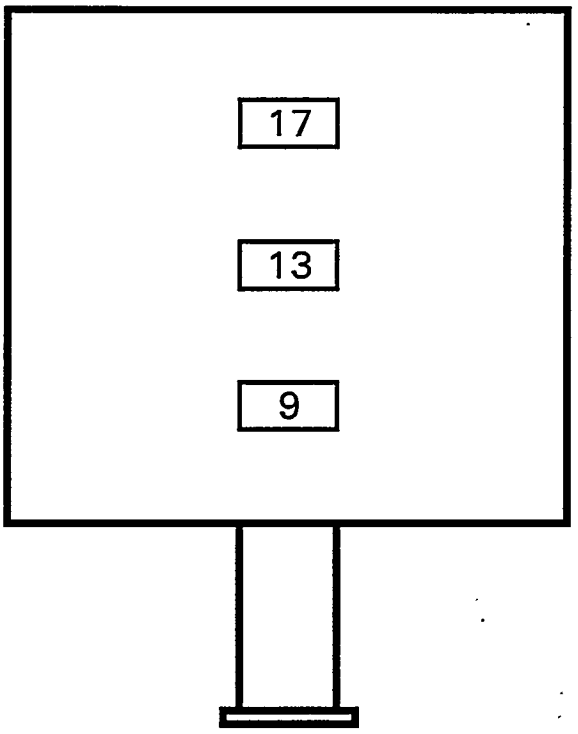

Average = 13 ft/s
σ = 4 ft/s

- Reactor F

Table 11 shows the parametric test data on intermediate ammonia, slip ammonia, and sulfur dioxide oxidation collected during this reporting period for the Haldor Topsoe catalyst. All the ammonia data are corrected to reactor inlet oxygen concentration. The long term NO_x reduction is also given in this table as an average over the operating periods shown, i.e., for January - March and April - July of 1995. The long term NO_x reduction data indicates the average performance of the catalyst at or near the design operating conditions of 0.8 NH_3/NO_x ratio, 400 SCFM flow rate, and 700 °F reactor temperature. As can be noted in both quarter data averages, analytical errors and drift in calibrations led to values falsely indicating NO_x reduction being higher than the NH_3/NO_x ratio.

The intermediate ammonia measurements were made after the first catalyst bed and at conditions thought to give the best kinetic information. The NO_x removals reported with the intermediate ammonia measurements are computed from the measured ammonia concentration using standard material balance techniques.

The ammonia slip data given in Table 11 are presented below in three plots: ammonia slip versus each of flow rate, NH_3/NO_x ratio, and temperature. Figure 30 shows ammonia slip versus flow rate for roughly 70% NO_x reduction. As expected, the trend shows increasing ammonia slip with increasing reactor flow rate. The ammonia slip is, however, relatively minor indicating the ability of the catalyst design to withstand significant increases in flow while maintaining ammonia slip limits. Since a portion of the overall reaction rate is due to mass transfer limitations, improvements in bulk mass transfer coefficients are likely mitigating the effect of increased flow on slip ammonia increases. This plot demonstrates the ability of an SCR system to follow load variations dictated by the host boiler while maintaining design specifications.

Figure 31 shows ammonia slip versus NH_3/NO_x ratio at design temperature and low flow rate. The plot shows a slight increase in ammonia slip as the NH_3/NO_x ratio increases from 0.55 to 0.75. This finding is in keeping with published data of this type.

Ammonia slip versus temperature for design flow and roughly 70% NO_x reduction is plotted in Figure 32. Some improvement (decrease) in ammonia slip is noted between 620 and 700 °F, likely due to improvements in the kinetic reaction rate with increasing temperature. The slight increase shown between the 700 and 750 °F points is likely due to measurement variability and is

not considered significant. In this case, the plot should not be construed as demonstrating increases in ammonia slip with increasing temperature above 700 °F. It is expected that the 700 and 750 °F values are roughly equivalent which may be due in part to mass transfer limitations that have become controlling at these higher temperatures.

SO_2 oxidation at design temperature and flow rate was -0.32%. In this case, there was an apparent loss in sulfur trioxide across the reactor. It is believed that the apparent loss is cause by acid condensation on cold spots at the reactor surface. The SO_2 oxidation data is corrected to reactor outlet oxygen concentrations. The value for sulfur trioxide produced in the reactor is based on measured inlet and outlet sulfur trioxide concentration values (table showing SO_2 oxidation rate quotes reactor flow rate as calculated for the reactor exit, since outlet SO_3 is measured at this point).

Flue gas velocity (three-point) profiles were conducted near design operating conditions (700 °F, 400 SCFM) at the reactor inlet and reactor outlet. The flue gas velocity profiles are presented in Figure 33 (reactor inlet) and Figure 34 (reactor outlet). The average inlet and outlet velocities were 13.3 ± 0.4 ft/sec and 18.7 ± 2.2 ft/sec, respectively. The N_2O concentrations were also measured at the reactor inlet (2.0 ppmv) and at the reactor outlet (2.2 ppmv, both measurements are dry at 3% O_2).[1]

TABLE 11. REACTOR F DATA (5TH SEQUENCE)

INTERMEDIATE AMMONIA PARAMETRIC TEST DATA

FLOW RATE (SCFM)	TEMP. (°F)	INLET O_2 (%)	INLET NO_x (ppmv)	NH_3/NO_x RATIO	INT. NH_3 (ppmv)	INT. NO_x REDUCTION (%)
394	624	6.137	310	0.616	67.6	39.8
243	704	6.776	276	0.656	26.0	56.1
393	705	5.219	276	0.456	29.8	34.9
396	706	3.686	335	0.685	45.9	54.8
398	706	6.324	316	0.767	52.4	60.1
589	706	5.755	326	0.618	79.3	37.5
394	754	5.219	277	0.607	38.4	46.9

SLIP AMMONIA PARAMETRIC TEST DATA

FLOW RATE (SCFM)	TEMP. (°F)	INLET O_2 (%)	INLET NO_x (ppmv)	NH_3/NO_x RATIO	SLIP NH_3 (ppmv)
240	626	4.230	375	0.688	BDL
397	623	3.932	343	0.542	0.8
397	626	3.907	342	0.729	1.4
390	628	6.570	278	0.721	1.5
586	624	5.729	305	0.715	9.7
397	704	3.752	378	0.526	1.1
398	706	6.130	353	0.738	1.2
391	705	5.814	279	0.718	0.9
596	706	3.404	331	0.536	2.5
596	706	3.926	334	0.710	4.0
580	709	5.228	296	0.728	4.2
397	754	4.053	327	0.549	1.1
397	755	3.996	341	0.721	1.3
392	756	5.952	303	1.341	1.4

TABLE 11. REACTOR F DATA (5TH SEQUENCE) - Continued

SULFUR DIOXIDE OXIDATION PARAMETRIC TEST DATA

FLOW RATE (SCFM)	TEMP. (°F)	OUTLET O_2 (%)	INLET SO_2 (ppmv)	NH_3/NO_x RATIO	MEAS. SO_3 IN (ppmv)	SO_3 OUT (ppmv)	SO_3 formed (ppmv)	OXID. RATE (%)
421	706	7.702	833	0.752	3.4	0.8	-2.6	-0.32

LONG TERM NO_x REDUCTION

TIME PERIOD	FLOW RATE (SCFM)	INLET NO_x (ppmv)	NH_3/NO_x RATIO	OUTLET NO_x (ppmv)	NO_x RED. (%)
JAN. - MAR.	400	404	0.78	43	88
APRIL - JULY	391	334	0.66	69	75

FIGURE 30

AMMONIA SLIP VS. FLOW RATE

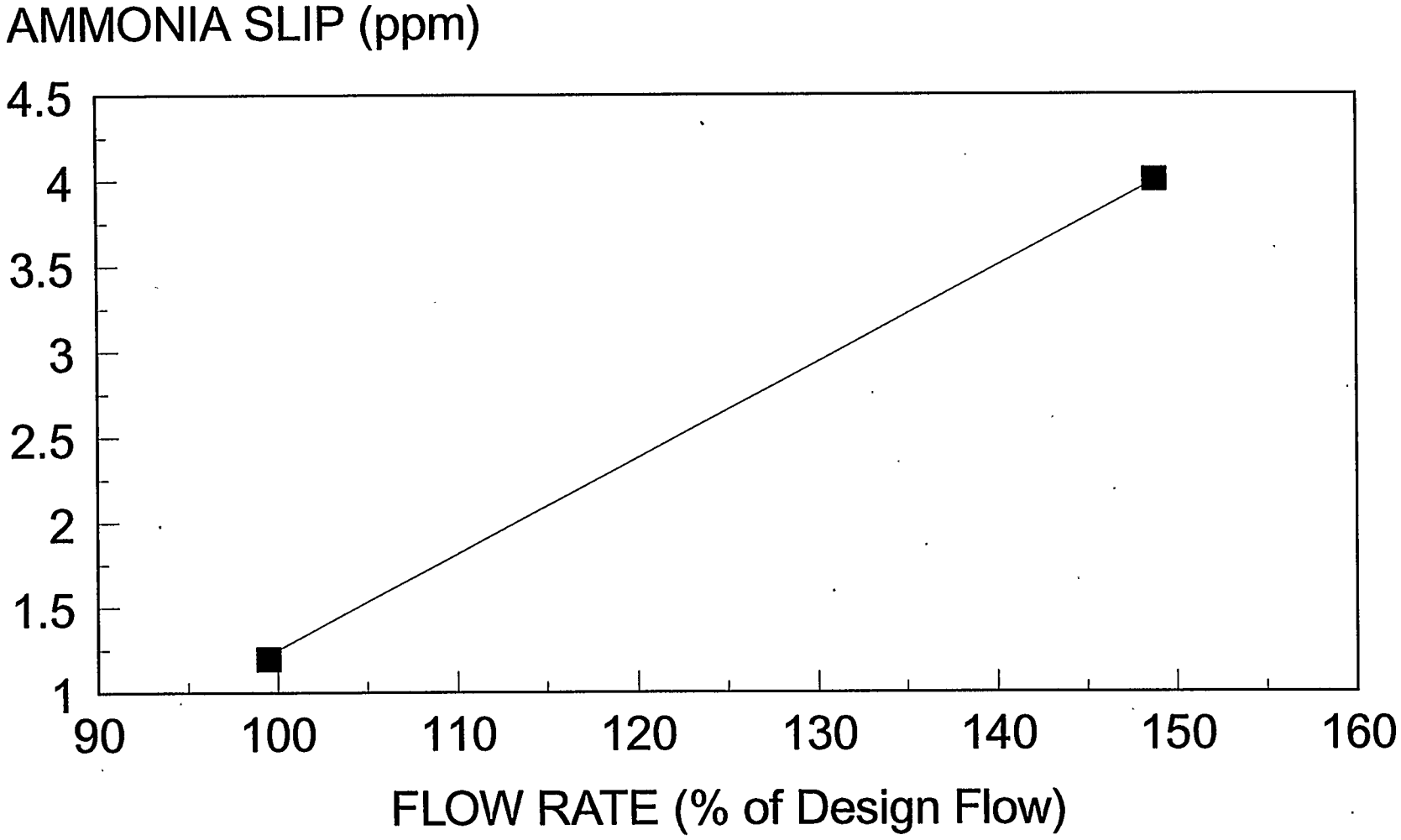

HALDOR: NH3/NOx=0.70, 700 F

FIGURE 31

AMMONIA SLIP VS. NH3/NOx RATIO

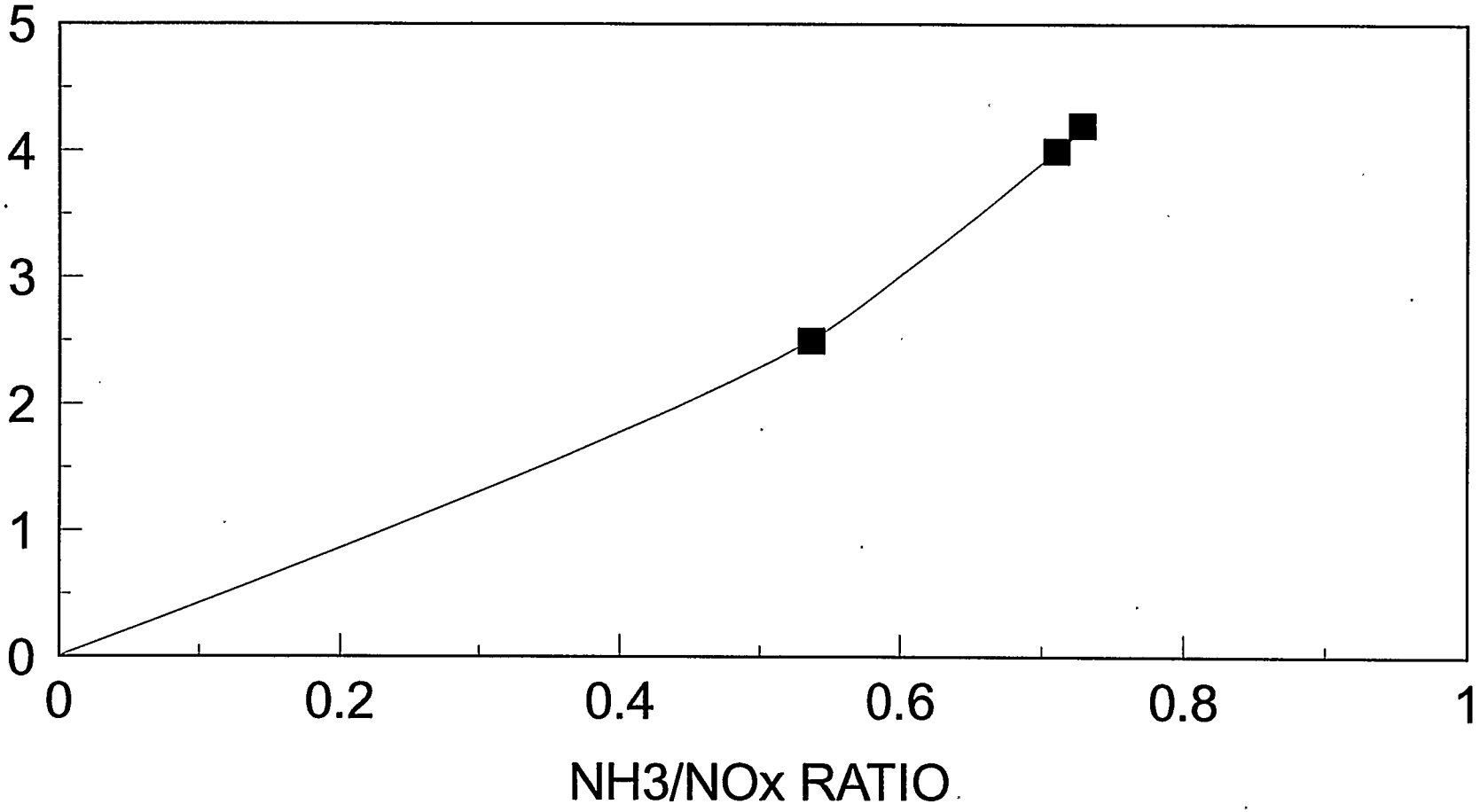

HALDOR: High Flow, 700 F

FIGURE32

AMMONIA SLIP VS. TEMPERATURE

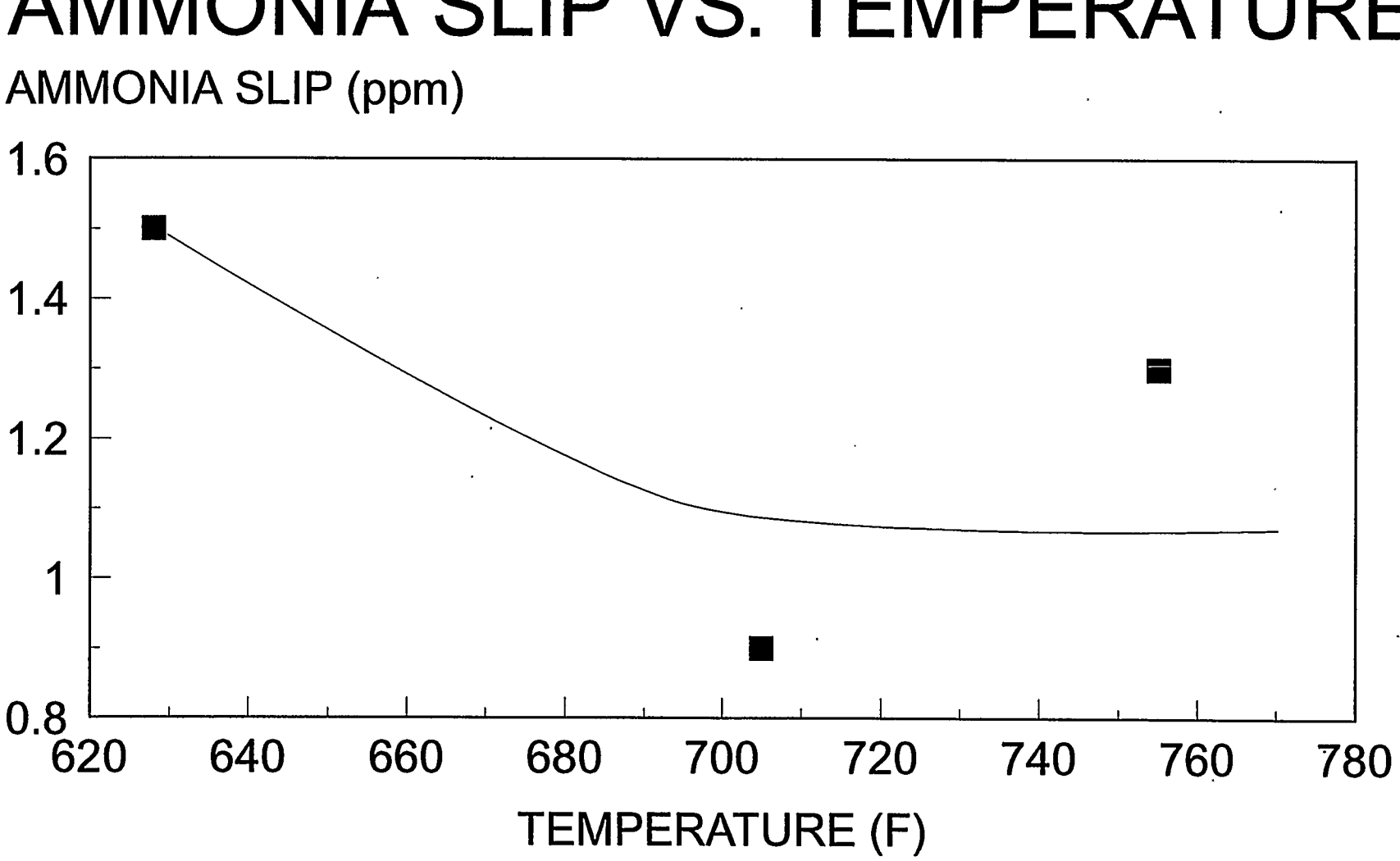

HALDOR: Design Flow, NH3/NOx=0.70

FIGURE 33

REACTOR F

CATALYST LAYER 1 INLET

Velocity Profile
ft/s

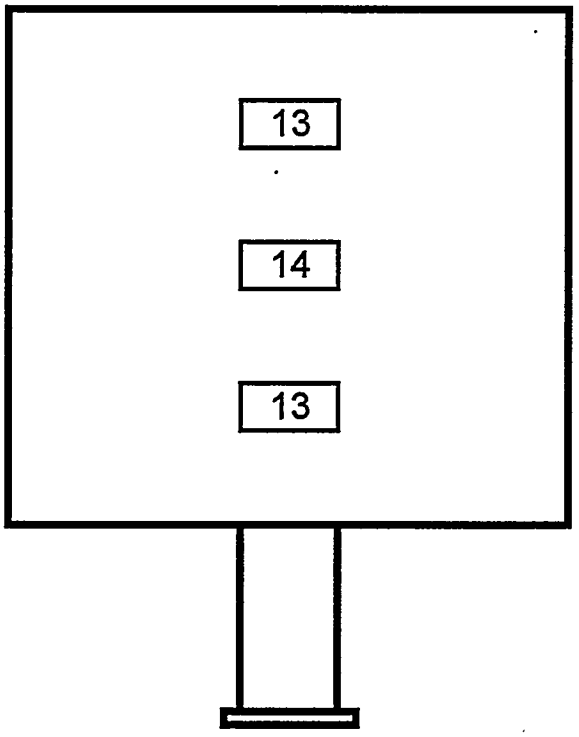

Average = 13 ft/s
σ = 0.4 ft/s

FIGURE 34

REACTOR F
REACTOR EXIT

Velocity Profile
ft/s

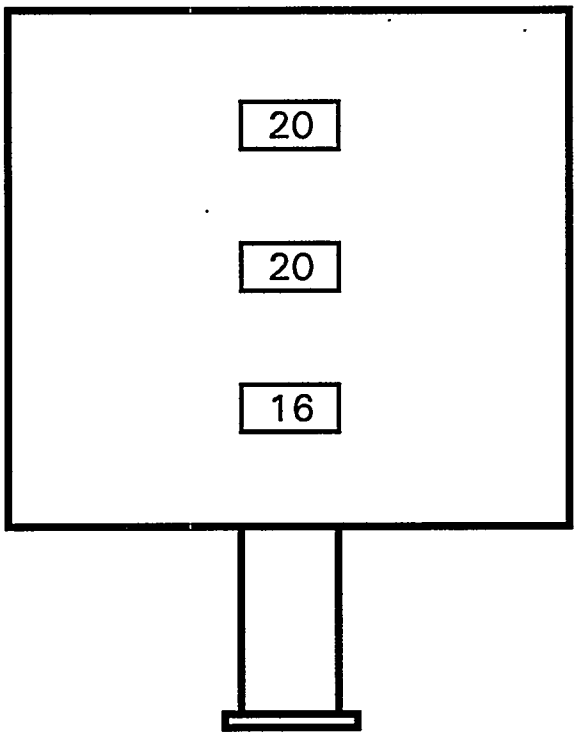

Average = 19 ft/s
σ = 2 ft/s

- Reactor G

Table 12 shows the parametric test data on intermediate ammonia, slip ammonia, and sulfur dioxide oxidation collected during this reporting period for the Hitachi Zosen catalyst. All the ammonia data are corrected to reactor inlet oxygen concentration. The long term NO_x reduction is also given in this table as an average over the operating periods shown, i.e., for January - March and April - July of 1995. The long term NO_x reduction data indicates the average performance of the catalyst at or near the design operating conditions of 0.8 NH_3/NO_x ratio, 400 SCFM flow rate, and 700 °F reactor temperature.

The intermediate ammonia measurements were made after the first catalyst bed and at conditions thought to give the best kinetic information. The NO_x removals reported with the intermediate ammonia measurements are computed from the measured ammonia concentration using standard material balance techniques.

The ammonia slip data given in Table 12 are presented below in three plots: ammonia slip versus each of flow rate, NH_3/NO_x ratio, and temperature. Figure 35 shows ammonia slip versus flow rate for roughly 65% NO_x reduction and 700 °F. As expected, the trend shows increasing ammonia slip with increasing reactor flow rate. The ammonia slip is, however, relatively minor indicating the ability of the catalyst design to withstand significant increases in flow while maintaining ammonia slip limits. Since a portion of the overall reaction rate is due to mass transfer limitations, improvements in bulk mass transfer coefficients are likely mitigating the effect of increased flow on slip ammonia increases. This plot demonstrates the ability of an SCR system to follow load variations dictated by the host boiler while maintaining design specifications.

Figure 36 shows ammonia slip versus NH_3/NO_x ratio at low temperature and design flow rate. The plot shows a slight increase in ammonia slip as the NH_3/NO_x ratio increases from 0.45 to 0.65. This finding is in keeping with published data of this type.

Ammonia slip versus temperature for design flow and roughly 55% NO_x reduction is plotted in Figure 37. Some improvement (decrease) in ammonia slip is noted between 620 and 700 °F, likely due to improvements in the kinetic reaction rate with increasing temperature. Only slight improvements could be noted in the kinetic reaction rate with increasing temperature. Thus may possibly be due to mass transfer limitations that become controlling at these higher temperatures. In general, the plot demonstrates that in terms of ammonia slip, significant improvements are not

realized with temperatures above 700 °F. Losses in boiler efficiency would probably outweigh any improvements that may be obtained in ammonia slip by designing an SCR reactor to operate at temperatures near 750 °F.

SO_2 oxidation at design temperature and flow rate was -0.51%. In this case there was an apparent loss in sulfur trioxide across the reactor. It is believed that the apparent loss is caused by acid condensation on cold spots at the reactor surface. The SO_2 oxidation data is corrected to reactor outlet oxygen concentrations. The value for sulfur trioxide produced in the reactor is based on measured inlet and outlet sulfur trioxide concentration values (table showing SO_2 oxidation rate quotes reactor flow rate as calculated for the reactor exit, since outlet SO_3 is measured at this point).

Flue gas velocity (three-point) profiles were conducted near design operating conditions (700 °F, 400 SCFM) at the reactor inlet and reactor outlet. The flue gas velocity profiles are presented in Figure 38 (reactor inlet) and Figure 39 (reactor outlet). The average inlet and outlet velocities were 14.0 ± 2.7 ft/sec and 18.4 ± 1.3 ft/sec, respectively. The N_2O concentrations were also measured at the reactor inlet (2.0 ppmv) and at the reactor outlet (1.6 ppmv, both measurements are dry at 3% O_2).[1]

TABLE 12. REACTOR G DATA (5TH SEQUENCE)

INTERMEDIATE AMMONIA PARAMETRIC TEST DATA

FLOW RATE (SCFM)	TEMP. (°F)	INLET O_2 (%)	INLET NO_x (ppmv)	NH_3/NO_x RATIO	INT. NH_3 (ppmv)	INT. NO_x REDUCTION (%)
470	624	4.581	322	0.568	71.6	34.5
291	707	4.496	310	0.551	23.0	47.7
478	703	6.710	333	0.409	26.4	32.9
464	708	4.296	298	0.582	39.3	45.1
479	696	4.442	332	0.682	59.0	50.4
617	711	5.271	317	0.512	45.2	36.9
492	753	4.764	343	0.508	41.4	38.7

SLIP AMMONIA PARAMETRIC TEST DATA

FLOW RATE (SCFM)	TEMP. (°F)	INLET O_2 (%)	INLET NO_x (ppmv)	NH_3/NO_x RATIO	SLIP NH_3 (ppmv)
272	624	5.210	368	0.622	BDL
443	624	4.256	325	0.489	BDL
445	625	4.168	338	0.650	0.7
518	623	5.218	324	0.558	2.1
665	629	5.075	320	0.542	5.5
437	704	4.165	337	0.501	BDL
438	705	4.158	337	0.661	0.7
531	709	4.903	325	0.534	2.0
624	706	3.967	361	0.451	2.3
649	706	4.059	372	0.623	5.1
460	740	6.626	360	0.450	BDL
455	754	6.028	356	0.609	0.8
533	756	4.849	301	0.539	2.7

TABLE 12. REACTOR G DATA (5TH SEQUENCE) - Continued

SULFUR DIOXIDE OXIDATION PARAMETRIC TEST DATA

FLOW RATE (SCFM)	TEMP. (°F)	OUTLET O_2 (%)	INLET SO_2 (ppmv)	NH_3/NO_x RATIO	MEAS. SO_3 IN (ppmv)	SO_3 OUT (ppmv)	SO_3 formed (ppmv)	OXID. RATE (%)
523	706	10.026	794	0.695	4.2	0.2	-4.0	-0.51

LONG TERM NO_x REDUCTION

TIME PERIOD	FLOW RATE (SCFM)	INLET NO_x (ppmv)	NH_3/NO_x RATIO	OUTLET NO_x (ppmv)	NO_x RED. (%)
JAN. - MAR.	400	420	0.79	66	81
APRIL - JULY	462	323	0.58	111	46

FIGURE 35

AMMONIA SLIP VS. FLOW RATE

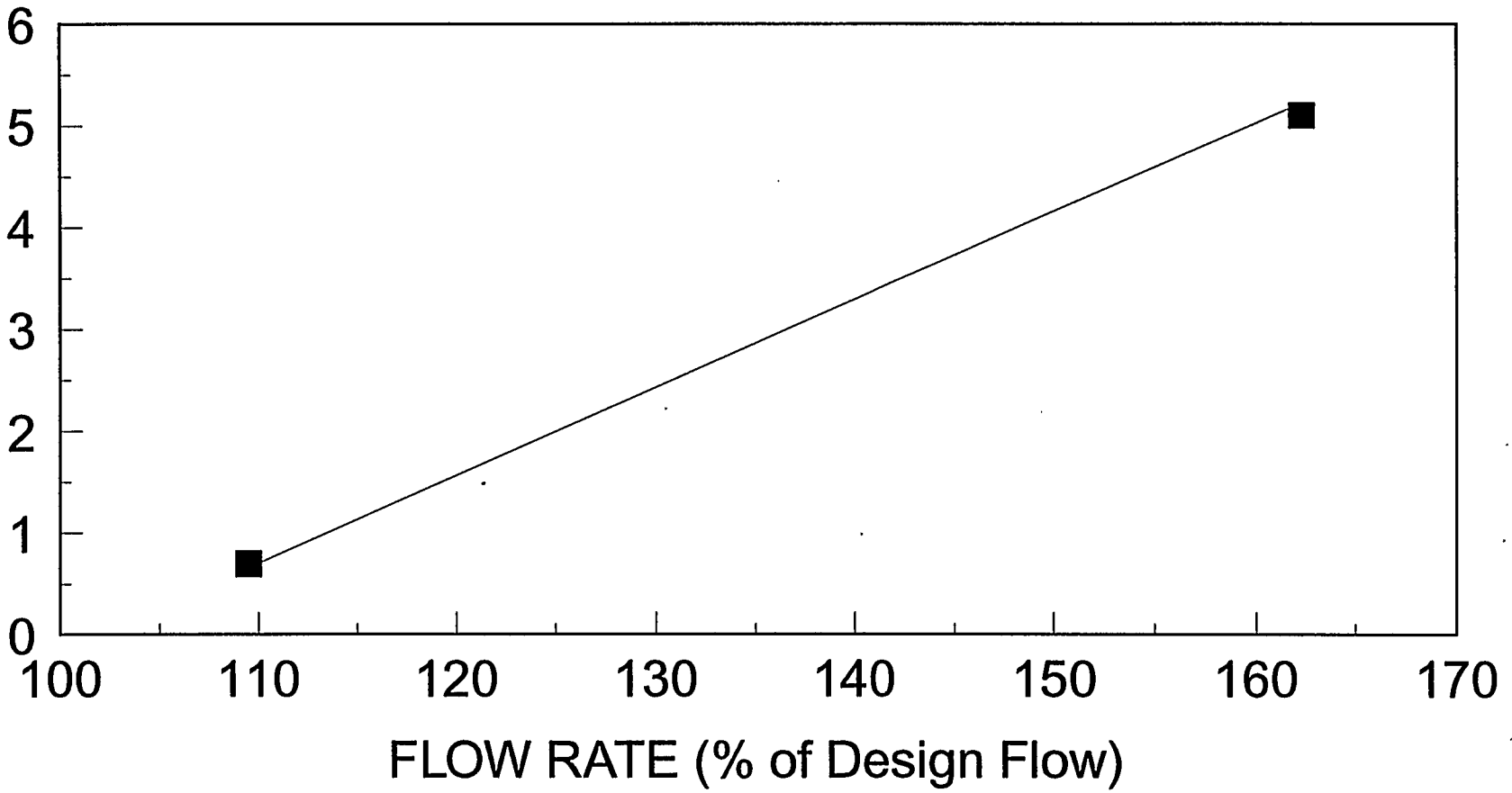

HITACHI: NH3/NOx=0.65, 700 F

FIGURE 36

AMMONIA SLIP VS. NH3/NOx RATIO

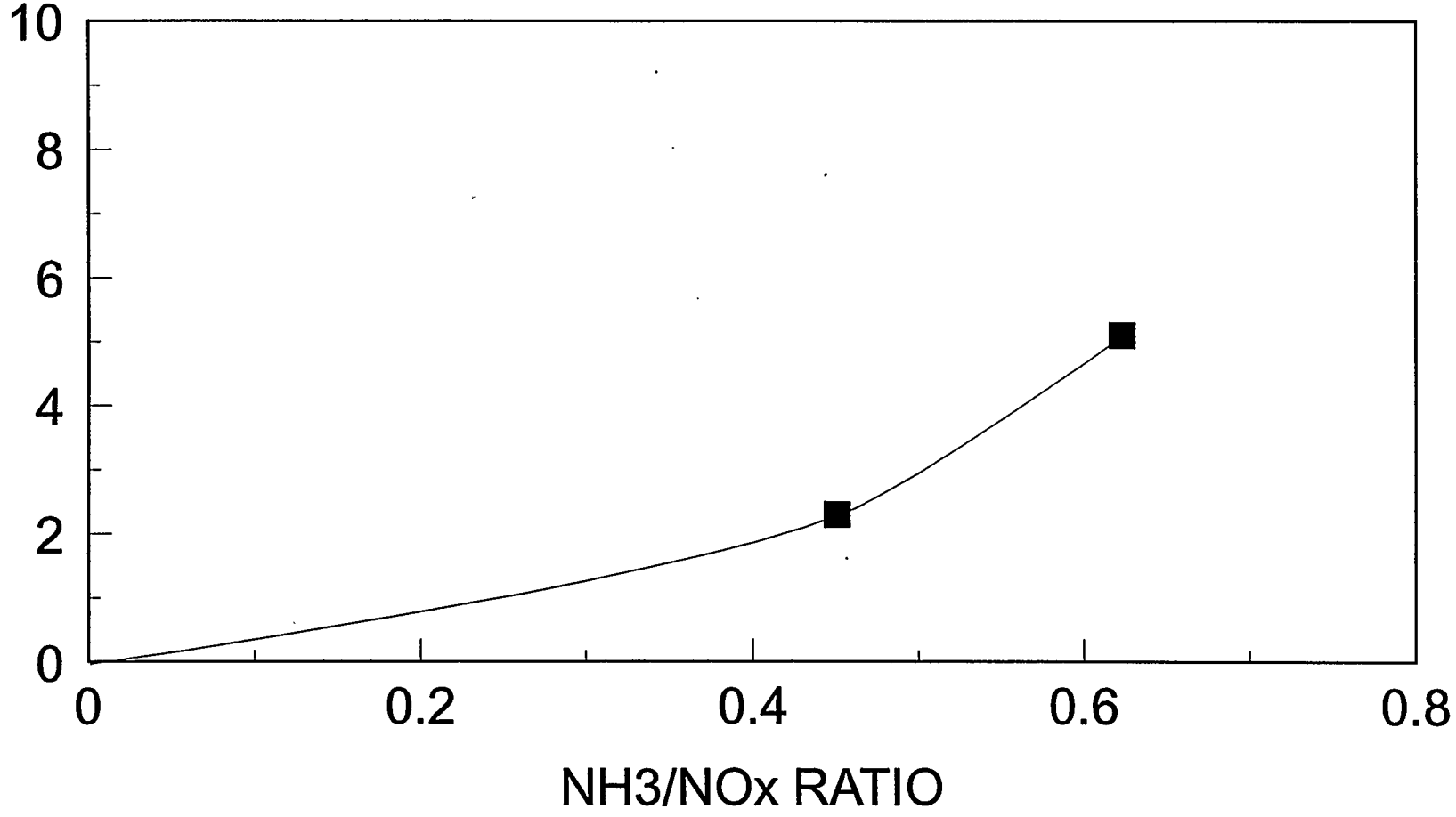

HITACHI: High Flow, 700 F

FIGURE 37

AMMONIA SLIP VS. TEMPERATURE

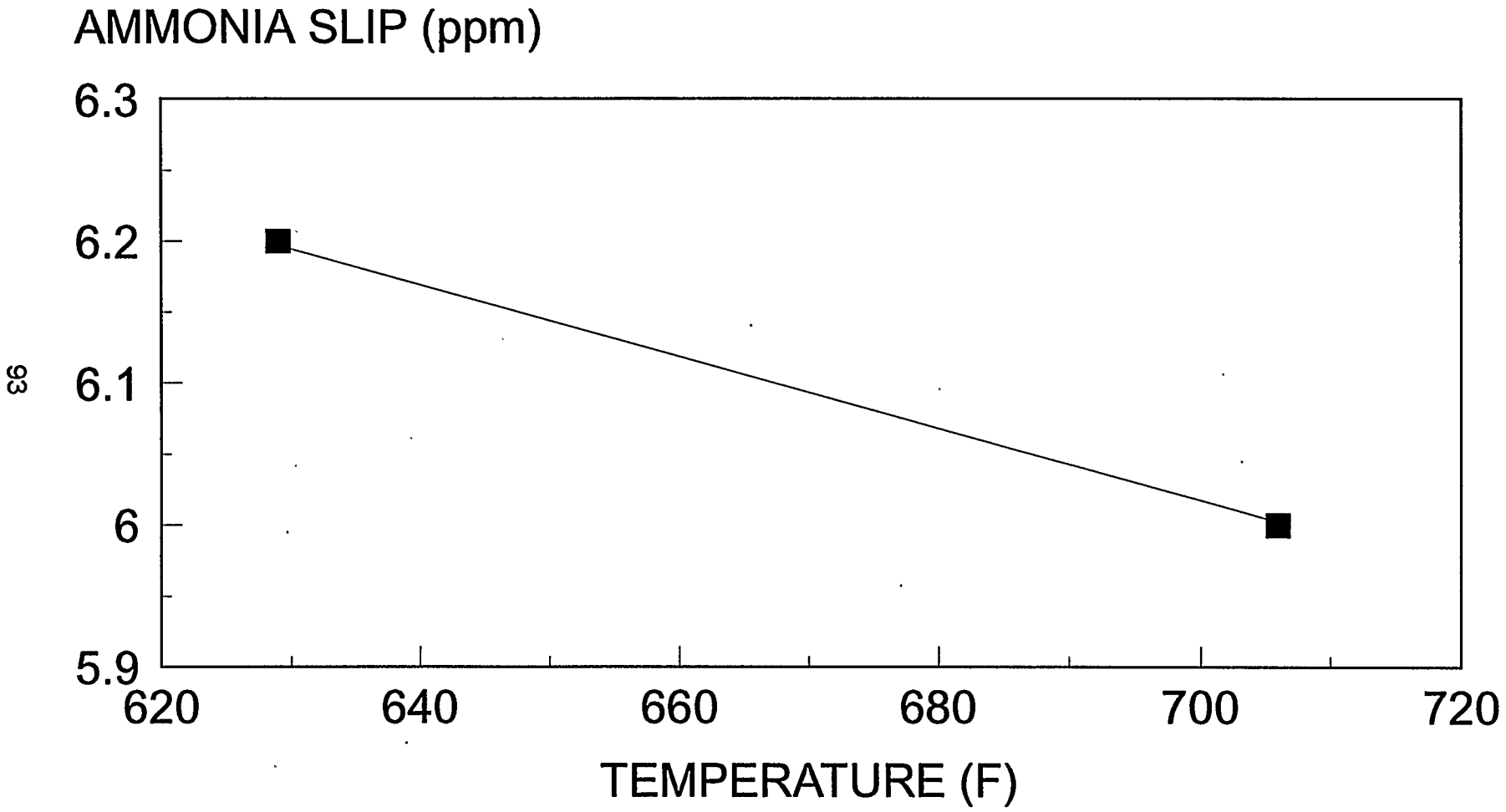

HITACHI: High Flow, NH3/NOx=0.55

FIGURE 38

REACTOR G

CATALYST LAYER 1 INLET

Velocity Profile
ft/s

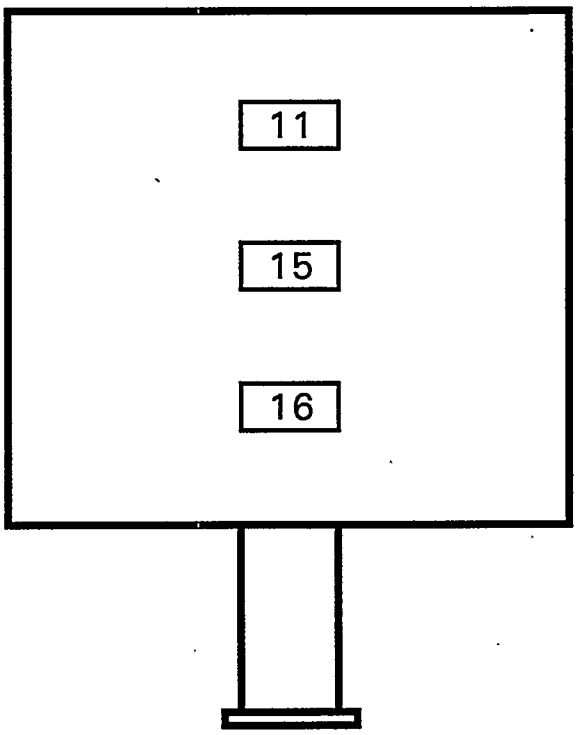

Average = 14 ft/s
σ = 3 ft/s

FIGURE 39

REACTOR G

REACTOR EXIT

Velocity Profile
ft/s

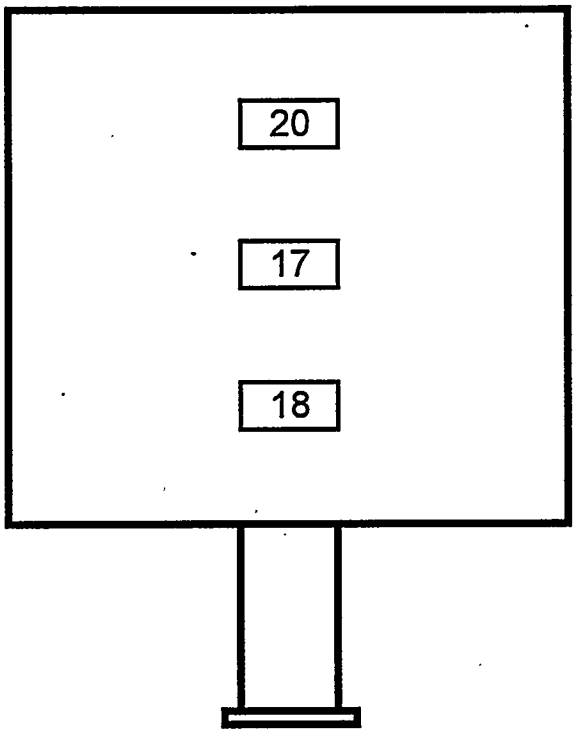

Average = 18 ft/s
σ = 1 ft/s

- Reactor J

Table 13 shows the parametric test data on intermediate ammonia, slip ammonia, and sulfur dioxide oxidation collected during this reporting period for the Cormetech low-dust catalyst. All the ammonia data are corrected to reactor inlet oxygen concentration. The long term NO_x reduction is also given in this table as an average over the operating periods shown, i.e., for January - March and April - July of 1995. The long term NO_x reduction data indicates the average performance of the catalyst at or near the design operating conditions of 0.8 NH_3/NO_x ratio, 400 SCFM flow rate, and 700 °F reactor temperature. As can be noted in the first quarter data averages, analytical errors and drift in calibrations led to valued falsely indicating NO_x reduction higher than the NH_3/NO_x ratio.

The intermediate ammonia measurements were made after the first catalyst bed and at conditions thought to give the best kinetic information. The NO_x removals reported with the intermediate ammonia measurements are computed from the measured ammonia concentration using standard material balance techniques.

The ammonia slip data given in Table 13 are presented below in three plots: ammonia slip versus each of flow rate, NH_3/NO_x ratio, and temperature. Figure 40 shows ammonia slip versus flow rate for roughly 55% NO_x reduction and 700 °F. As expected, the trend shows increasing ammonia slip with increasing reactor flow rate. The ammonia slip is, however, relatively minor indicating the ability of the catalyst design to withstand significant increases in flow while maintaining ammonia slip limits. Since a portion of the overall reaction rate is due to mass transfer limitations, improvements in bulk mass transfer coefficients are likely mitigating the effect of increased flow on slip ammonia increases. This plot demonstrates the ability of an SCR system to follow load variations dictated by the host boiler while maintaining design specifications.

Figure 41 shows ammonia slip versus NH_3/NO_x ratio at low temperature and design flow rate. The plot shows sharp increases in ammonia slip as the NH_3/NO_x ratio increases from 0.45 to 0.65. This finding is in keeping with published data of this type.

Ammonia slip versus temperature for design flow and roughly 50% NO_x reduction is plotted in Figure 42. Some improvements (decrease) in ammonia slip is noted between 620 and 700 °F, likely due to improvements in the kinetic reaction rate with increasing temperature. No improvements are noted with increasing temperatures above 700 °F. This may possibly be due to

mass transfer limitations that have become controlling at these higher temperatures. In general, the plot demonstrates that in terms of ammonia slip, significant improvements are not realized with temperature above 700 °F. Losses in boiler efficiency would probably outweigh any improvements that may be obtained in ammonia slip by designing an SCR reactor to operate at temperatures near 750 °F.

SO_2 oxidation at design temperature and flow rate was 0.18%. The SO_2 oxidation data is corrected to reactor outlet oxygen concentrations. The value for sulfur trioxide produced in the reactor is based on measured inlet and outlet sulfur trioxide concentration values (table showing SO_2 oxidation rate quotes reactor flow rate as calculated for the reactor exit, since outlet SO_3 is measured at this point).

Flue gas velocity (three-point) profiles were conducted near design operating conditions (700 °F, 400 SCFM) at the reactor inlet and reactor outlet. The flue gas velocity profiles are presented in Figure 43 (reactor inlet) and Figure 44 (reactor outlet). The average inlet and outlet velocities were 17.7 ± 0.5 ft/sec and 21.5 ± 0.3 ft/sec, respectively. The N_2O concentrations were also measured at the reactor inlet (2.0 ppmv) and at the reactor outlet (2.9 ppmv, both measurements are dry at 3% O_2).[1] Although an apparent increase in N_2O occurred across the reactor, this increase was within measurement variability.

TABLE 13. REACTOR J DATA (5TH SEQUENCE)

INTERMEDIATE AMMONIA PARAMETRIC TEST DATA

FLOW RATE (SCFM)	TEMP. (°F)	INLET O_2 (%)	INLET NO_x (ppmv)	NH_3/NO_x RATIO	INT. NH_3 (ppmv)	INT. NO_x REDUCTION (%)
411	624	7.823	220	0.609	7.0	57.7
252	706	9.672	192	0.588	2.9	57.3
427	706	7.852	232	0.426	4.4	40.7
417	706	8.243	225	0.564	6.0	53.7
423	704	8.096	243	0.638	10.5	59.4
563	704	7.075	234	0.510	12.9	45.5
417	754	8.124	223	0.557	6.5	52.7

SLIP AMMONIA PARAMETRIC TEST DATA

FLOW RATE (SCFM)	TEMP. (°F)	INLET O_2 (%)	INLET NO_x (ppmv)	NH_3/NO_x RATIO	SLIP NH_3 (ppmv)
236	624	9.982	211	0.648	0.5
403	625	8.285	229	0.471	0.6
403	624	8.309	234	0.619	0.8
447	622	7.649	255	0.382	1.5
561	625	6.623	233	0.534	3.7
404	706	7.671	223	0.47	BDL
403	707	7.677	225	0.63	0.5
453	707	6.929	238	0.538	1.8
552	705	7.673	231	0.467	0.7
537	753	7.667	224	0.615	0.9
552	706	5.925	235	0.538	2.8
407	756	7.667	208	0.458	BDL
405	753	7.665	211	0.603	0.6
452	756	6.378	308	0.400	1.9

TABLE 13. REACTOR J DATA (5TH SEQUENCE) - Continued

SULFUR DIOXIDE OXIDATION PARAMETRIC TEST DATA

FLOW RATE (SCFM)	TEMP. (°F)	OUTLET O_2 (%)	INLET SO_2 (ppmv)	NH_3/NO_x RATIO	MEAS. SO_3 IN (ppmv)	SO_3 OUT (ppmv)	SO_3 formed (ppmv)	OXID. RATE (%)
517	708	9.920	904	0.477	4.7	6.3	1.6	0.18

LONG TERM NO_x REDUCTION

TIME PERIOD	FLOW RATE (SCFM)	INLET NO_x (ppmv)	NH_3/NO_x RATIO	OUTLET NO_x (ppmv)	NO_x RED. (%)
JAN. - MAR.	399	422	0.75	26	88
APR. - JUL.	395	333	0.61	87	60

FIGURE 40

AMMONIA SLIP VS. FLOW RATE

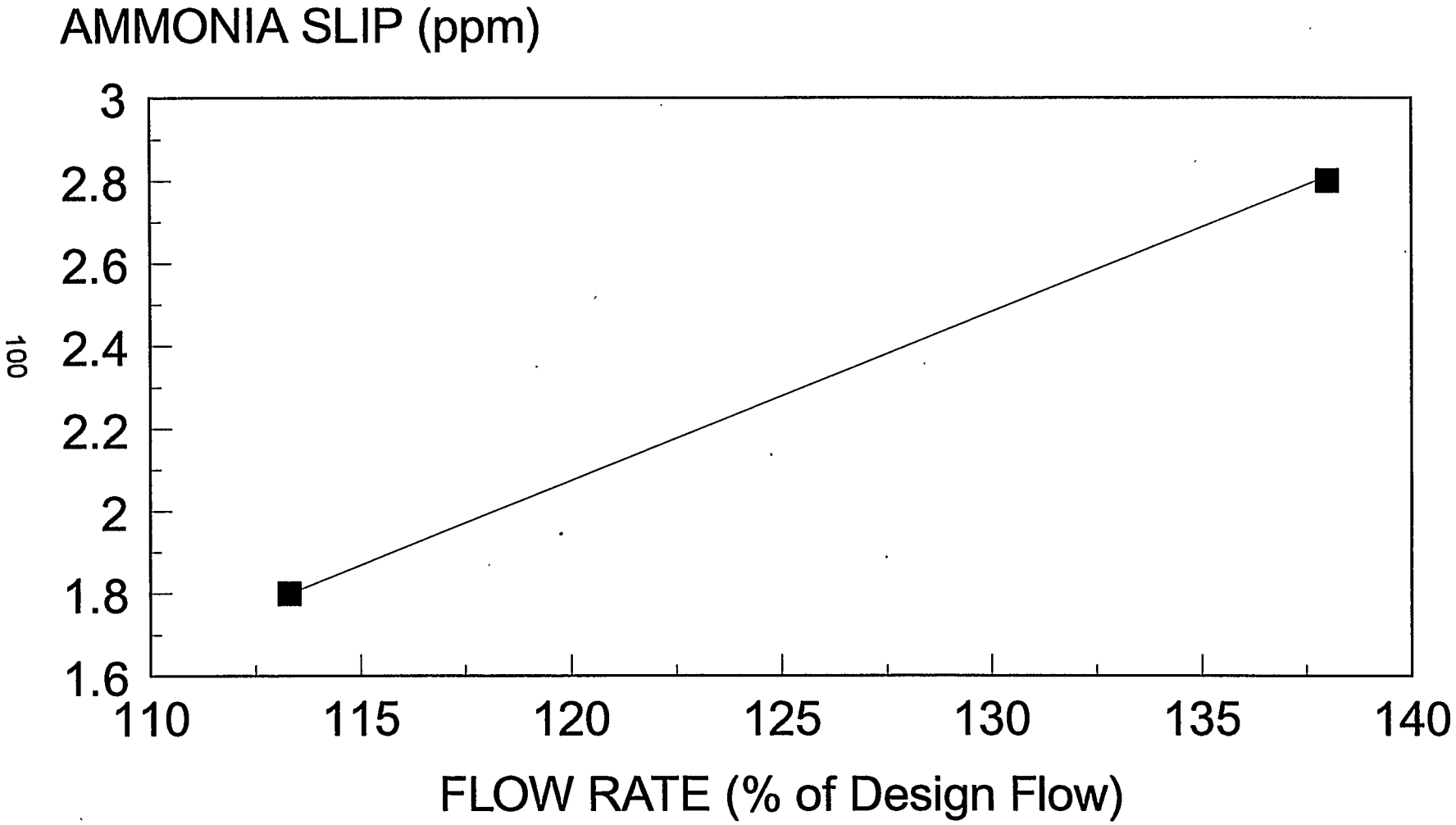

CORM LD: NH3/NOx=0.55, 700 F

FIGURE 41

AMMONIA SLIP VS. NH3/NOx RATIO

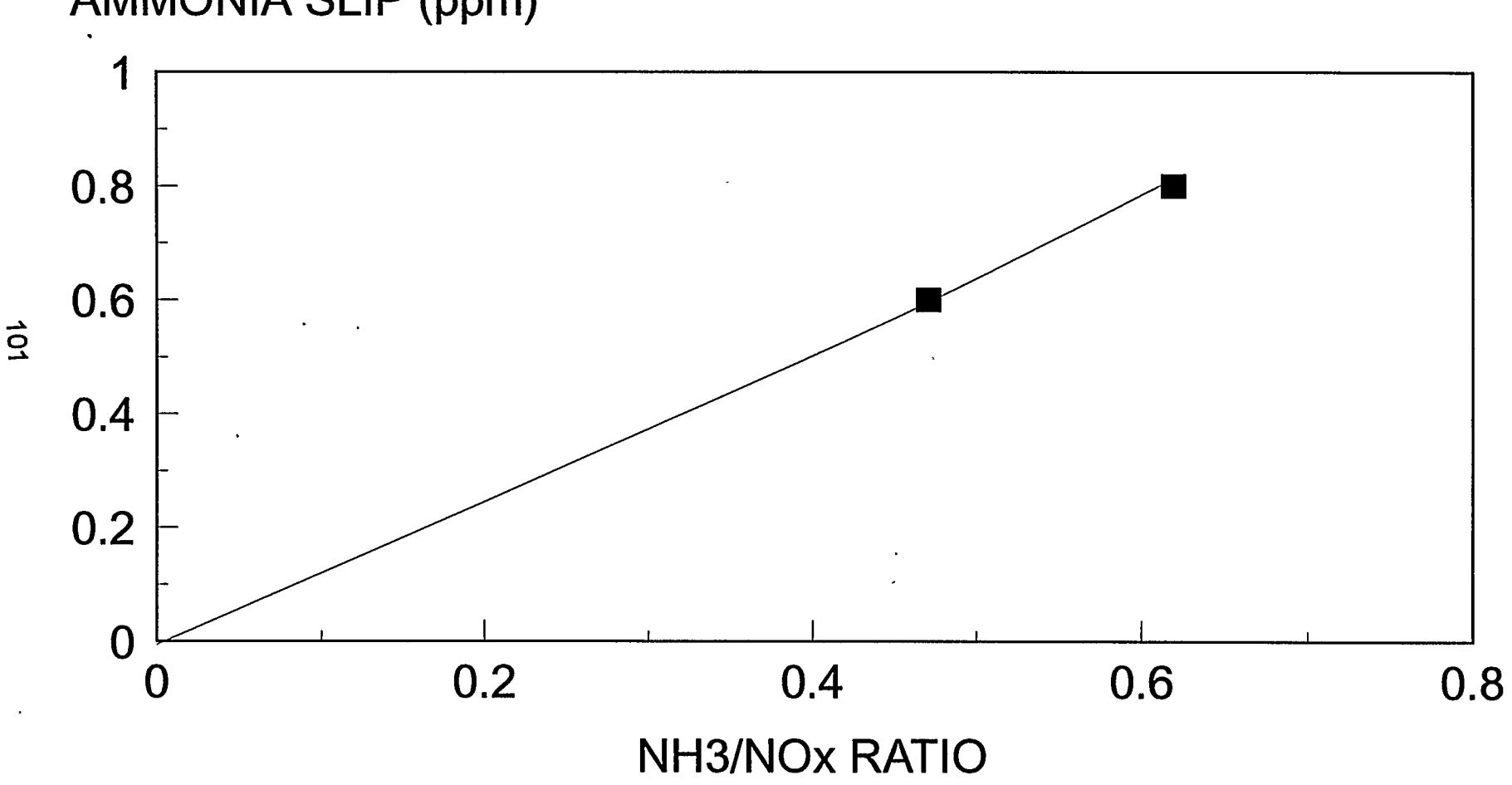

CORM LD: Design Flow, 620 F

FIGURE 42

AMMONIA SLIP VS. TEMPERATURE

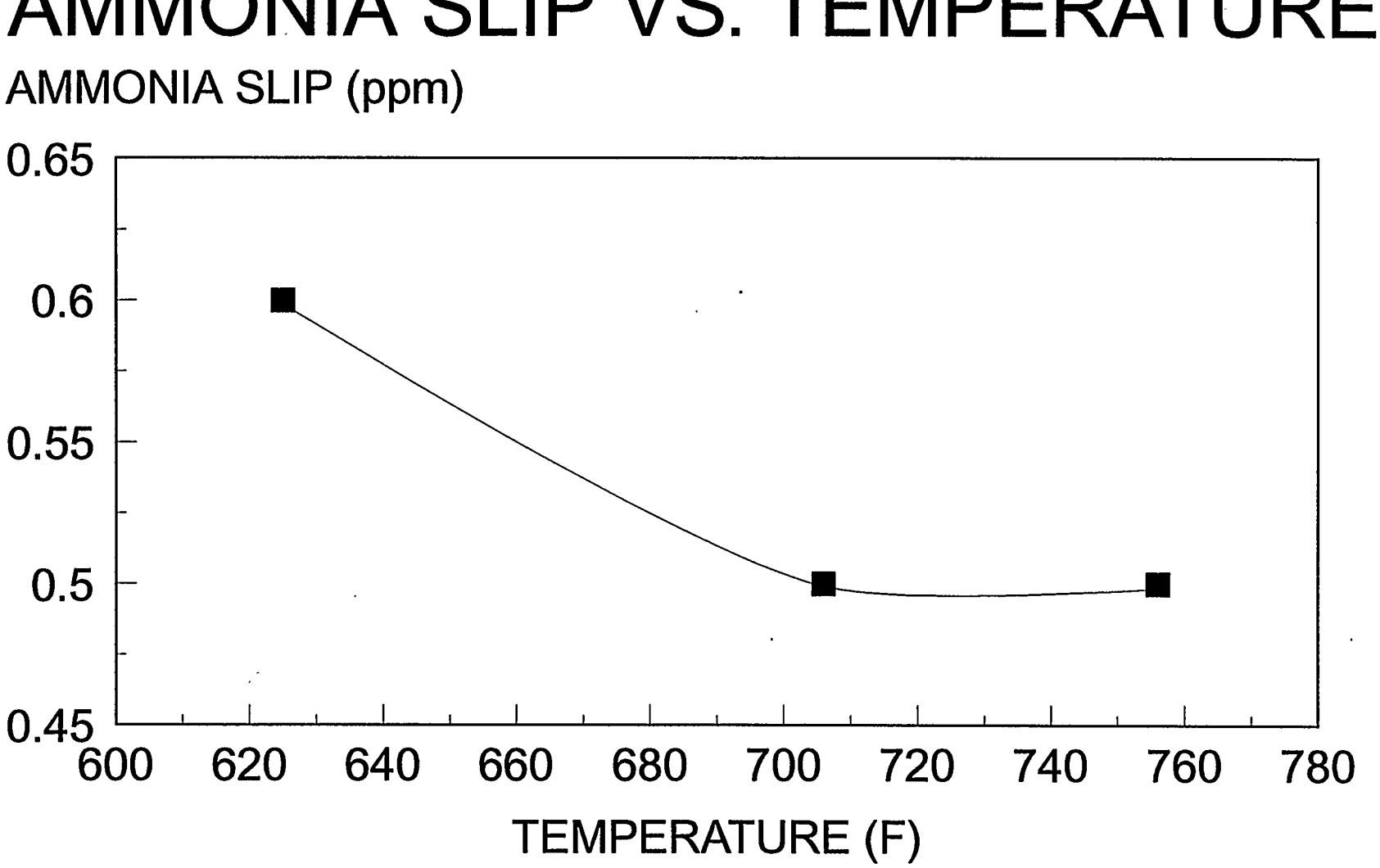

CORM LD: Design Flow, NH3/NOx=0.50

FIGURE 43

REACTOR J

CATALYST LAYER 1 INLET

Velocity Profile
ft/s

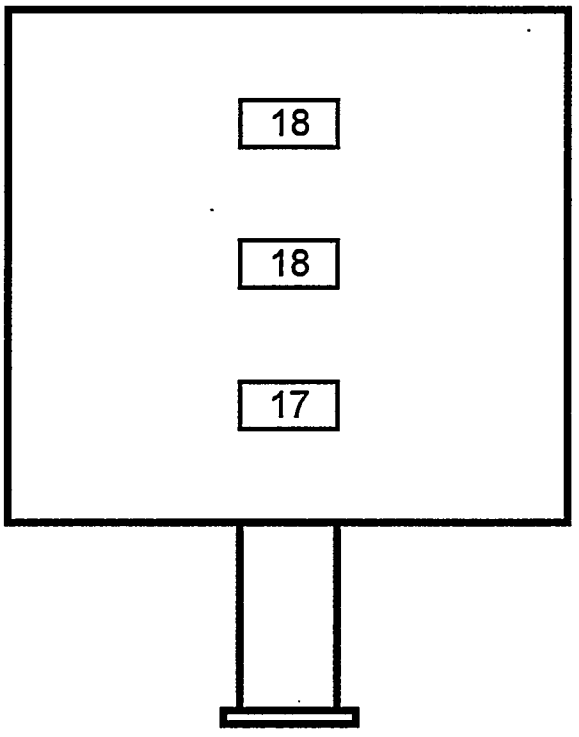

Average = 18 ft/s
σ = 0.5 ft/s

FIGURE 44

REACTOR J
REACTOR EXIT

Velocity Profile
ft/s

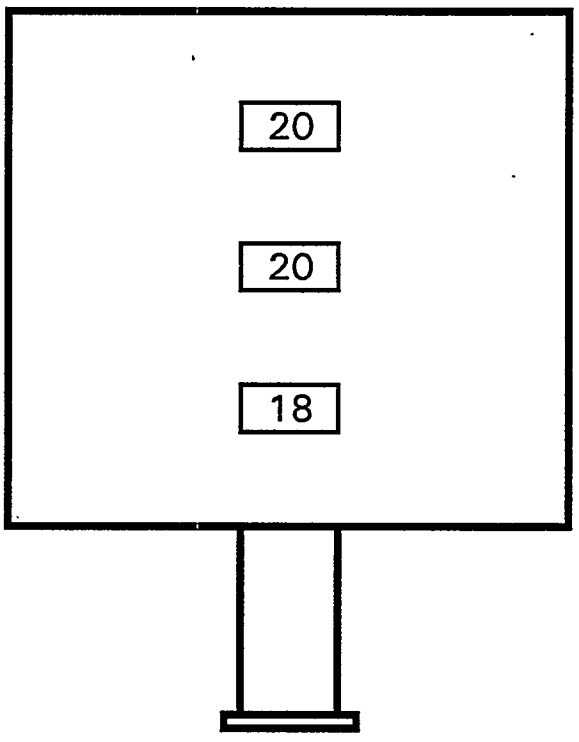

Average = 19 ft/s
σ = 1 ft/s

Task 1.3.6 - Project Management and Reporting

The Management Information System, developed for tracking overall budget and schedule information, was used to monitor budget and schedule and to help fulfill DOE reporting requirements. Monthly progress reports were submitted to DOE.

A paper was presented at the EPRI/EPA Joint Symposium on Stationary Combustion NO_x Control, Kansas City, Missouri, May 16-19, 1995, titled, "Demonstration of SCR technology for the Control of NO_x Emissions from High Sulfur Coal-Fired Utility Boilers at Plant Crist SCR Test Facility."

Facility dismantling specifications were released for solicitation.

Section 5

PLANNED ACTIVITIES

During the last two quarters of 1995, the following activities are planned:

- Award dismantling contract and complete the dismantling process by the end of 1995.
- Complete analysis of test facility data.
- Continue work on project reporting, focusing on final report.
- Continue technology transfer to both internal and external parties.
- Hold final project review meeting with all project participants.

REFERENCES

1. Testing and Analytical Services for the Innovative Clean Coal Technology Demonstration of Selective Catalytic Reduction (SCR) Technology for the Control of Nitrogen Oxide (NO_x) Emissions from High Sulfur Coal, Interim Report for Task 4, Parts 1 - 7(Reactors A - G), Long-Term Parametric Tests, Draft SRI report to SCS.

APPENDIX A

Effects of SCR Ammonia on Ammonia Volatilization, Ammonia Extraction, and Metals Extraction from SCR Fly Ash

TESTING AND ANALYTICAL SERVICES FOR THE INNOVATIVE CLEAN COAL TECHNOLOGY DEMONSTRATION OF SELECTIVE CATALYTIC REDUCTION (SCR) TECHNOLOGY FOR THE CONTROL OF NITROGEN OXIDE (NO_x) EMISSIONS FROM HIGH SULFUR COAL

Final Report

Effects of SCR Ammonia on Ammonia Volatilization, Ammonia Extraction, and Metals Extraction from SCR Fly Ash

Prepared by

Kenneth M. Cushing
Robert F. Heaphy
Edward B. Dismukes

SOUTHERN RESEARCH INSTITUTE
P.O. Box 55305
2000 Ninth Avenue, South
Birmingham, Alabama 35255-5305

Prepared for

SOUTHERN COMPANY SERVICES, INC.
P.O. Box 2625
Birmingham, Alabama 35202-2625

DOE Prime Contract Number DE-FC22-89-PC89652
SCS Contract Number C-92-000320
SRI Project Number 7613
SRI Report Number SRI-ENV-95-415-7613

October 20, 1995

TABLE OF CONTENTS

LIST OF FIGURES

LIST OF TABLES

ACKNOWLEDGEMENTS

The authors wish to thank the many Southern Research Institute employees who contributed their efforts in performing the testing and analytical services reported herein, especially Mr. Randy Hinton and Mr. James Garrett, the SRI on-site staff at the Plant Crist SCR Test Facility, and Ms. Wynema Kimbrough and Mr. Dave Smith of our Birmingham office. We are also grateful to Scott Hinton, Ph.D., Southern Company Services' on-site SCR Project Engineer, for his support and encouragement during this test program.

Section 1

EXECUTIVE SUMMARY

This report summarizes the results of a laboratory study, conducted at Southern Research Institute for Southern Company Services, Inc., to evaluate the effects of SCR ammonia on ammonia volatilization, ammonia extraction, and metals extractability from fly ash. To conduct the study, samples of pre-reactor (ammonia-free) and post-reactor (ammonia-exposed) fly ash were collected at SCR Reactors B and C at Plant Crist.

Ammonia Extractability and Volatilization from SCR Fly Ash

Almost no ammonia volatilized from the SCR ash until a significant amount of water vapor was absorbed by the ash. A plausible mechanism for the apparent volatilization that occurred is that enough water was gained by the ash to form a moist layer with a pH high enough to evolve gas-phase ammonia from the ammonium compounds on the ash. Nearly all of the ammonia on the ash evolved to the gas phase in the closed-container experiments. Ammonia concentrations in enclosed spaces depend on the ammonia concentration of the ash, the volume of air above the ash available for dilution, and the presence of a humid atmosphere.

The extraction of ammonia from fly ash seems to depend upon pH. Evidently, all or nearly all of the ammonia present was extracted in the buffered solutions at pH 4.7 and pH 6.2, but not all was recovered in alkaline unbuffered extracts. In the pH 6.2 buffer, however, the completeness of extraction seemed to fall off somewhat as the ratio of ash to buffer increased. At 3 g of ash per 50 mL of pH 6.2 buffer, the amount of ammonia extracted was about 200 μg/g, whereas at 1 g per 50 mL, the amount was near 250 μg/g.

Ammonia concentration in the ash was much higher for the smaller particle sizes, but most of the total ammonia was found to reside with the larger particles simply because these comprise the vast majority of the ash mass. The implication is that very little slip ammonia will exit the process when high efficiency particulate emission controls are in place since all detectable ammonia is in the solid phase at the air heater exit and most of the ammonia is associated with the larger particle sizes which are most readily collected.

Metals Extractability from SCR Fly Ash

The SCR fly ash samples were subjected to extraction with water, and the extracts were analyzed for each of 28 metals. This was done to ascertain whether exposure of the fly

ash to ammonia vapor caused an enhancement of the metals extractabilities under conditions resembling those that might exist in an ash pond.

Of the 28 metals included in the study, only 17 could be detected in the fly-ash extracts. Of these 17 detectable metals, only barium underwent an increase in extractability following exposure to ammonia. The magnitude of the increase was found to depend directly on the magnitude of the NH_3/NO_x ratio in the SCR unit, however, the increase was slight for all NH_3/NO_x ratios tested. Of the 16 additional metals that could be detected in the fly-ash extracts, none displayed what we considered to be genuine enhancements in extractability, and several exhibited decreases in extractability as a result of exposure of the fly ash to ammonia. Although one of these metals -- Se -- displayed a large apparent increase in extractability on exposure to ammonia, we concluded that the selenium found in the reactor-outlet sample extracts must have condensed from the gas phase onto the fly ash at the reactor outlet. Finally, a deliberate downward adjustment in the pH of one sample solution caused enhancements in the extractabilities of several metals, most notably Mg, but also Mn, Ca, As and Fe to a lesser degree.

Section 2

INTRODUCTION

The Selective Catalytic Reduction (SCR) process is a pollution-control strategy that is designed to reduce the emissions of NO_x from power plants. In this process, gaseous ammonia is injected into the flue-gas stream, where it chemically reduces the NO_x to nitrogen gas at an elevated temperature. The SCR process has recently been evaluated at DOE's SCR Demonstration Plant at Gulf Power Company's Plant Crist.

Unfortunately, the ammonia added in the SCR process does not completely react with NO_x. Of course, it is possible to increase the efficiency of NO_x removal by increasing the amount of ammonia (i.e., by boosting the NH_3/NO_x ratio in the reactor). But this also increases the amount of excess, unreacted ammonia in the flue stream. Much of this excess ammonia is known to be taken up by the entrained fly ash, however, this almost always occurs because of a reduction in flue gas temperature as happens in an air heater. The injection of ammonia in the presence of fly ash at 700°F may not cause any ammonia to deposit or be absorbed on the fly ash. Nevertheless, the effects of absorbed ammonia on the properties of the fly ash are not well understood.

One of the major concerns about fly ash that has been exposed to ammonia in the SCR process is how the ammonia in the ash may be extracted and what will be the resulting ammonia concentration measured in the laboratory. The species is likely to occur in the ash as ammonium sulfate $(NH_4)_2SO_4$. Either the ammonium ion (NH_4^+) or free ammonia (NH_3) is likely to be easily dissolved in water. The completeness of extraction, however, may depend on the pH of the extracting medium, which regulates the balance between NH_4^+ and NH_3 in the extract. Either the innate alkalinity of the ash and the pH the ash produces when wet, or the pH of a buffer used for extraction, may influence the efficiency of ammonia removal from the ash.

Another concern is the volatility of ammonia in ash. In the form NH_4^+ there is likely to be only an infinitesimal volatility. Moisture in air, however, is capable of hydrolyzing the ammonium ion and forming the much more volatile NH_3 species:

$$NH_4^+ (aq) + H_2O (l) = NH_3 (aq) + H_3O^+ (aq)$$

The hydronium ion, or hydrated proton shown as a product in this reaction, will be neutralized by alkalinity in the ash, and thus the reaction made to proceed further toward completion. Air with a high relative humidity which may lead to a high concentration of adsorbed moisture, or liquid water that actually wets the ash, are likely to increase volatilization.

Still another major concern about the presence of ammonia in the fly ash is whether the ammonia influences the water extractability of pollutant metals from the ash. That is, will the presence of ammonia in the ash lead to an increase in the amount of dissolved metals in the ash ponds? Clearly, the answer to this question could have a significant impact on the ability of a power plant to meet the requirements of its regulatory pollutant-discharge permits.

This report describes a brief laboratory study performed at Southern Research Institute (Southern Research), for Southern Company Services, Inc., to address the questions of ammonia extractability, ammonia volatilization, and metals extractability from ammonia-exposed fly ash. Samples of fly ash were collected both upstream and downstream from SCR Reactor B and C at Plant Crist. Because the upstream ash samples had not been exposed to ammonia, their presence in this study allowed a direct comparison between ammonia-free and ammonia-containing ash from the same flue gas stream, as well as the attendant effects of temperature reduction as the flue gas passed through the air heater.

Section 3 of this report describes the various ash samples collected for these studies. Section 4 describes the results of the ammonia extractability and volatilization tests. The results of tests on metals extractability from SCR fly ash are summarized in Section 5. Test data are presented in various tables throughout each section.

Section 3

DESCRIPTION OF ASH SAMPLES

Ash samples for this work were obtained during the last two weeks of January 1995 during routine operation of the Plant Crist SCR Demonstration Plant. Three bulk samples of hopper ash were collected from the cyclones located downstream from the air heaters on large SCR reactors B and C. These ash samples were collected from the cyclone hoppers following a full day of reactor operation at one of three SCR parametric operating conditions. A full day of operation prior to sample collection at each test condition was required to provide sufficient time for ammonia equilibrium to be achieved. The reactor's flow rate and temperature were identical at all three parametric conditions - 5000 scfm (wet) and 700 °F, respectively. Only the ammonia to nitrogen oxides ratio (NH_3/NO_x) differed. The NH_3/NO_x ratios were 0.6 (Test Condition 21), 0.8 (Test Condition 22), or 1.0 (Test Condition 24). Hopper samples were collected from the Reactor B cyclone hopper for Test Conditions 21 and 24. For Test Condition 22 a cyclone hopper sample was collected from Reactor C.

A second set of fourteen ash samples was collected from Reactor B while operating at Test Conditions 21, 22, and 24. Table 3-1 provides information about each sample (test location, date of test, start time, end time, etc.). The samples were collected isokinetically using an in-stack filter simultaneously at two locations. Fly ash samples upstream of ammonia injection were collected at test ports located downstream of the reactor venturi flow meter. Ash samples downstream of ammonia injection were collected at the outlet of the Reactor B air heater.

A third set of size-segregated ash samples was collected at the outlet of the Reactor B air heater using a Southern Research five-stage cyclone, an in-stack sampling device. This device separated the particulate matter into five size fractions as it was collected. Since the cross-section of the duct at the test point was quite small (1 ft by 3 ft) in relation to the sampling device which is more than two feet in length, the samples were collected isokinetically at the center point of the duct. Two runs were completed while the reactor operated at parametric test condition 22, the normal baseline operating condition (a flue gas flow rate of 5000 scfm (wet), a flue gas temperature of 700 °F, a NH_3/NO_x ratio of 0.8).

Table 3-1. Identification of Reactor B inlet and air heater outlet ash samples.

Sample Code Number*	Test Identification Number*	Test Date	Start Time	End Time	NH_3/NO_x
BI 2	108-BI-M17-02	1/23/95	1530	1630	na
BI 3	108-BI-M17-03	1/24/95	1020	1220	na
BI 4	108-BI-M17-04	1/24/95	1445	1630	na
BI 5	108-BI-M17-05	1/25/95	930	1130	na
BI 6	108-BI-M17-06	1/25/95	1500	1630	na
BI 7	108-BI-M17-07	1/26/95	1010	1210	na
BI 8	108-BI-M17-08	1/26/95	1430	1615	na
BAO 2	108-BAO-M17-02	1/23/95	1535	1635	0.8
BAO 3	108-BAO-M17-03	1/24/95	1020	1220	0.8
BAO 4	108-BAO-M17-04	1/24/95	1446	1617	0.8
BAO 5	108-BAO-M17-05	1/25/95	930	1130	0.6
BAO 6	108-BAO-M17-06	1/25/95	1500	1630	0.6
BAO 7	108-BAO-M17-07	1/26/95	1010	1210	1.0
BAO 8	108-BAO-M17-08	1/26/95	1430	1615	1.0
Cyclone 1	128-BAO-CYC-01	6/17/95	959	1059	0.8
Cyclone 2	128-BAO-CYC-02	6/17/95	1330	1430	0.8

* – BI - Reactor B Inlet; BAO - Reactor B Air Heater Outlet
na – Not applicable to inlet tests.

Section 4

INVESTIGATION OF AMMONIA EXTRACTABILITY AND VOLATILIZATION FROM FLY ASH

Prior to the volatilization and extraction studies, the ammonia content of the hopper ash samples was determined by extracting a one-gram sample of the ash in fifty milliliters of deionized water to which 4 drops of 1:1 sulfuric acid had been added. Ammonia concentrations were determined by the ion-specific-electrode method. The results of these extractions are shown in Table 4-1. As expected, higher ammonia concentrations were measured for the fly ash samples collected during operation at higher NH_3/NO_x ratios. (It is important to note that the addition of 1:1 sulfuric acid, as described here, makes a pH of about 1.7 in the ash slurry. This pH is substantially more acidic than that in either of the buffers described later for controlling the pH during ammonia extraction.)

An ammonia train was run at the Reactor B air heater outlet after the collection of the seven isokinetic ash samples to measure total ammonia in the gas stream. All ammonia concentrations were determined by the ion-specific-electrode method. The total ammonia concentration measured by the ammonia train and the solid phase ammonia concentration from the ash sample collected at the outlet of the air heater were used to determine ammonia partitioning between the gas and solid phases. Table 4-2 shows the results of these analyses and the resulting ammonia partitioning. Solid-phase ammonia concentrations are shown both on a mass fraction basis and a volume basis corrected to 3% O_2 (dry). The gas-phase ammonia concentration was calculated as the difference between the total ammonia and solid-phase ammonia concentrations. Please note that the samples were collected on different days. This could account for some of the variability observed in the ammonia partitioning. The average ratio of solid-phase ammonia to gas-phase ammonia was 0.53, 3.3, and 0.38 for NH_3/NO_x ratios of 0.6, 0.8, and 1.0, respectively.

Solid-Phase Ammonia Concentration and Ash Slurry pH

Two preliminary analyses of the isokinetic ash samples were performed before they were forwarded to Southern Research's Birmingham laboratories for trace metals analysis. The pH of each sample when 0.1 g of ash from the filter catch was mixed with 50 mL of deionized water was measured. The mixture of ash and water was placed in a sealed bottle and agitated for four hours before measuring the pH. The pH of the ash-water mixtures for the samples collected upstream of ammonia injection ranged from 7.90 to 9.94. For the ash samples collected at the air heater outlet for NH_3/NO_x ratios of 0.6, 0.8, and 1.0, the average pH values were 9.20, 9.34, and 9.77, respectively. Also, one-gram samples of the ash were placed in 50 mL of deionized water with four drops of 1:1 sulfuric

Table 4-1. Ammonia concentrations of the SCR hopper ash samples used in the ammonia volatilization experiments.

Parametric Condition	SCR Reactor	NH_3/NO_x	Reactor Flow Rate, scfm; wet	Reactor Inlet Temperature, °F	Average NH_3* Conc., µg/g
21	B	0.6	5,000	700	48
22	C	0.8	5,000	700	254
24	B	1.0	5,000	700	352

*: Extractions performed by placing 1 g of ash in a beaker, adding 50.0 ml D.I. H_2O, 4 drops of 1:1 H_2SO_4, and stirring for 5 minutes.

Table 4-2. Partitioning of ammonia slip between gas phase and solid phase at the outlet of the B reactor air heater.

Sample Number Code	NH_3/NO_x	Total NH_3, ppm(v) @ 3%O_2 (dry)	Mass Conc., gr/dscf @ 3%O_2 (dry)	Solid-Phase NH_3, µg/g	Solid-Phase NH_3, ppm(v) @ 3%O_2 (dry)	Gas-Phase NH_3, ppm(v) @ 3%O_2 (dry)
BAO 5	0.6	2.9	2.74	93	1.0	1.9
BAO 6	0.6	2.9	3.13	79	1.0	1.9
BAO 2	0.8	3.5	3.10	185	2.5	1.0
BAO 3	0.8	3.3	2.89	236	2.9	0.3
BAO 4	0.8	3.2	3.14	175	2.2	1.0
BAO 7	1.0	32.1	2.83	888	10.2	21.9
BAO 8	1.0	34.6	2.68	735	8.0	26.6

acid, stirred for 5 minutes, and the ammonia concentration measured with an ion-specific electrode (these data are also included in Table 4-2). As expected, no ammonia (generally less than the detection limit) was found in the ash samples collected upstream of ammonia injection. Average ammonia concentrations in the ash samples collected at the air heater outlet for NH_3/NO_x ratios of 0.6, 0.8, and 1.0 were 86, 199, and 812 μg/g, respectively. The results of these analyses are shown in Table 4-3.

Also included in this table are the measured pH and ammonia concentrations for the three cyclone hopper samples from Reactors B and C. The pH values for the hopper ash samples were slightly higher on average (10.23) than those from the air heater outlet (9.42). A possible explanation for this is that the cyclone hopper ash is coarser in particle size, has a lower surface/mass ratio, contains less adsorbed SO_3, and therefore is more alkaline. The ammonia concentrations shown in Table 4-3 are different from those in Table 4-1 because separate analyses were performed. For comparison the pH of a de-ionized water blank is also presented.

Ammonia Volatilization from the Ash

Ammonia volatilization tests were performed by placing thirty-gram samples of hopper ash in a petri dish and a beaker containing 50 mL of 0.1 N sulfuric acid together in individual, sealed, 2.65 L plastic containers. The ammonia concentration of the acid solution was measured to determine the extent of transfer of ammonia from the ash to the liquid. Three trials were needed to produce appropriate results. Initially, it was assumed (incorrectly) that the ammonia on the ash would volatilize continuously. Duplicate samples of ash from each of the three operating conditions (at the three NH_3/NO_x ratios) were placed in six containers, two for each NH_3/NO_x ratio. The first sample for each NH_3/NO_x ratio was analyzed after 14 days had elapsed. It was found that nearly all of the ammonia from the ash had transferred to the acid solution. The second sample was then analyzed two days later, confirming the earlier result. Table 4-4 summarizes these test results. Between 71% and 99% of the original ammonia in the ash volatilized and was captured in the sulfuric acid solution. There appeared to be a dependency of volatilization on the original concentration of ammonia in the ash, however, the NH_3 remaining on the ash was more or less independent of the ammonia initially present on the ash. Ammonia recovery values were 87% or higher.

It should be noted that the samples in the initial closed-container experiment were subjected to wide variations in temperature. Overnight temperatures fell below 30°F in the laboratory when no heat was on over a weekend. Normal indoor temperatures above 70°F prevailed during working hours. At the cooler temperature, the air in the sealed containers became saturated with water vapor and condensation was observed on the interior container walls. When the containers were opened to analyze the acid solution for ammonia, it was also observed that the ash sample had agglomerated.

Table 4-3. Mass concentration, slurry pH, and NH_3 concentration for the isokinetic ash samples and the hopper ash samples used for the SCR ash study.

Sample Code Number	Mass Concentration gr/dscf @ 3% H_2O (dry)	NH_3/NO_x	pH *	NH_3 Conc. µg/g
BI 2	2.93	na	9.44	<6
BI 3	3.01	na	9.03	5
BI 4	3.20	na	7.98	<4
BI 5	3.15	na	7.90	8
BI 6	3.26	na	8.82	<6
BI 7	2.92	na	8.90	<6
BI 8	2.64	na	9.05	6
BAO 2	3.10	0.8	9.94	185
BAO 3	2.89	0.8	8.87	236
BAO 4	3.14	0.8	9.22	175
BAO 5	2.74	0.6	9.21	93
BAO 6	3.13	0.6	9.19	79
BAO 7	2.83	1.0	9.69	888
BAO 8	2.68	1.0	9.85	735
Hopper Ash Sample		0.6	10.17	49
Hopper Ash Sample		0.8	10.10	234
Hopper Ash Sample		1	10.43	349
D.I. H_2O Blank			5.60	

* samples were agitated in sealed bottles for 4 hours before measuring pH (except D.I. H_2O)

The initial attempt to characterize ammonia volatilization from the SCR ash indicated that water absorption and the resulting pH may play an important role in the mechanisms involved. The behavior of the pH of a mixture of SCR ash and deionized water over a period of about 8 minutes is shown in Figure 4-1. Fifty milliliters of deionized water were allowed to come to pH equilibrium with the atmosphere and one gram of ash was then added while the mixture was stirred. The pH of the slurry dropped immediately from 5.3 to 3.7 and then rose rapidly until finally stabilizing at 11.1. The volatilization of the ammonium compounds on the ash to gaseous ammonia would be expected to begin as the pH rose to 9 and above.

The results of a second closed-container volatilization experiment are shown in Table 4-5. Samples of condition 22 ash, prepared as in the first closed-container test, were analyzed after 1, 2, 3, and 7 days. The air temperature in the laboratory was kept near 70 °F. Almost no ammonia was found in the sulfuric acid solution for the first three days (0.1 to 0.2%), however, a significant percentage of the ammonia (87%) had transferred to the acid solution after 7 days. The weight gain of the ash samples, presumably due to absorbed water, was also measured. Almost no ammonia transfer was noted when the weight gain of the 30 g ash sample was 1.6% after three days, however, a significant percentage of the ammonia (87%) had transferred to the acid solution when the weight gain of the ash was only 2.1% after seven days. Ammonia recovery values for this experiment were very good (87.0 to 104.3%).

A third closed-container volatilization experiment was conducted to determine when ammonia transfer from the ash to the acid solution occurred. Seven samples of condition 22 ash were placed in separate containers along with beakers of 1:1 sulfuric acid. Laboratory temperature was kept near 70 °F. A container was opened and the ash and acid solution analyzed for ammonia daily for the succeeding 7 days. Table 4-6 shows the results of these tests. Most of the ammonia was transferred from the solid to the liquid between the fourth and sixth days. As in the earlier experiment, little ammonia transfer was observed until the ash weight had increased by 1.8% or greater. Figure 4-2 shows a plot of the fractions of ammonia on the ash and in the sulfuric acid solution over the seven days of this experiment. This graph shows the rate of transfer of ammonia from one phase (solid) to another (gaseous). The two points from the fourteenth day and the sixteenth day from the earlier work were added to show the continuing nature of the ammonia volatilization.

A dynamic volatilization experiment was also run in which a large volume of ambient air was passed over a sample of ash before being scrubbed of ammonia in a set of impingers filled with 0.1 N sulfuric acid. This experiment with ash in the sample container was run twice. To determine whether ammonia actually volatilized from the ash, a third, blank test was conducted in which the identical sampling procedure was followed, but there was no ash in the sample container. A set of 100 mL impingers, two containing 50 mL of acid and a third serving as a trap, was used for the first test. Due to the small volume of acid and the long duration of the run, the liquid was lost by evaporation and it was necessary to

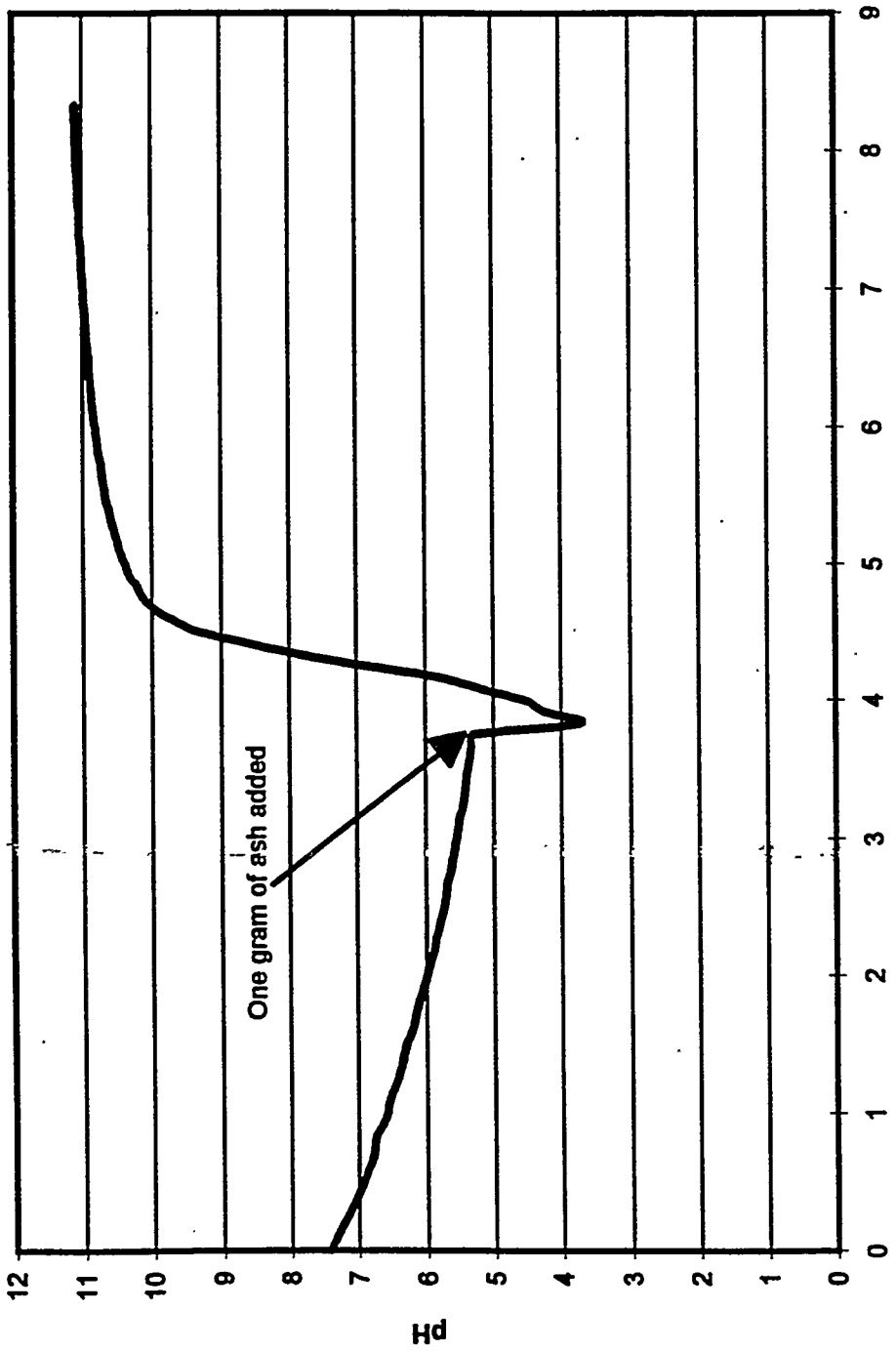

Figure 4-1. pH of a slurry of one gram of ash in fifty milliliters of deionized water.

Table 4-5. Summary of the second closed container volatilization experiment using ash collected at 0.8 NH_3/NO_x ratio.

Test Duration, days	Initial NH_3 On Ash, µg	Final NH_3 On Ash, µg	Ash Mass Gain, %	Final NH_3 in H_2SO_4, µg	NH_3 Volatilized, %	NH_3 Recovery, %
1	7,054	6,965	0.9%	7	0.1%	98.8%
2	7,053	7,344	1.3%	13	0.2%	104.3%
3	7,167	7,144	1.6%	0	0.0%	99.7%
7	7,184	333	2.1%	5,920	82.4%	87.0%

Table 4-6. Summary of the third closed container volatilization experiment using ash collected at 0.8 NH_3/NO_x ratio.

Test Duration, days	Initial NH_3 On Ash, µg	Final NH_3 On Ash, µg	Ash Mass Gain, %	Final NH_3 in H_2SO_4, µg	NH_3 Volatilized, %	NH_3 Recovery, %
1	7,358	7,285	0.8%	< 6	0.1%	99.1%
2	7,355	6,806	1.2%	11	0.2%	92.5%
3	7,325	6,949	1.5%	8	0.1%	94.9%
4	7,325	6,731	1.7%	6	0.1%	92.0%
4	7,425	6,918	1.7%	7	0.1%	93.2%
5	7,322	3,883	1.8%	1,943	26.5%	79.6%
6	7,331	1,258	1.9%	6,056	82.6%	99.8%
7	7,418	490	2.0%	5,768	77.8%	84.4%

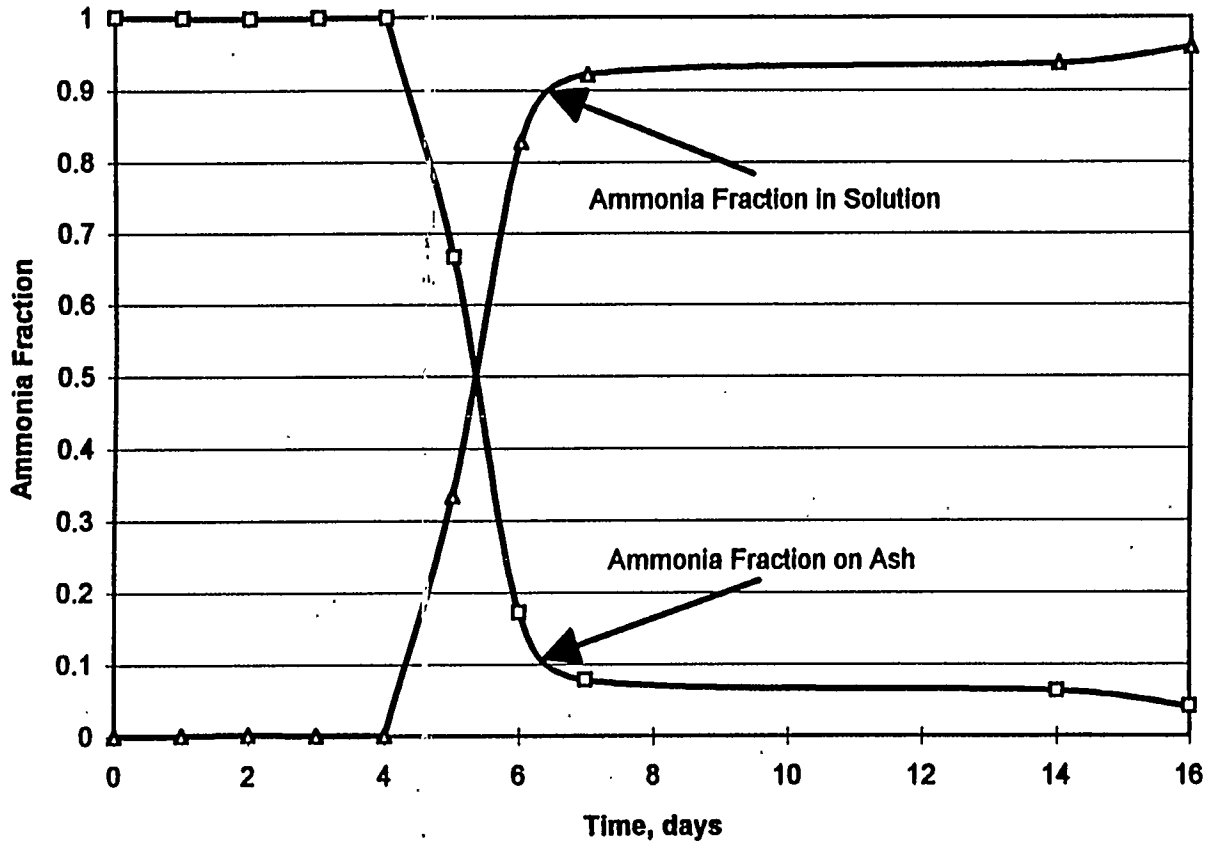

Figure 4-2. Transfer of ammonia from the solid phase to a sulfuric acid solution. Both the ash and the acid solution were in a in a sealed container.

replenish the acid solution periodically during the first run which was terminated after five days (sample 115-NHx-ASH-01). For the second test and the third blank test, three 500-mL Smith-Greenburg impingers, two containing 200 mL of 0.1 N sulfuric acid and the third serving as a trap, were used (sample 115-NHx-ASH-02 and blank 121-NHx-ASH-01). The second test was run for ten days. The blank test was run for eight days.

The analytical results of these three tests are shown in Table 4-7. A small, but measurable, mass of ammonia was collected in the impingers during all three tests, indicating that there was no measurable volatilization of ammonia from the dry ash. The ambient air used for this experiment contained an unknown and unmeasured concentration of water vapor, but it was known to be well below the saturation point (< 100% RH). Thus, in this experiment, the water vapor could not be taken up to reach the nominal 2% level and therefore little NH_3 volatilization occurred. For this test then, volatilization was prevented, not by the dynamics, but by the absence of water vapor.

Ammonia Extraction

The extraction of ammonia in an ash/water slurry was also investigated. A test matrix of nine samples defined by three different quantities of ash and three different pH levels were analyzed for ammonia content. Samples of approximately 1, 2, and 3 grams of the condition 22 hopper ash were placed in fifty milliliters of deionized water, fifty milliliters of an acetate buffer, and in fifty milliliters of a phosphate buffer, allowed to stand for 24 hours, and analyzed for ammonia concentration. The resulting pH levels and ammonia concentrations are shown in Table 4-8. Ammonia concentration of the buffered solutions agreed with predicted concentrations based on ammonia extractions in dilute sulfuric acid. However, the ammonia concentration of the ash samples extracted in deionized water were much lower than predicted.

Two factors may have produced the lower ammonia concentrations observed in the deionized water slurry. First, a portion of the ammonia may not have been extracted from the ash, and secondly, the ammonia may have escaped from the open beakers as gas-phase ammonia. Because gas-phase ammonia is liberated in solutions at higher pH levels like those observed when SCR ash was mixed with water, the water extractions were repeated using sealed bottles. The ammonia concentrations shown in Table 4-9 for the ammonia extractions in sealed bottles with deionized water were higher than when open beakers were used, but still lower than predicted. The ash filtrate was re-extracted in the acetate buffer solution with results as shown in the table. These results indicate that a portion of the ammonia escaped from the solution before the analysis was completed and that another portion was not extracted from the ash by the deionized water.

Table 4-7. Dynamic ammonia volatilization experiment.

Sample	Ash Mass, g	Liquid Sample Volume, ml	Dilution Factor	Conc., µg/ml as N	NH_3 Mass, µg	Air Volume, Standard L	NH_3 Conc. in Air, ppm(v) (dry)
115-NHx-ASH-01	260	1 3.4	1	0.645	89	23,263	0.005
115-NHx-ASH-02	220	473.8	1	0.201	116	33,927	0.004
121-NHB-ASH-01	0	388.9	1	0.0601	28	12,178	0.003

Table 4-8. Ammonia extractions from Test Condition 22 (0.8 NH_3/NO_x) hopper ash at three pH values.

Sample	Ash Mass, g	Volume, ml	Solvent	pH	D_F	Conc., µg/ml as N	NH_3 Mass, µg	Apparent NH_3 Concentration on Ash, µg/g
Buffer 1				4.62				
Buffer 2				6.18				
1	1.0155	50	Buffer 1	4.68	5	0.814	247	243
1D	1.0526	50	Buffer 1	4.67	5	0.852	259	246
2	3.0071	50	Buffer 1	4.67	10	1.19	723	240
2D	3.1297	50	Buffer 1	4.67	10	1.26	765	244
3	5.1103	50	Buffer 1	4.67	10	2.05	1245	244
3D	5.2750	50	Buffer 1	4.67	10	2.19	1330	252
4	1.0423	50	Buffer 2	6.16	10	0.485	294	283
4D	1.1374	50	Buffer 2	6.16	10	0.465	282	248
5	3.0744	50	Buffer 2	6.17	10	1.15	698	227
5D	3.0890	50	Buffer 2	6.17	10	1.19	723	234
6	5.0583	50	Buffer 2	6.18	10	1.66	1008	199
6D	5.0772	50	Buffer 2	6.19	10	1.84	1117	220
7	1.0153	50	D.I. H_2O	9.10	1	1.69	103	101
7D	1.0442	50	D.I. H_2O	9.19	1	1.68	102	98
8	3.0233	50	D.I. H_2O	9.51	1	3.3	200	66
8D	3.0824	50	D.I. H_2O	9.54	1	3.3	200	65
9	5.0525	50	D.I. H_2O	9.75	1	4.05	246	49
9D	5.0933	50	D.I. H_2O	9.67	1	6.39	388	76
3D spike	(+2.0 µg/ml)					4.14		
6D spike	(+2.0 µg/ml)					3.54		
1.00 STD						1.06		
D.I. H_2O blank						0.013/BDL		

Table 4-9. Closed-container ammon'a extractions from Test Condition 22 hopper ash in D.I. water.

Sample	Ash Mass, g	Volume, ml	Solvent	pH	D_F	Conc., µg/ml as N	NH_3 Mass, µg	Apparent NH_3 Concentration on Ash, µg/g
10	1.013	111.99	D.I. H_2O	11.06	2	0.693	188	186
11	3.020	93.76	D.I. H_2O	11.31	2	1.74	396	131
12	5.000	96.38	D.I. H_2O	11.45	2	3.44	805	161
Re-extractions in acetate buffer, pH 4.8								
10	1.013	37.0	4.8	na	5	0.249	56	55
11	3.020	42.9	4.8	na	5	0.254	66	22
12	5.000	41.1	4.8	na	5	0.306	76	15
Extraction of ash in 0.1 N sulfuric acid								
Ash	1.004	42.5			25	0.232	299	298

Particle Size Dependency of Ammonia Concentration

To investigate the dependency of ammonia concentration on particle size, two special tests were conducted at the outlet of the Reactor B air heater with a five-stage cyclone particle size instrument. This device which is operated in situ samples the flue gas isokinetically and then passes it though five sequential cyclones. Each cyclone is designed to remove a smaller size particle. For this test the cyclone "cut" sizes were approximately 7.8, 4.5, 2.5, 1.8, and 0.8 micrometers diameter (Stokes aerodynamic).

Tables 4-10 and 4-11 show data summaries for the two cyclone tests at the outlet of the Reactor B air heater. The analysis of the distribution of ammonia was confined to the ash actually captured in the five cyclone stages since a quantitative analysis of pre-collector and back-up filter material was not conducted. For the purpose of this study, the median particle diameter for each stage, the mass of ash collected in each stage, and the mass-basis ammonia concentration of the particulate in each stage were of primary interest. The data in the tables confirmed that the ammonia concentration (mass basis) of the fly ash is strongly dependent on particle size. The ammonia concentration in the ash increased by nearly two orders of magnitude from the 7.8 micrometer diameter particles to the 0.8 micrometer diameter particles. This relationship is illustrated in Figure 4-3. A power curve is superimposed on the data to illustrate the apparent trend of the relation but is not meant to suggest any definitive relationship.

The ammonia concentration in the ash was much higher in the smaller particle sizes, but most of the total ammonia was found to reside with the larger particles simply because these comprise the vast majority of the ash mass. The ammonia distribution is presented as a fraction of the total ammonia resident in each particle size group in Figure 4-4. The linear trend line superimposed on the data is included only to aid the visual presentation of the data and is not meant to show that any relationship has been conclusively demonstrated. The average total mass of ash collected for the two cyclone runs was 6.026 grams and the average mass of ammonia extracted form all the ash was 528.7 micrograms. These values give a ammonia concentration (mass basis) of 88 ppm(w) or micrograms of ammonia/gram of ash.

Figure 4-5 shows the cumulative ammonia distribution plot of the sum of all ammonia in the particle size at which the point is plotted plus all of the ammonia in the smaller particle size stages. These data imply that very little slip ammonia will exit the stack when high efficiency particulate emission controls are in place since all detectable ammonia is in the solid phase at the air heater exit and most of the ammonia is associated with the larger particle sizes which are most readily collected.

Table 4-10. Summary of the first five-stage cyclone test.

TEST DESIGNATOR:	Cyclone 1	
TEST TYPE:	INLET	
RUN NUMBER:	128-BAO-CYC-01	
Actual Flow Rate:	0.889	ft^3/min
Standard Flow Rate:	0.532	ft^3/min
% Isokinetic:	96.57	%
Viscosity:	229.3E-06	g/g-s
Calculated Cyclone ΔP:	1.92	in. Hg

Stage	Cunningham Correction Factor	D_{50}, μm (Classical Aerodynamic)	D_{50}, μm (Stokes Aerodynamic)	Cumulative Frequency, %	Reynolds Number	$\sqrt{\psi_{50}}$	Mass, g	NH_3 Conc., μg/g
1	1.033	7.639	7.765	15.7444	1461	0.195	5.1647	24.6
2	1.059	4.277	4.402	5.0997	1856	0.158	0.6525	98.8
3	1.109	2.333	2.456	1.7113	2475	0.136	0.2077	198.2
4	1.158	1.616	1.739	0.3051	3639	0.172	0.0862	421.4
5	1.401	0.677	0.802	0.2007	6085	0.172	0.0064	734.0
Back-Up Filter							0.0123	

Stage Cut Diameters Based on Particle Density = 2.5 g/cm^3

Total Mass Concentration:	6780	mg/m^3 (dry), STD
	4060	mg/m^3 actual
	2.96	gr/scf, dry
	1.77	gr/acf

Table 4-11. Summary of the second five-stage cyclone test.

TEST DESIGNATOR:	Cyclone 2	
TEST TYPE:	INLET	
RUN NUMBER:	128-BAO-CYC-02	
Actual Flow Rate:	0.866	ft^3/min
Standard Flow Rate:	0.516	ft^3/min
% Isokinetic:	93.78	%
Viscosity:	229.3E-06	g/g-s
Calculated Cyclone ΔP:	1.82	in. Hg

Stage	Cunningham Correction Factor	D_{50}, μm (Classical Aerodynamic)	D_{50}, μm (Stokes Aerodynamic)	Cumulative Frequency, %	Reynolds Number	$\sqrt{\psi_{50}}$	Mass, g	NH_3 Conc., μg/g
1	1.033	7.781	7.907	15.5336	1423	0.196	5.0951	22.8
2	1.058	4.393	4.518	5.0065	1807	0.160	0.6350	104.3
3	1.106	2.399	2.522	1.7606	2409	0.138	0.1958	189.7
4	1.154	1.660	1.783	0.3597	3543	0.174	0.0845	403.3
5	1.387	0.698	0.822	0.2039	5924	0.174	0.0094	734.0
Back-Up Filter							0.0652	

Stage Cut Diameters Based on Particle Density = 2.5 g/cm^3

Total Mass Concentration:	6880	mg/m^3 (dry), STD
	4100	mg/m^3 actual
	3.01	gr/scf, dry
	1.79	gr/acf

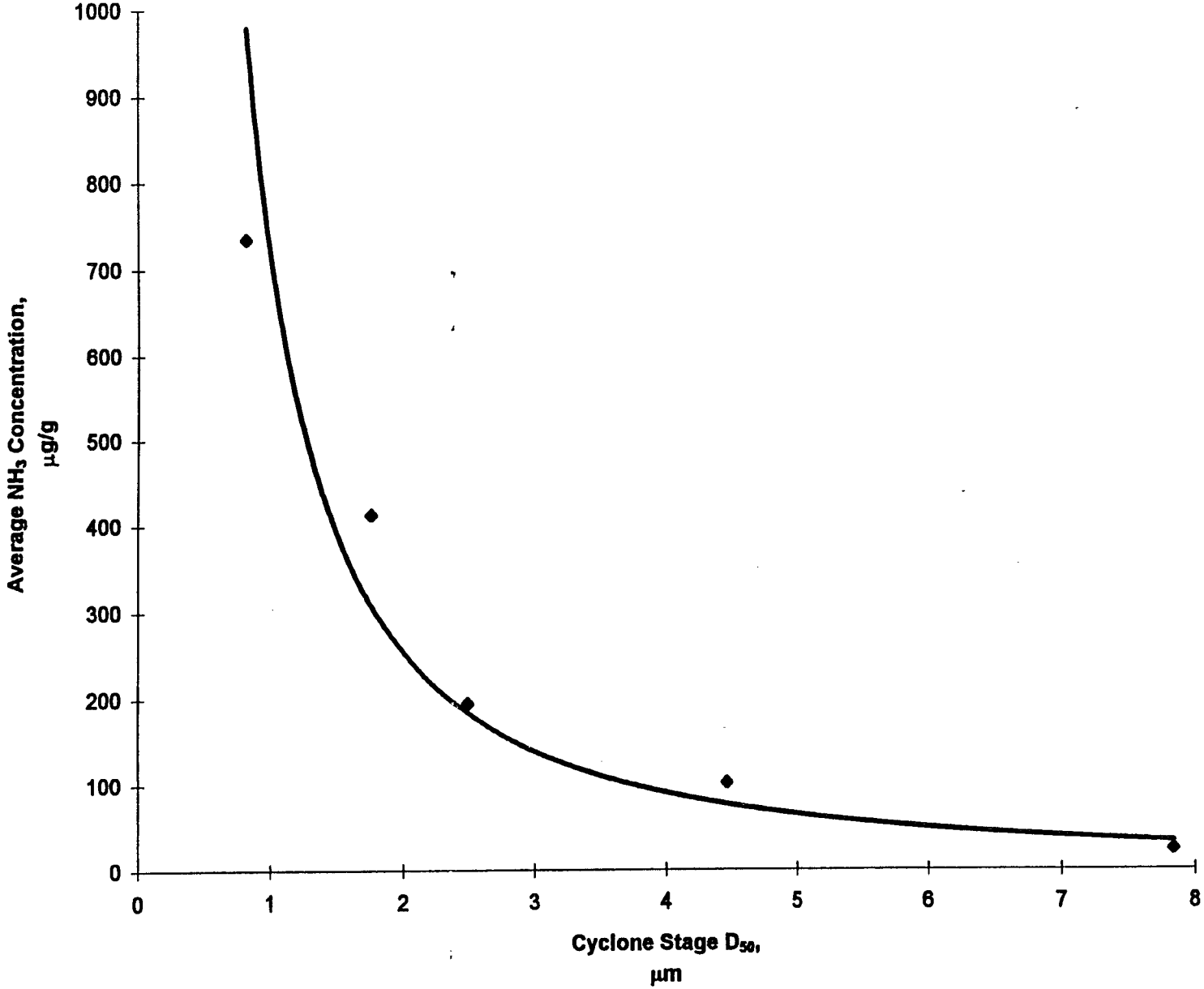

Figure 4-3. Mass concentration of ammonia as a function of particle size.

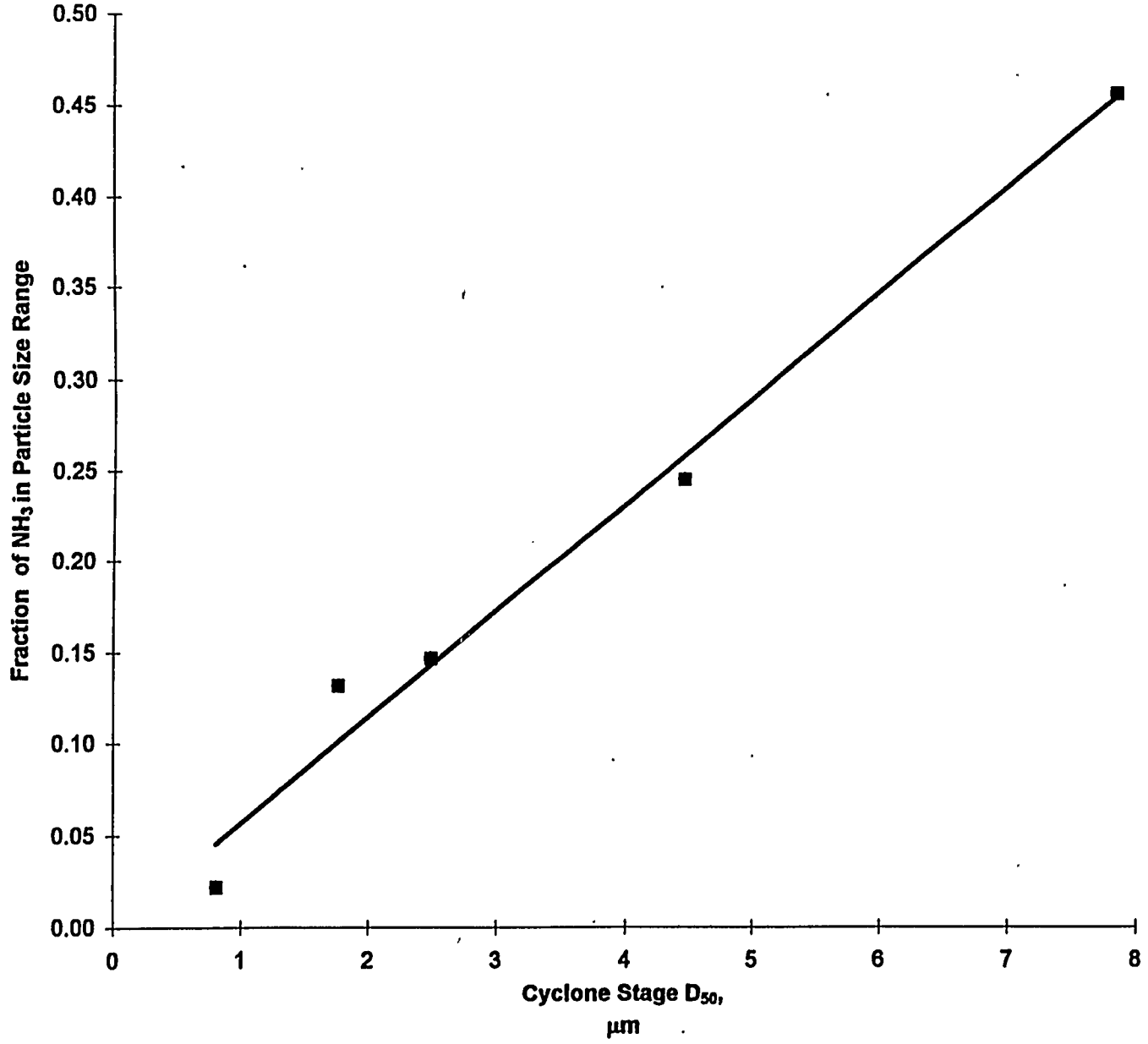

Figure 4-4. Distribution of ammonia among the five particle size ranges.

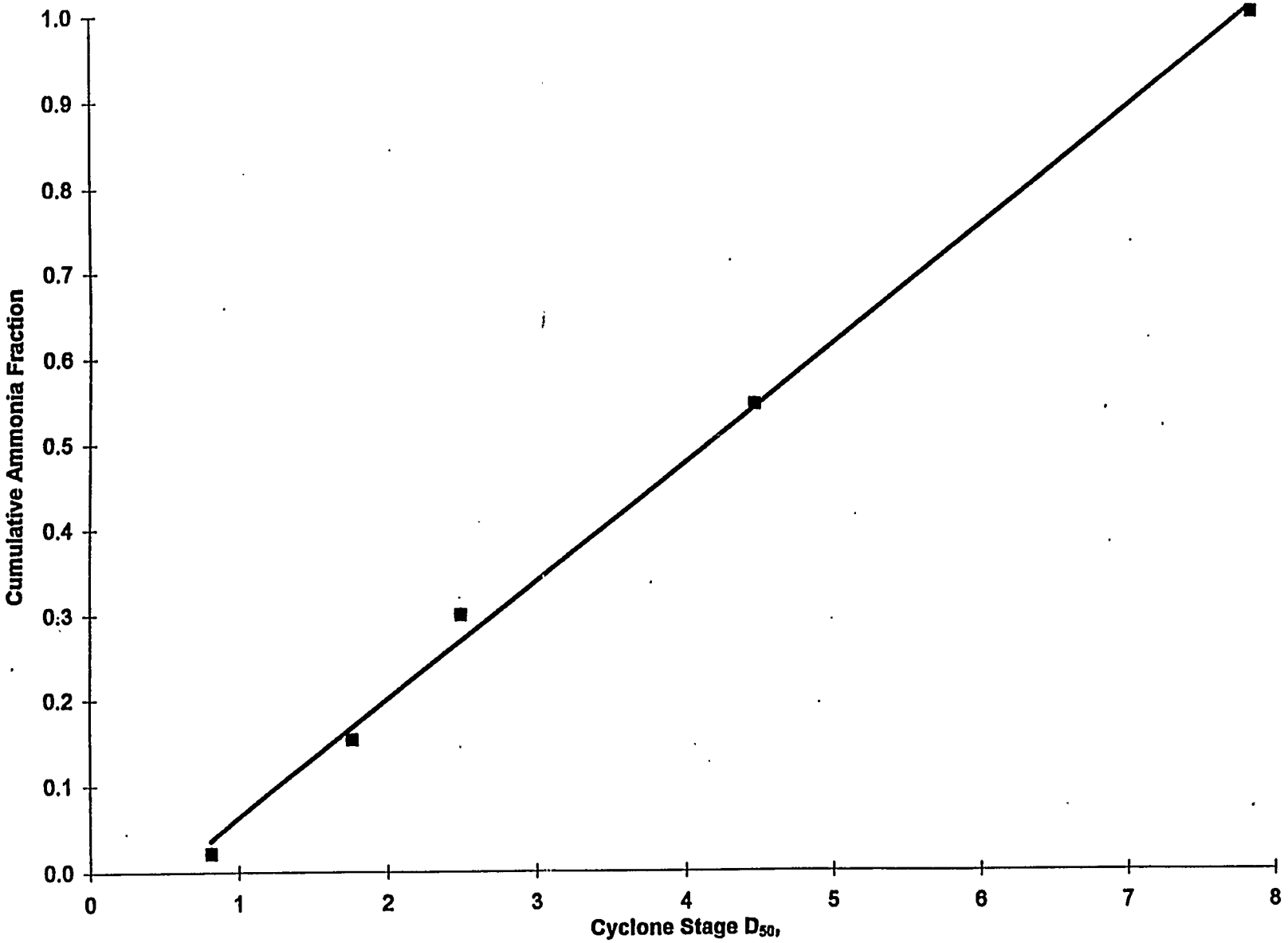

Figure 4-5. Cumulative solid-phase ammonia fraction as a function of particle size.

Conclusions

Almost no ammonia volatilized from the SCR ash until a significant amount of water vapor was absorbed by the ash. A plausible mechanism for the apparent volatilization that occurred is that enough water was gained by the ash to form a moist layer with a pH high enough to evolve gas-phase ammonia from the ammonium compounds on the ash. Nearly all of the ammonia on the ash evolved to the gas phase in the closed-container experiments. Ammonia concentrations in enclosed spaces will depend on the ammonia concentration of the ash, the volume of air above the ash available for dilution, and the presence of a humid atmosphere.

The extraction of ammonia from fly ash seems to depend upon pH. Evidently, all or nearly all, of the ammonia present was extracted in the buffered solutions at pH 4.7 and pH 6.2, but not all was recovered in alkaline unbuffered extracts. In the pH 6.2 buffer, however, the completeness of extraction seemed to fall off somewhat as the ratio of ash to buffer increased. At 3 g of ash per 50 mL of pH 6.2 buffer, the amount of ammonia extracted was about 200 μg/g, whereas at 1 g per 50 mL, the amount was near 250 μg/g.

The hopper ash that was collected at the same NH_3/NO_x ratio as the suspended fly ash (ratio, 0.8) was extracted with sulfuric acid (at pH 1.7) and found to contain ammonia at a concentration of about 250 μg/g, or about the same concentration as in the fly ash extracted with pH 4.7 buffer. The ashes differ in particle size and perhaps in ammonia content; if the hopper ash contains less ammonia, as may reasonably be suspected, because of its coarser particle size, then it is conceivable that the equivalent amounts of ammonia extracted from both ashes mean the pH 4.7 buffer is somewhat less effective for extraction than the dilute sulfuric acid. The available data do not permit this uncertainty to be fully resolved.

The effect of pH described above indicates that extraction is more complete when ammonia appears in the extract as the ammonium ion NH_4^+ rather than the free base molecule NH_3. At pH 1.7, the ratio NH_4^+/NH_3 is approximately 10,000,000. At pH 4.7, the value decreases to about 10,000, and at pH 6.2 it is roughly 100. When the pH reaches 11, however, in the absence of a buffer, NH_3 is predominant, and the NH_4^+ ratio is only about 0.01. The correlation of extraction with NH_4^+ ion, however, cannot be explained theoretically. The solubility of NH_3 is not limited in a practical way by pH. The volatility of NH_3, on the other hand, is appreciable, and this property of NH_3 may be substantially responsible for the data indicating that NH_3 is not completely extracted.

It is surprising to see that the addition of ammonia apparently makes the ash more alkaline (shown by comparing outlet ash with inlet ash). It is probably not the ammonia per se, however, that is responsible. Even without ammonia, the ash makes such a high pH in a slurry that ammonia can contribute nothing as a base. Near pH 11, dissolved ammonia is too weak as a base to capture protons and thus exhibit the property of a base. Ammonia can capture protons when the pH is well below 9 and the proton concentration is relatively

high. It cannot capture protons when the pH is much above 9 and the proton concentration is very low. In such an alkaline medium, the NH_3 molecule is not reactive; its behavior is not very different from that of the water molecule.

The paradox of increased slurry pH is likely due to an indirect effect from ammonia. Ammonia will neutralize the sulfuric acid that would otherwise occur on the ash surface. If sulfuric acid is neutralized by ammonia, it is not available to neutralize other extractable base in the ash and thus the pH of the slurry rises to a higher value.

All sample and blank solutions were placed in a tumbling apparatus and tumbled for approximately 96 hr. About 24 hr before the end of this period, however, the extra reactor outlet sample mentioned above was briefly removed from the tumbling apparatus and combined with 0.85 mL of 1.0 N sulfuric acid. The sample pH immediately dropped to 7, then began to slowly increase. The Teflon-coated magnetic stir bar added to this sample to facilitate the pH adjustment could not be removed from the solution without losing part of the ash sample. Thus, the stir bar was left in place, and another stir bar was added to one of the blanks to enable it to serve as a blank for this sample. Then all samples were returned to the tumbling apparatus, and tumbling was continued for the duration of the 96-hr agitation interval.

After the above extraction process, each sample was removed from the tumbling apparatus and allowed to stand for about three days to permit the undissolved ash to settle out of the solution. We then checked the solution pH with a pH meter and filtered the aqueous phase through an Acrodisc syringe filter into a precleaned 125-mL polyethylene (Nalgene) bottle. From each filtered sample, a 25-mL aliquot was transferred to a precleaned 60-mL amber glass bottle for mercury determination. The remainder was reserved for microwave digestion and analysis for other metals. The pertinent sample-preparation data are synopsized in Table 5-1.

Preparation of Fly-Ash Extracts for Analysis

The sample extracts were ultimately analyzed for all metals that were thought to be pertinent to the problem at hand, including the 20 metals that were previously determined in Plant Crist fly ash: arsenic (As), barium (Ba), beryllium (Be), cadmium (Cd), cerium (Ce), cobalt (Co), chromium (Cr), copper (Cu), mercury (Hg), manganese (Mn), molybdenum (Mo), nickel (Ni), lead (Pb), rubidium (Rb), antimony (Sb), selenium (Se), tin (Sn), strontium (Sr), vanadium (V), and zinc (Zn). In addition, we also analyzed the extracts for silver (Ag), boron (B), phosphorus (P), thallium (Tl), aluminum (Al), calcium (Ca), iron (Fe), and magnesium (Mg).

The sample extracts were prepared for Hg analysis essentially by the preparation method given in EPA Method 7470. Using this method as a guideline, we diluted a 10-mL aliquot of each extract to 100 mL. The diluted solution was transferred to a BOD (biological oxygen demand) bottle and combined with 5 mL of concentrated sulfuric acid, 2.5 mL of concentrated nitric acid, 15 mL of 5% (w/v) aqueous potassium permanganate, and 8 mL of 5% (w/v) potassium persulfate. The bottle was then placed on a hot plate at 95 °C for 2 hr. Afterward, the sample solution was cooled and combined with 6 mL of an aqueous reagent solution consisting of 12% (w/v) hydroxylamine hydrochloride and 12% (w/v) sodium chloride.

For the purpose of matrix matching, the calibration standards were treated in the same manner as set forth above. A digestion blank and an independent QC sample (i.e., water

Table 5-1. Sample Preparation Data for Plant Crist SCR Fly Ash Samples

Reactor B Inlet Samples

Sample No.	NH_3/NO_x	Ash Weight, g	Extract Volume, mL	Final pH
1A-1	0.8	5.0092	100	11.1
1A-2	0.8	4.9848	100	11.1
2A-1	0.6	5.0093	100	11.3
2A-2	0.6	5.0161	100	11.2
3A-1	1.0	5.0080	100	11.3
3A-2	1.0	5.0022	100	11.3

Reactor B Air Heater Outlet Samples

Sample No.	NH_3/NO_x	Ash Weight, g	Extract Volume, mL	Final pH
1B-1	0.8	5.0139	100	11.3
1B-2	0.8	5.0028	100	11.3
1B-3*	0.8	5.0026	100.85	9.1
2B-1	0.6	5.0012	100	11.4
2B-2	0.6	5.0062	100	11.3
3B-1	1.0	5.0071	100	11.7
3B-2	1.0	5.0171	100	11.7

Extraction Blanks

Sample No.	NH_3/NO_x	Ash Weight, g	Extract Volume, mL	Final pH
WB-1	------	------	100	5.5
WB-2	------	------	100	5.5

*This sample received 0.85 mL of 1.0 N sulfuric acid in an attempt to adjust its pH downward (see text).

containing spiked mercury at a level that was unknown to the analyst) were also prepared in this way. Furthermore, two additional aliquots of one of the real samples were spiked with mercury and carried through the above preparation procedure exactly like the other samples. Real samples spiked and treated in this manner are referred to subsequently in this report as "matrix spikes".

For determinations of all other metals except Rb, the sample extracts were digested according to EPA Method 3015 - Microwave Assisted Acid Digestions for Aqueous Samples and Extracts. That is, a 40-mL aliquot of each sample was placed into a Teflon microwave digestion vessel. After the addition of 5 mL of concentrated nitric acid to each vessel, the vessels were capped and placed in the microwave oven. The samples were heated for a total of 20 min in a two-stage heating program. After a brief cooling period, 0.5 mL of an internal standard solution (scandium, Sc) was added to each vessel, and the contents of each vessel were rinsed into a 50-mL polyethylene (Nalgene) volumetric flask. After mixing the solutions, we transferred them to 125-mL Nalgene bottles.

Two separate digestions of the type described above were required to prepare all of the samples. Thus, each digestion run included a digestion blank. In addition, a certified QC sample was included in one of the runs. Moreover, two matrix spikes were prepared as described previously, i.e., by spiking a real sample with the elements of interest. The spike levels were chosen to be roughly the same as the natural (i.e., unspiked) metal concentrations in the sample, as determined in a preliminary analysis of the sample in question. If the natural metal concentration was at or below our detection limit, then the sample was spiked with that metal at a concentration that was very close to the detection limit to enable us to identify even minor spectral and matrix interferences. All metals of interest were included in the matrix spikes except Ca and B, which were present at such high levels that a comparable spike would have required an unacceptable expansion of the solution volume. For all analyses, calibration standards were made up in 5% (v/v) nitric acid from certified 1000-ppm stock solutions.

For determinations of Rb, the sample extracts were not digested; they were merely combined with concentrated nitric acid to form a 5% (v/v) solution and further combined with potassium chloride to form a 0.2% (w/v) solution.

Analysis of Sample Extracts

All metals except Hg, Pb, Tl, and Rb were initially determined by inductively-coupled plasma atomic emission spectrometry (ICPAES). The ICPAES conditions and methods were essentially those set forth in EPA Method 6010. The instrument was a Perkin-Elmer Plasma 400 Spectrometer with QC Expert software and an AS-90 Autosampler. A six-point calibration curve (including a calibration blank) was used for each element except Ag, which tends to fall out of solution at high concentrations when other metals are present at high concentrations. For Ag, therefore, we used a five-point calibration curve

covering a relatively short concentration range. A calibration check standard was analyzed at the beginning and end of each instrumental run. To check for spectral interferences, As, Sb, and Se were analyzed at each of two wavelengths. All quantitation was performed by computing the ratio of the response from the analyte to the response from the internal standard (Sc).

Graphite-furnace atomic absorption spectrometry (GFAAS) was the only analysis method used for determining Pb and Tl. In addition, after we reviewed the ICPAES data, we decided to use this technique also to redetermine Ag, As, Cd, Cu, and Sb, mainly in an attempt to achieve lower detection limits. A calibration check standard and two calibration blanks were run essentially as described above for ICPAES. A 20-ppm Ni solution was used as a matrix modifier for the Tl, As, and Sb analyses. Our GFAAS methods were adapted from the 7000 series of methods promulgated in EPA SW-846. The instrument used for this work was a Perkin-Elmer Model 3100 Atomic Absorption Spectrometer equipped with an HGA-600 Graphite Furnace assembly, an AS-60 Autosampler, and Perkin-Elmer 5100 Software. The instrument uses deuterium background correction, electrodeless discharge lamps (for As and Sb), hollow cathode lamps (for all other elements), and a pyrocoated graphite tube fitted with a L'Vov platform.

After a review of the GFAAS data for Cu, we decided that the ICPAES method had provided a slightly better detection limit; hence, the Cu data reported here are those from the ICPAES analyses. But for those samples that yielded an unambiguously positive ICPAES response to Cu, we were able to confirm the found concentrations from the GFAAS data.

Our Hg analyzer, a PSA Analytical Merlin-Plus System with a hydride/vapor generator and an autosampler, has the unique feature of analyzing samples simultaneously by two different methods: atomic absorption and atomic fluorescence. The atomic fluorescence unit is the more sensitive one; it is able to measure Hg concentrations down to about 20 parts per trillion in calibration standards. With regard to calibration check standards and other QC samples, this instrument was evaluated during use in much the same way as the others.

Determinations of Rb were carried out by the atomic emission technique on a Perkin-Elmer Model 2380 instrument. A slot-type air-acetylene flame was used as the emission source. Again, QC checks were much the same as for the other instruments.

In this test program, we used an aggressive but risky definition of detection limit. Specifically, we chose to report numerical concentration values for all analyte responses lying more than one standard deviation above the average response to two digestion blanks, two calibration blanks, and two extraction blanks. (There were generally no significant differences in response from these three different types of blanks.) In a table of normal curve areas, one finds that about 14% of blank responses can be expected to lie at

Table 5-2. Metals Concentrations in Extracts of SCR Fly Ash Samples

Concentration, mg/mL (ppb)

Element	NH3/NOx	Reactor Inlet			Reactor Air Heater Outlet			
		Replicate #1[a]	Replicate #2[a]	Average	Replicate #1[a]	Replicate #2[a]	Average	Low pH Sample[b]
Ag	0.6	<2.5	<2.5	<2.5	<2.5	<2.5	<2.5	
	0.8	<2.5	<2.5	<2.5	<2.5	<2.5	<2.5	<2.5
	1	<2.5	<2.5	<2.5	<2.5	<2.5	<2.5	
As	0.6	104	101	103	68.6	64.9	66.8	
	0.8	86.9	84.4	85.6	67.3	60.5	63.9	98.8
	1	93.6	90.8	92.2	53	49	51	
B[c]	0.6	15	15.1	15.1	10.8	11.9	11.4	
	0.8	17	18.9	18	12.5	14	13.3	17.9
	1	16.3	18.3	17.3	11.3	12.5	11.9	
Ba	0.6	192	191	192	211	238	225	
	0.8	198	215	207	226	264	245	142
	1	200	241	221	271	294	283	
Be	0.6	<5.09	(5.25)	<5.25	<5.09	6.05	<5.57	
	0.8	<5.09	(5.25)	<5.19	<5.09	<5.09	<5.09	5.66
	1	<5.09	<5.09	<5.09	<5.09	<5.09	<5.09	
Cd	0.6	1.32	0.488	0.904	<0.250	<0.250	<0.250	
	0.8	0.712	3.68	2.2	2.24	<0.250	<1.25	1.4
	1	0.55	0.475	0.513	<0.250	<0.250	<0.250	
Ce	0.6	<46.2	<46.2	<46.2	<46.2	<46.2	<46.2	
	0.8	<46.2	<46.2	<46.2	<46.2	(50.2)	<48.2	<46.2
	1	<46.2	<46.2	<46.2	<46.2	<46.2	<46.2	
Co	0.6	(6.44)	<5.76	<6.10	(9.91)	(12.2)	11.1	
	0.8	(10.2)	(11.4)	10.8	<5.76	13.9	<9.83	<5.76
	1	<5.76	(8.23)	<7.00	(11.4)	(12.8)	12.1	
Cr	0.6	74.9	66.5	70.7	59.3	60.6	60	
	0.8	84.8	82.8	83.8	81.5	77.6	79.6	69.1
	1	109	91.9	100	84.1	73	78.6	
Cu	0.6	<3.21	<3.21	<3.21	(3.40)	(7.08)	5.24	
	0.8	<3.21	<3.21	<3.21	12.4	<3.21	<7.81	4.91
	1	(4.66)	(3.53)	4.1	<3.21	<3.21	<3.21	

Table 5-2. Metals Concentrations in Extracts of SCR Fly Ash Samples, continued

Concentration, mg/mL (ppb)

Element	NH3/NOx	Reactor Inlet			Reactor Air Heater Outlet			
		Replicate #1[a]	Replicate #2[a]	Average	Replicate #1[a]	Replicate #2[a]	Average	Low pH Sample[b]
Hg	0.6	<0.200	<0.200	<0.200	<0.200	<0.200	<0.200	
	0.8	<0.200	<0.200	<0.200	<0.200	<0.200	<0.200	<0.200
	1	<0.200	<0.200	<0.200	<0.200	<0.200	<0.200	
Mn	0.6	<0.240	<0.240	<0.240	<0.240	<0.240	<0.240	
	0.8	<0.240	<0.240	<0.240	(0.28)	<0.240	<0.26	2.63
	1	3.43	<0.240	<1.84	<0.240	<0.240	<0.240	
Mo	0.6	722	743	733	737	798	867	
	0.8	810	866	838	745	844	795	880
	1	771	877	824	758	835	797	
Ni	0.6	<6.60	<6.60	<6.60	(7.79)	(8.24)	8.02	
	0.8	<6.60	<6.60	<6.60	68	<6.60	<37.3	9.75
	1	(13.0)	<6.60	<9.80	(9.80)	<6.60	<8.20	
P	0.6	(98.8)	(79.6)	89.2	<76.1	<76.1	<76.1	
	0.8	(105)	(95.2)	100	<76.1	<76.1	<76.1	92.5
	1	<76.1	(77.1)	<76.6	<76.1	<76.1	<76.1	
Pb	0.6	<6.25	<6.25	<6.25	<6.25	<6.25	<6.25	
	0.8	<6.25	<6.25	<6.25	<6.25	<6.25	<6.25	<6.25
	1	<6.25	<6.25	<6.25	<6.25	<6.25	<6.25	
Rb	0.6	140	140	140	120	120	120	
	0.8	140	140	140	100	100	100	100
	1	120	120	120	80	80	80	
Sb	0.6	116	103	110	65.1	57.5	61.3	
	0.8	116	124	120	47.6	54.5	51.1	152
	1	97.4	89.6	93.5	33	30.6	31.8	
Se	0.6	<48.8	<48.8	<48.8	244	228	236	
	0.8	<48.8	<48.8	<48.8	469	518	494	516
	1	<48.8	<48.8	<48.8	350	390	370	
Sn	0.6	<22.0	(24.0)	<23.0	<22.0	<22.0	<22.0	
	0.8	<22.0	<22.0	<22.0	<22.0	<22.0	<22.0	(22.5)
	1	<22.0	<22.0	<22.0	<22.0	<22.0	<22.0	

condensate on the surface of the ash, where it would be relatively easy to extract. But we currently have no explanation for the high extractability of Mo.

The data of Table 5-2 appear to suggest that exposure of the fly ash to ammonia enhanced the extractability of Se and possibly also Ba. But the apparent enhancement of Se extractability is probably due to the condensation of Se on the reactor outlet fly-ash particles, as explained above. The observed effect on Ba was quite weak; the average increase in Ba extractability due to ammonia exposure was 22%. This is such a small increment that it may not be real. In other words, a variation of this magnitude could have resulted from a combination of variability in sample composition and error in analytical measurement. However, the data do reflect a consistent upward trend in Ba extractability as the NH_3/NO_x ratio increases. This observation, together with the consistently higher Ba extractabilities in the reactor outlet samples (versus the inlet samples), leads us to suspect that the observed effect of ammonia on Ba extractability may be genuine, but leaves the unanswered question as to the mechanism for the effect.

None of the other detectable metals appeared to undergo an extractability enhancement due to ammonia exposure. Indeed, the ammonia exposure actually seemed to diminish the extractabilities of several metals, most notably Al, Cd, and Sb, and possibly also P, B, Rb, and As. Exposure to ammonia seemed to have no effect on the extractabilities of Cr, Mo, Co, Sr, V, Zn, Ca, and Mg.

Correlations between metal extractability and NH_3/NO_x ratio were frequently inconsistent and hence inconclusive. Apparently, the combined effects of variability in sample composition and variability due to analytical error were often sufficient to mask any effects caused by the intentional variation of the NH_3/NO_x ratio. As has already been noted, however, there was a consistent trend of increasing Ba extractability with increasing NH_3/NO_x ratio. In addition, the opposite trend, i.e., decreasing metal extractability with increasing NH_3/NO_x ratio, was observed for several other metals, e.g., Rb, Sb, As, and Mg. Note that, for each of these metals except Mg, this trend was consistent with the extractability-decreasing effect of ammonia exposure (versus no ammonia exposure) that was observed for these metals.

In the last column of Table 5-2, data are given for the sample in which a pH adjustment was attempted. In this column, one sees that the pH adjustment greatly enhanced the extractability of Mg from the fly ash. It may also have enhanced the extractabilities of Mn, Ca, As, and Fe. Some of these observations are explainable on the basis of the differing solubilities of the corresponding metal hydroxides at the two pH levels (see Table 5-1). For example, the solubility of $Mg(OH)_2$ at pH 11 is markedly lower than it is at pH 9, and a similar but smaller solubility difference exists for Mn. But this explanation may not fully account for all of the observed solubility increases.

QC Data

Our QC data generally indicated very few problems with interferences, calibration errors, and so on. Responses to both extraction blanks were uniformly below or (occasionally) very near our detection limits for all metals except Hg. For Hg, our blank responses were more than two-fold higher than our detection limit. But no Hg blank response above the detection limit was obtained for any of the real-sample extracts. Thus, the background Hg in the real-sample extracts may have been precipitated by the alkalinity or absorbed by the fly ash in these extracts.

Among the more revealing QC samples are the matrix spikes. Because they represent the recovery of spiked analyte from the actual sample-extract matrix, they are capable of identifying the presence of a variety of different types of matrix and spectral interferences. Hence, the matrix-spike recoveries are summarized in Table 5-3 and are discussed further here. In view of the very low spike levels that were used in this work, we considered the vast majority of these recoveries to be satisfactory for the intended purpose.

However, the recoveries for Sb and Fe were systematically high, which suggested a possible matrix or spectral interference in each case. Moreover, the recovery of Sn was erratic; this is a common problem with this element. But Sn and Fe were not detected at high enough levels in the sample extracts to enable us to draw any conclusions with regard to the effects of ammonia. Therefore, these interferences were of no particular significance to this study. But the problem with Sb is significant to the extent that the absolute magnitudes of the Sb found concentrations may be in error. However, the precision of the Sb responses was good, and thus the observed changes (i.e., trends) in Sb extractability as a function of ammonia exposure were, in our opinion, quite valid.

Conclusions

We concluded from this study that the extractability of Ba from fly ash by water is slightly enhanced by prior exposure of the fly ash to ammonia in the SCR system. In addition, the magnitude of this enhancement depends directly on the magnitude of the NH_3/NO_x ratio in the SCR unit. Of the 16 additional metals that could be detected in the fly-ash extracts, none displayed what we considered to be genuine enhancements in extractability, and several exhibited decreases in extractability as a result of exposure of the fly ash to ammonia. Although one of these metals -- Se -- displayed a large apparent increase in extractability on exposure to ammonia, we concluded that the Se found in the reactor-outlet sample extracts must have condensed from the gas phase onto the fly ash at the reactor outlet. Finally, a deliberate downward adjustment in the pH of one sample solution caused enhancements in the extractabilities of several metals, most notably Mg, but also Mn, Ca, As and Fe to a lesser degree.

Table 5-3. Recoveries of Matrix Spikes

Element	Matrix Spike Recovery, %			Element	Matrix Spike Recovery, %		
	Matrix Spike #1	Matrix Spike #2	Average Recovery		Matrix Spike #1	Matrix Spike #2	Average Recovery
Ag	96	104	100	P	110	118	114
As	91	108	100	Pb	122	124	123
B	—[a]	—[a]	—[a]	Rb	102	102	102
Ba	105	95	100	Sb	159	145	152
Be	87	86	87	Se	100	102	101
Cd	76	130	103	Sn	228	71	150
Ce	111	114	113	Sr	99	96	98
Co	84	94	89	Tl	106	108	107
Cr	108	118	113	V	100	100	100
Cu	121	128	125	Zn	91	94	93
Hg	89	93	91	Al	106	119	113
Mn	92	91	92	Ca	—[a]	—[a]	—[a]
Mo	104	100	102	Fe	127	193	160
Ni	90	102	96	Mg	104	89	97

[a] No matrix spikes were attempted for B and Ca because of their high natural concentrations in the samples (see text).

The results of our analyses raise several questions requiring discussion from theoretical perspectives:

* Should ammonia alter the extractability of any of the metals?

* Could the very marked apparent increase in the extractability of selenium actually be due to ammonia rather than the temperature change already suggested?

* How can the increase in extractability of barium be explained?

* How can the decreases in extractability of certain other metals be explained?

Increase in metal solubility due to complex ion formation with ammonia

Several metals react with ammonia to form a series of complex ions. This phenomenon is illustrated by the following reactions beginning with Co^{+2} ion:

$$Co^{+2} + NH_3 = Co(NH_3)^{+2} \qquad K_1$$

$$Co(NH_3)^{+2} + NH_3 = Co(NH_3)_2^{+2} \qquad K_2$$

$$Co(NH_3)^{+2} + NH_3 = Co(NH_3)_3^{+2} \qquad K_3$$

$$Co(NH_3)^{+2} + NH_3 = Co(NH_3)_4^{+2} \qquad K_4$$

The enhanced solubility of cobalt can be expressed as the ratio R of total dissolved cobalt, including the complexed and uncomplexed metal, to the uncomplexed metal as a function of the several complexation constants and the concentration of excess, uncomplexed ammonia:

$$R = [\text{Total Co}]/[\text{Uncomplexed Co}]$$

$$= 1 + K_1[NH_3] + K_1 K_2[NH_3]^2 + K_1 K_2 K_3[NH_3]^3 + K_1 K_2 K_3 K_4[NH_3]^4$$

The values of the logarithms of these complexation constants involving Co^{+2} and NH_3 are approximately as follows:

$$\log K_1 = 1.99$$

$$\log K_2 = 3.50$$

$$\log K_3 = 4.43$$

$$\log K_4 = 5.07$$

If the concentration of uncomplexed NH_3 is, for example, 0.009 M, the value of the ratio R is 1.32. If there were no other form of cobalt in solution, then, the presence of NH_3 in an amount providing an uncomplexed concentration of 0.009 M would increase the solubility of cobalt by 32%.

The compilation of complexation constants published by Bjerrum indicates that there are six metal ions that are significantly complexed by ammonia. These are the ions of cadmium, cobalt, copper, nickel, silver, and zinc. All but silver produce at least four complexes as illustrated above for cobalt; silver, on the other hand, produces only the complexes with one and two moles of ammonia. Bjerrum lists several sets of values for the complexation constants of each metal; the reader cannot easily establish the best set of values for each metal. For the present purposes, however, a set of approximately correct values has been selected for each metal; these sets of values are presented in Table 5-1 (the selected set for cobalt is the same as the one listed above in the text). The ratios of concentrations of each metal in all forms to that in uncomplexed form have subsequently been calculated, with the results given in Table 5-2. As before, the uncomplexed concentration of NH_3 was assumed to be 0.009 M (a value to be commented upon momentarily).

The concentrations ratios listed in Table 5-2 are provisional values only, which require further discussion. They indicate, however, that ammonia has a far greater solubilizing effect on copper than on any of the other metals, because of course the complexes based on copper are more stable than those of any other metal. For copper, the multiplying factor is 5430; for cobalt it is just 1.32.

The assumed value of 0.009 M for uncomplexed ammonia is more than of incidental value. Suppose that ammonia is retained by fly ash at a concentration of 1000 μg/g, a value just slightly higher than that measured for any NH_3/NO_x ratio in this investigation. If this ash is then placed in water in the ratio of 5 g per 100 mL and all the ammonia goes into solution, the ammonia concentration will be 0.009 M. Moreover, if only a very much smaller concentration of a metal is extracted, as in all solutions analyzed in this investigation, the concentration of uncomplexed ammonia will remain near 0.009 M. This concentration, then, and the results in Table 5-2 based on this concentration have a provisional applicability for predicting enhanced metal extractabilities in this investigation.

None of the observed enhancements that can be assigned numerical values clearly conforms to the prediction. This perhaps can be said most emphatically for copper, for which the enhancement seems certainly not to be three orders of magnitude. Whether silver satisfies the prediction of an enhancement by the factor 158 cannot be said, because this metal was not measurable with or with ammonia added. Cadmium is not enhanced by

---

J. Bjerrum et al., Stability Constants of Metal-Ion Complexes, with Solulbility Products of Inorganic Substances, Part II: Inorganic Ligands, The Chemical Society, London, 1958.

SeO_2 between 700° and 300° F. The reduction in volatility from that of SeO_2 to that of the element at 300° F provides a less dramatic driving force for the deposition of selenium.

Increase in extractability of barium

Bjerrum gives no indication that barium reacts with ammonia to produce complex ions. Thus, if ammonia is the cause of increased extractability of this metal, the effect must be through another mechanism, none of which is apparent as a direct process. Conceivably, the effect on barium is not due to ammonia even indirectly. It may be the result of the change in temperature that accompanied the addition of ammonia (because samples containing ammonia were collected after the temperature had decreased in a heat exchange process). No way to explain an increased extractablity of barium at a lower sampling temperature, however, is evident. Specifically, no process analogous to the condensation of SeO_2 on ash surfaces as the temperature falls can be postulated. Barium is essentially as involatile at the higher temperature (around 700° F) as at the lower temperature (300° F).

Decrease in extractability of other metals

These effects occurred with several metals and require comment just as does the contrary effect with barium. It is reasonable to ask the question of whether processes can be suggested whereby ammonia directly or indirectly lowers metal solubility. There are rare processes if any that produce relatively insoluble aggregates of a metal ion with ammonia. None can be suggested that are associated with those metals that seems to have decreased extractability from fly ash as the result of the presence of ammonia.

Aluminum is perhaps the metal with the greatest apparent reduction in extractability with ammonia present. This metal has no reaction with ammonia known to the present investigators. Its behavior is not readily explained by the decrease in temperature that accompanied the addition of ammonia, nor is it explained by the other phenomenon known to occur -- the increased pH of the extract. In fact, aluminum is amphoteric and if influenced by the change in pH it should have increased in extractability, not decreased.